UNIVERSITÀ DI PADOVA **FACOLTÀ DI INGEGNERIA**

MASTER'S THESIS

ENERGY DISAGGREGATION

USING A SINGLE VOLTAGE SENSOR

Author: Silvia Bertagna De Marchi

Supervisors: *University of Padua*:
Dr. Stefano Tomasin.
Philips Research:
Dr. Alessio Filippi,
Dr. Ronald Rietman.

Corso di Laurea Magistrale in Ingegneria delle Telecomunicazioni

Anno Accademico 2011/2012

Abstract

Continuous and detailed energy monitoring is essential to ensure the energy efficient operation of complex systems, for instance, buildings. Energy efficiency is becoming a relevant topic in the last years because of the growing concerns on sustainability and the will of reducing the energetic costs.
The idea behind this Master's thesis is a novel energy monitoring solution that with a single sensor enables the monitoring of energy consumption per each single device in an electrical group. The proposed method enables an extremely simple energy monitoring since it does not require monitoring the overall current. All other existing methods need to have access to the electrical current to estimate correctly the power consumption of the different devices. The current meter has to be clamped around a wire inside the electrical cabinet and its installation is a non-trivial task. The main advantage of this novel method is that the unit of sensing can be installed by any user in any socket.
Our method monitors only the voltage signal and maps the voltage variations to the power jumps caused by the different devices.

Keywords:
energy management systems, energy meters, energy measurement, event detection, energy saving, power load, energy power management, energy detection, energy disaggregation. nonintrusive load monitoring, voltage analysis, voltage method, voltage monitoring.

Acknowledgement

First of all, thanks to my supervisors. Thanks to Alessio Filippi, Ronald Rietman and Ying Wang for supporting me in my time at Philips Research, for helping me in the redaction of my Master's thesis.
Thanks to Professor Stefano Tomasin for his guidance and for being my supervisor also in the Bachelor's thesis.
Thanks to my parents for supporting me in all these years of study. Thanks to my mother for all the afternoon and evening that we have spent together and thanks to my father for all the advices.
Thanks to my brother for being always near also when he is another city.
Thanks to Philips Research for the opportunity that it gives to me in the last months.

Contents

List of Figures

List of Tables

Chapter 1

Introduction

This Master's Thesis describes a novel technology being developed which enables very detailed insights into electricity consumption via an extremely simple installation of a single voltage sensor.
This novel technology is designed to monitor, continuously and non intrusively, an electrical circuit that contains a certain number of devices which are turned on/off independently. Furthermore it checks the steps of the power level and determines the energy consumption of individual appliances using only the voltage signal.
The method is based on the assumption to have access only to the voltage signal and to have a known reference load in the electrical network that is under control. The reference load is used to estimate the required electrical network parameters to map the observed voltage variations into power jumps.
This Master's Thesis is organized as follows:

- Chapter 2 is about the System Model. Some basic notions are recalled to permit the understanding of the the development of the following Chapters;

- Chapter 3 argues about the motivation behind works on energy monitoring. Furthermore it describes briefly the State of the Art in the field of Appliance Load Monitoring and it explains our innovative method;

- Chapter 4 discusses the design of the system. In This Chapter the best solution in term of implementation of the novel technology is proposed as result of our theoretical analysis;

- Chapter 5 reports some performed experiment to test the novel method. They constitute preliminary tests about the reliability of the novel approach;

- Chapter 6 shows the results that we have obtained in the analysis of high frequency components of the voltage signal;

- Chapter 7 ends this Master's Thesis with the conclusion about our method and some suggestions for future works.

Chapter 2

System Model

2.1 General

The novel voltage method, as introduced in Chapter 1, provides the energy disaggregation of the devices running in a environment only looking at the voltage.
The measured voltage signal depends on the position of the voltage sensor and the existing electrical network, for this reason it is useful to introduce some notions about the electrical system model.
The Chapter is organized as follows: Section 2.2 focuses on a basic ideal model of the network to recall some electrical definition, Section 2.3 introduces a more complex model of the network including different electrical branch circuits and also wire cables, Section 2.4 recalls theory about power consumption, Section 2.5 models the Root Mean Square (RMS) amplitude of the voltage signal and also reports the conducted experiments in the Philips's Laboratory for the estimation of the variability of the delivered voltage signal, finally Section 2.6.1 models also the phase information of the voltage signal and provides some considerations about the recorded phase of the delivered voltage.

2.2 Basic Ideal Model

This Section introduces a basic ideal model of the electrical network that represents a generic environment.
A general equivalent electrical scheme of a single phase environment is illustrated in Fig. 2.1. By using Thevenin's theorem the source of the delivered voltage can be represented as an ideal voltage source $v_0(t)$ in series with an equivalent impedance Z_0. The devices in the household, numbered from 1 through N, are connected in parallel. Each device is represented by its admittance Y_i and it could be turned on by closing the corresponding switching. The delivered voltage is, in first approximation, a sinusoidal wave with a time-varying peak amplitude equal to $\sqrt{2}V_{RMS}(k)$.
The frequency of the delivered voltage f_0 is assumed to be constant, and is equal to 50 Hz in the EU (60 Hz in U.S.), so the period of the sinusoidal wave is $T = 0.02$s ($T = 0.0167$s in U.S). The

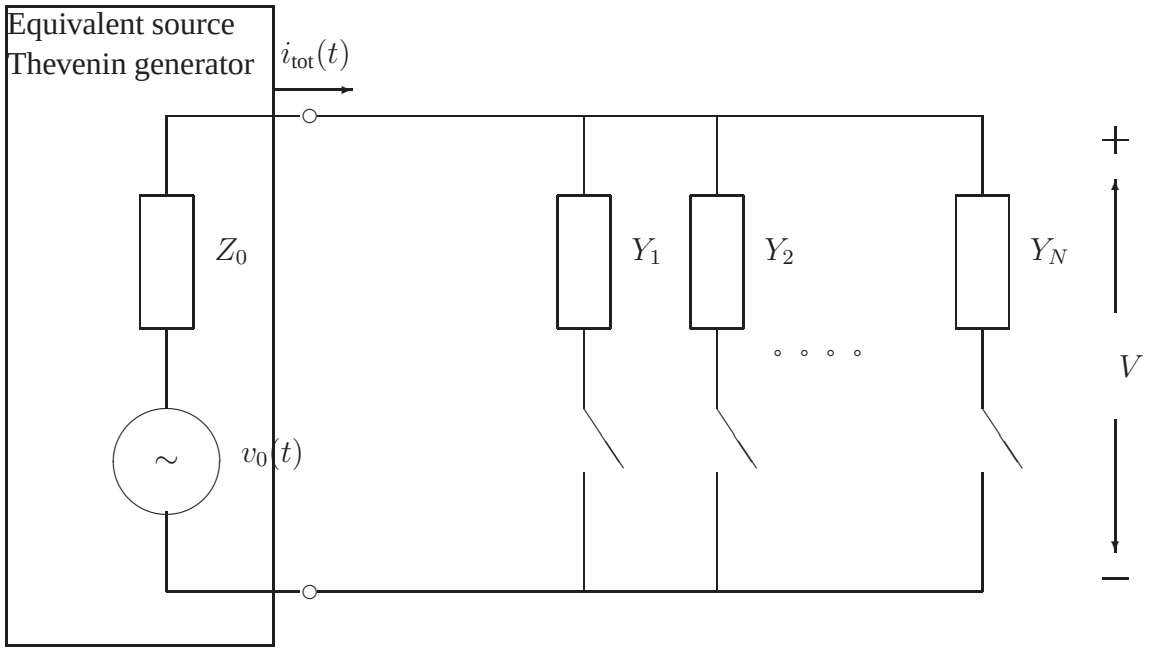

Figure 2.1: *Equivalent electrical scheme of a single phase house.*

Root Mean Square (RMS) at the period k is defined as:

$$V_{RMS}(k) = \sqrt{\frac{1}{T}\int_{t_k}^{t_k+T} v^2(t)dt}, \tag{2.1}$$

where t_k is an arbitrary starting time.
A simple expression of the equivalent delivered voltage $v_0(t)$ observed at the period k is:

$$v_{0,k}(t) = \sqrt{2}V_{RMS}(k)\sin\left(\omega t + \phi(k)\right), \tag{2.2}$$

where $\omega = 2\pi f_0$ is the angular frequency and $\phi(k)$ is the phase of the sinusoidal wave.
The novel method, discussed in this Master's Thesis, is based on the assumption to look only at fundamental frequency signatures, in this way is possible to express the voltage through the phasor notation because the entire analysis is developed at the fixed frequency f_0.
This last consideration permits to define the delivered voltage phasor as a complex number in the following way:

$$V_0(k) = V_{RMS}(k)e^{j\phi(k)}. \tag{2.3}$$

In Chapter 3 and 4 the entire explanation of the method assumes to use the phasor notation.

2.3 Electrical Network

In this Section some notions about a generic electrical network are recalled. This Section first recalls some of the performances that have to be guarantee in a generic electrical network, then

introduces two fundamental elements of a generic network that are cables and circuit breakers, finally it recalls the concept of Crosstalk that can afflict different branch circuits that constitute the network. To recall all these notions the Section refers to Fig. 2.3, in which a simplified model of a distribution network with two electrical branch circuits is represented.
In a network with different electrical branches, as in Fig. 2.3, the distribution network has to assure certain performances as:

- It has to guarantee to all the electrical branch circuits a minimum level of voltage also in presence of a big variation of the voltage. Example of big variations: in the branch circuit (A) a short-circuit happens and this could cause a black out of the voltage for the other branches.

- It has the task to protect the users of all the electrical branch circuits from abrupt variations. Example of abrupt variation: in the branch circuit (A) a big load (with a big absorption of current) is switched on/off.

- It has to try to avoid wide range of variation of the voltage. Example of wide uncontrolled variations: a elevated number of users are present and an high number of applications are switched on/off in a random way during the day so that the variation of the voltage is slow and it can be dangerous.

To partially solve all these problems two different approaches are implemented: user's side and network side. The first consists in the fact that all the users (applications) are designed taking into account the rules relating to immunity that they need to respect (different rules depending on the class of the product) and the rules of compatibility:

- Each device has to guarantee to generate disturbances under certain levels. These limits depend on the type of the device and the environment for which the device is designed to work. These conditions are called "compatibility".

- Each device has to work correctly also in presence of other devices and other disturbances. These limits also depends on the type of the device and they are referred to the "immunity".

On the network's side, in general, it is important that the network guarantees a quality of supply voltage, the requirements depend on the countries and on other parameters (see Section 3.5). Network design and operations, protection strategy, relaying and grounding and so forth are key points to guarantee certain voltage quality (reported in Section 3.5).
One of the designed measures to realize this aim is the presence of **miniature circuit-breakers** to isolate different electric branch circuits. They operated as automatic electrical switches. They are designed to detect a fault condition and to protect the network and the final user, by interrupting the electrical flow in case of dangerous situations. They are usually mounted in a central electrical panel: electrical panels are easily accessible junction boxes used to reroute and switch electrical services (they are also called circuit breaker panels or "fuseboxes"). The circuit breakers are used to detect short circuits between the live and the neutral wires, or the drawing of more current than the wires are rated to handle to prevent overheating and fire. They have an

impedance which must be taken into account in the design of the system (see Fig. 2.3).
In addiction to circuit breakers, the **wire cables** constitute another important part of a generic electrical network.
First of all a small introduction about the electricity line is reported, after that the general expression of the impedance of the wire cables is recalled.
Despite competition from other materials, copper remains the preferred electrical conductor in nearly all categories of electrical wiring. Indeed, copper is used to conduct electricity in high, medium and low voltage power networks (our case), including power generation, power transmission, power distribution, telecommunications, electronics circuitry, and countless other types of electrical equipment.
Regarding the electricity line, this last one usually is of limited length and, at the fundamental frequency f_0, can be summarized with the following distributed components (transmission line theory, referred to Fig. 2.2):

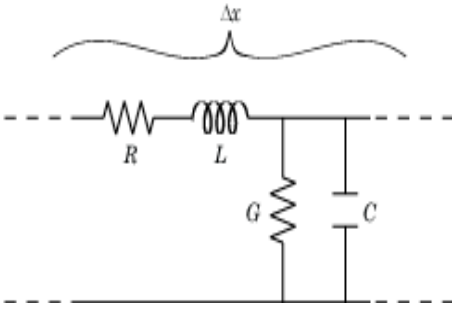

Figure 2.2: *Transmission line.*

- The distributed resistance R of the copper cable:

$$R = \frac{\rho}{S}\,[\frac{\Omega}{m}] \tag{2.4}$$

  - ρ : electrical resistivity (also known as resistivity, specific electrical resistance). For the copper wire is equal to $1.68 \cdot 10^{-8}\ \Omega \cdot \mathrm{m}$ at 20 °C;
  - S: section of the cable (usually is equal to $2.5\ \mathrm{mm}^2$ in the considered cases).

- The distributed inductance L (due to the magnetic field around the wires) $[\frac{H}{m}]$;
- The distributed capacity C between the two conductors $[\frac{F}{m}]$;
- The distributed conductance G of the dielectric material separating the two conductors $[\frac{S}{m}]$.

The relevant term at the fundamental frequency f_0 is the resistance of the copper line that expresses the physical resistance of the copper to the current and it causes a voltage drop proportional to current through the cable. Therefore the impedance of the wire cables is equivalent

to:

$$Z_{\mathrm{i}} = R \cdot l_{\mathrm{i}}, \tag{2.5}$$

where l_{i} is the length of the i copper wire in meters.

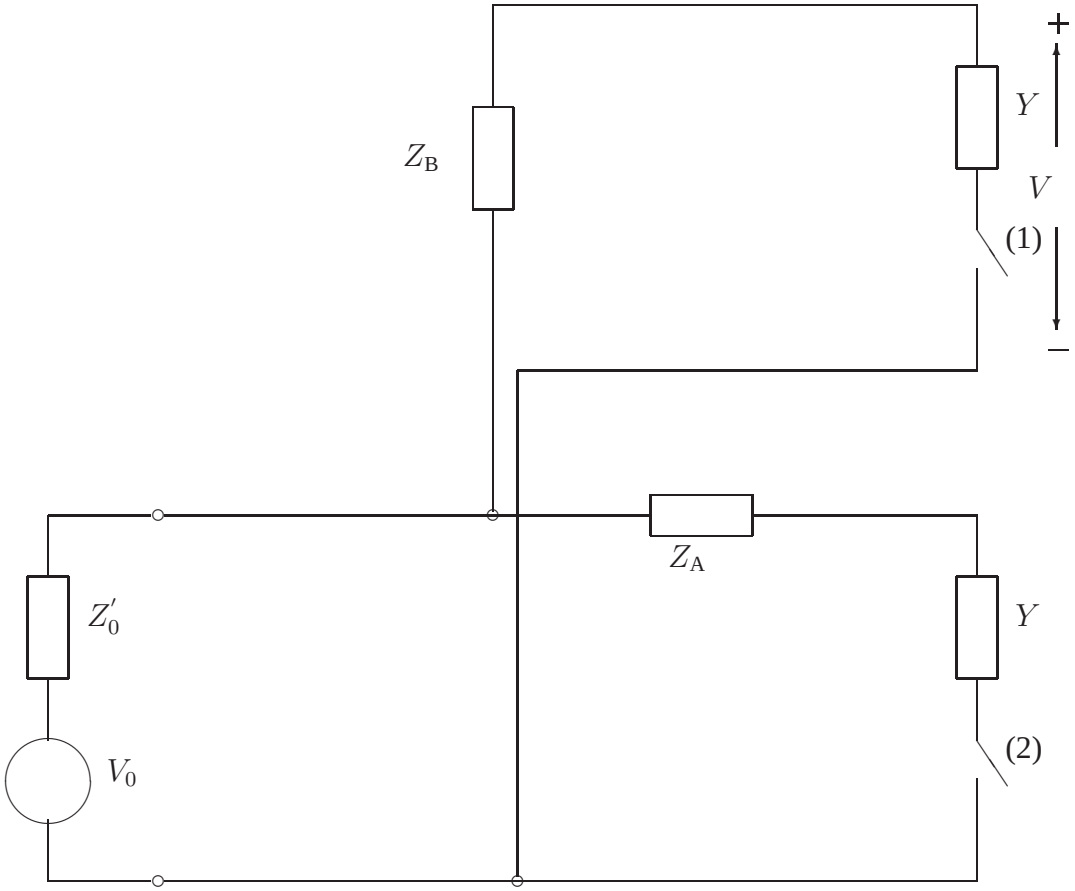

Figure 2.3: *Network model.*

2.3.1 Crosstalk between different electrical branch circuits of the electrical network

As already introduced, an electrical network is composed of different branch circuits.
The mutual interference between different electrical branch circuits of the same electrical network (Fig. 2.3) is a problem known as crosstalk.

Definition 1 *Crosstalk:*
Crosstalk is any phenomenon by which a signal transmitted on one circuit or channel of a transmission system creates an undesired effect in another circuit or channel.

In ideal conditions two electrical circuits should work independently, in reality there are different causes of reciprocal influence: for example the common impedance that they share, the inductive coupling, the capacitive coupling.
The last two interferences are not of interest in our analysis because the inductive and capacitive components are not relevant at the fundamental frequency (see [1]). The relevant term, for the development of our method in the next Chapters, is the interference due to the common impedance that different electrical circuits share.

2.4 Complex power

In this Section some quantities of fundamental importance and their meaning are recalled.
Our work is focused on the estimation of the power consumption.
The complex power P is composed of:

- Real Power $ReP\ [W]$: the average rate of delivery of energy, it represents the useful power consumed by loads to perform real work, i.e., to convert electric energy to other forms of energy;
- Reactive Power $ImP\ [VAR]$: the portion of complex power that is out of phase with the active power. It is generally associated with reactive elements (inductors and capacitors). It is not very useful by itself. However it is useful to distinguish between different loads with the same active power and different reactive powers.

For the estimation of the consumption in term of energy the important term is the Real Power , indeed the active power is the rate at which energy is dissipated or consumed by the load. The Real power can be computed by averaging the product of the instantaneous voltage and current:

$$ReP = \frac{1}{T} \int_{t_k}^{t_k+T} v(t)i(t)dt, \tag{2.6}$$

which is valid for both sinusoidal and nonsinusoidal conditions. In particular we suppose in Section 2.2 to work in the sinusoidal condition and so (2.6) can be written as:

$$ReP = V_{RMS} I_{RMS} \cos\theta, \tag{2.7}$$

where θ is the phase angle between voltage and current at the fundamental frequency f_0.

2.5 Voltage RMS

2.5.1 Model of the Root Mean Square of the voltage source

The voltage method is sensitive to the quality of the supplied voltage. As first step the variability of the voltage has been investigated by measuring the voltage signal, without any load turned on in our electrical branch circuit. The measurements have been performed in the set-up of Fig. 5.1 and the measured data is processed by calculating the RMS value:

$$V_{RMS}(k) = \frac{1}{N_S} \sum_{i=kN_s-1}^{(k+1)N_S} V(i)^2, \tag{2.8}$$

with $N_S = 1000$ (five periods of the AC signal, $5T = 0.1$s). The resulting pattern of the RMS voltage within one hour of observation is not stable because it includes different contributions of the devices from the other branch circuits (crosstalk) and also the voltage variations. The choice of having a single electrical branch circuit permits to avoid the problems of the crosstalk of other devices that share the same electrical branch circuit (also the instrument equipment is supplied from a different branch circuit).
Since the measurements are corrupted by random variations, they are said to be affected by **noise**, one of the simple modality to attenuate the noise component is by using a moving average filter. In our case a sliding window has been used to clear the track and keep into account the variations of the delivered voltage in a short interval of time. Indeed we are interested in short intervals of time before/after the switching on/off events, so we want to define the variability of the voltage in limited intervals of time.
The difference between each RMS (2.8) and the average value of the correspondent sliding (2.10) has been calculated for each RMS value of (2.8).
At any instant, a **moving window** of $2r + 1$ values is used to calculate the average of the data sequence to understand how much a certain value of the voltage can differs from the mean value calculated around it. That difference is assumed to be the noise component:

$$n(k) = V_{RMS}(k) - V_{RMS_{mean}}(k), \tag{2.9}$$

where:

- $V_{RMS}(k)$ is calculated as 2.8;
- $$V_{RMS_{mean}}(k) = \frac{1}{2r+1} \sum_{i=k-r}^{k+r} V_{RMS}(i), \tag{2.10}$$

  in which r is the length of the sliding window;
- $n(k)$ is the component of noise that afflicts the measurement.

2.5.2 Experimental data

A complete statistical description of the voltage trend is not available in literature.
To compensate this gap the voltage behaviour has been studied in the Laboratory of Philips Research at the High Tech Campus. The voltage have been recorded in order to evaluate the nature of the noise $n(k)$ and choose a suitable threshold for the implementation of the algorithm. Let us see some performed experiments.
All these experiments have been performed with a reserved electrical branch circuit with the electrical setup explained in Section 5.2.
In the first example the RMS voltage (2.8) has been recorded for 25 minutes, the trend of the voltage is reported in Fig. 2.4. The voltage in Fig. 2.4 appears to be very stable and it is necessary

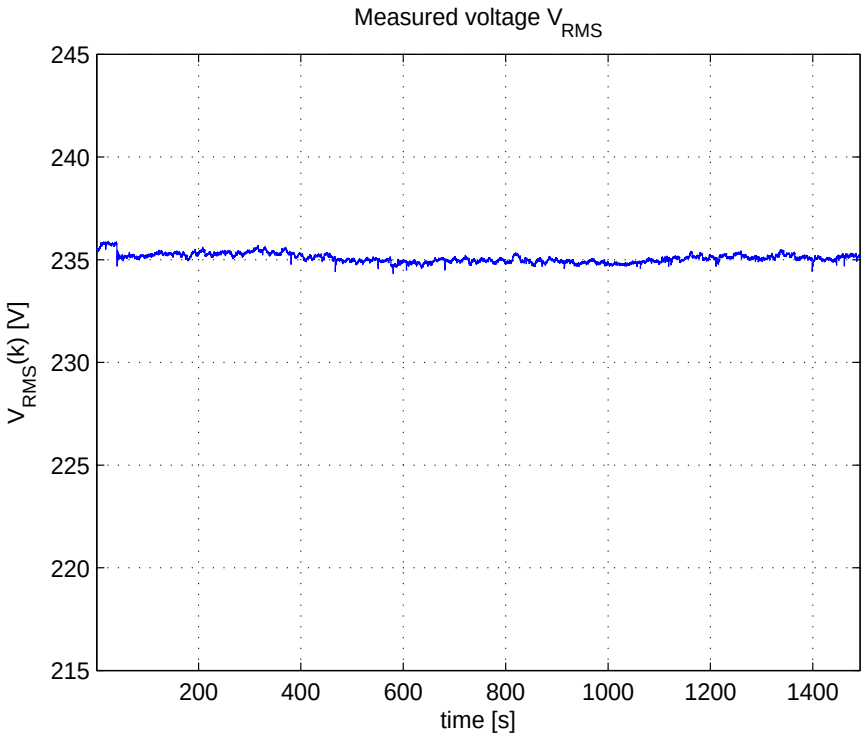

Figure 2.4: *RMS voltage recorded with no loads on. Experiment 1.*

to reduce the range of y-axis, a zoom of that trend is reported in Fig. 2.5, to see in a clearly way the fluctuations of the RMS voltage. In the initial trend of Fig. 2.5 one jump in the voltage happens, this can be due or to the variation of the delivered voltage or to a big load that has been switched on in another branch circuit (crosstalk).
The more interesting part is the analysis of short intervals of time (on which the algorithm works). $n(k)$ has been evaluated as in (2.9) by using an average moving window with different values of r always of small amplitude. The histograms of Fig. 2.6 2.7 2.8 2.11 2.12 show the distribution of $n(k)$ (2.9) for different values of r in two different experiments.
All the histograms are normalized by applying the following rule: the normalized count is the

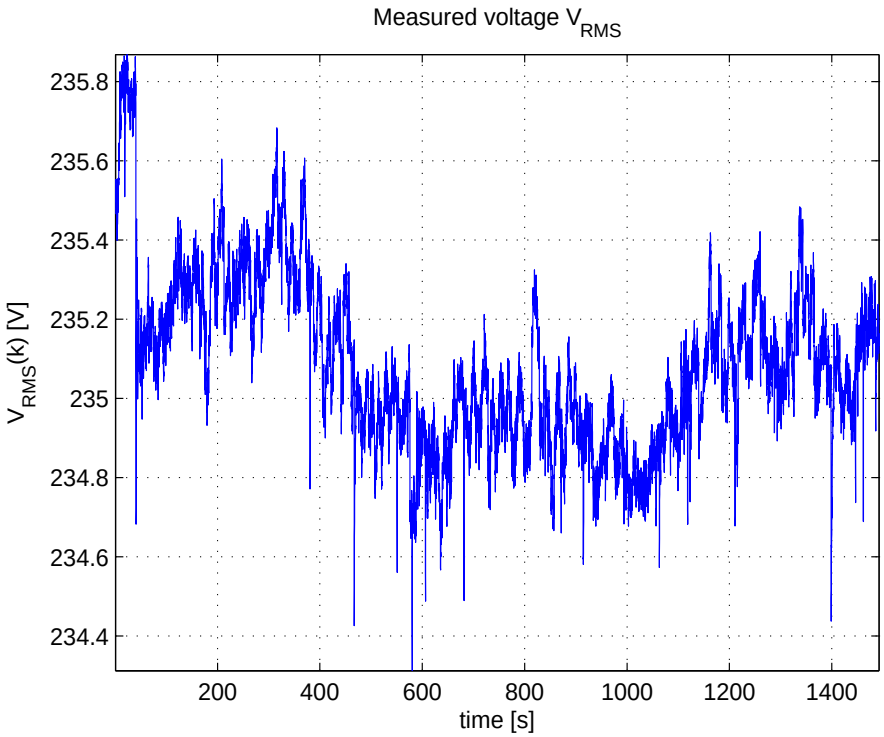

Figure 2.5: *RMS voltage recorded with no loads on. Experiment 1.*

count in the class divided by the number of observations times the class width (as class width is used the value 0.001).
We found through a series of experiments that their are afflicted by noise $n(k)$ that can really express as:

$$n(k) \in N(0, \sigma^2) \; . \tag{2.11}$$

Indeed the noise n is composed of different contributions but the important result is that, by evaluating a big number of realizations of the noise, is possible to approx it as a Gaussian function. This can be explained by the Central limit theorem. We can suppose that the noise can be approx indeed as a sum of independent, random variables and for this reason it tends towards the normal distribution with a probability density function:

$$f(n) = \frac{1}{\sigma\sqrt{2\pi}} \exp\left(-\frac{(n-\mu)^2}{2\sigma^2}\right). \tag{2.12}$$

The analysis has been performed by varying the radius r of the sliding window to understand how the variance changes (so also the standard deviation) by considering different intervals of time (relation between time and variations of the voltage). The standard deviation is important because it gives the range for a normal distribution: theoretically the amplitude of a Gaussian function can be an infinite value but in the reality nearly all values lie within 3 times the standard

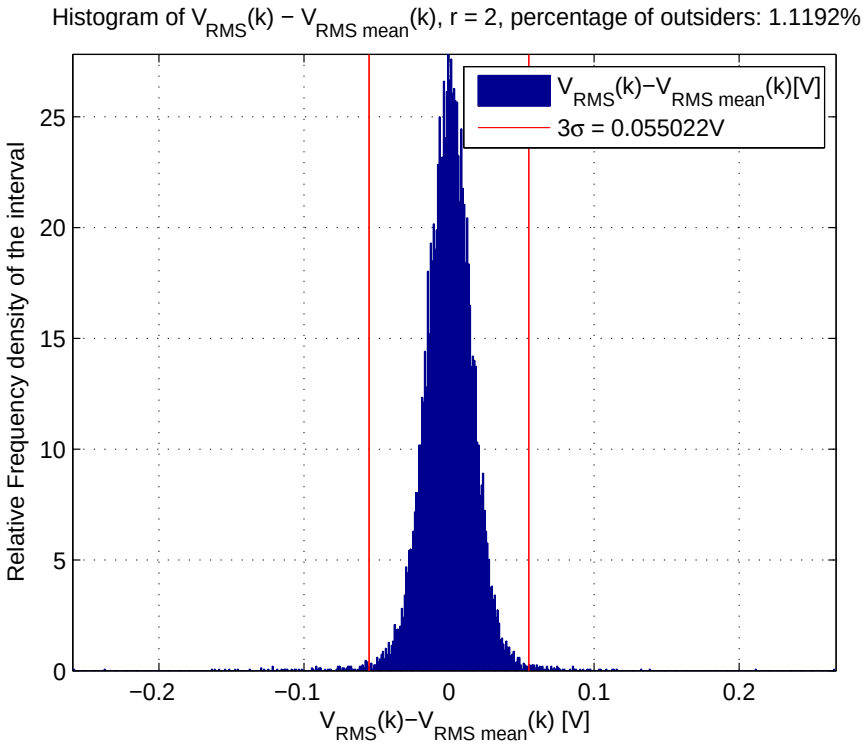

Figure 2.6: *Histogram of the noise $n(k)$ with $r = 2$. Experiment 1.*

deviations of the 2.10 following the 3 sigma rule.
In mathematical notation, this fact can be expressed as follows:

$$P[-3\sigma < n(k) < +3\sigma] \approx 0.9973 \tag{2.13}$$

where $n(k)$ has a normal distribution.

Definition 2 (Relative percentage of the outsiders) *Define the set I as:*

$$I = \{n(k) : n(k) < -3\sigma \vee n(k) > 3\sigma\}, \tag{2.14}$$

the set N as:

$$N = \{n(k)\ stored\ in\ the\ file\} \tag{2.15}$$

The percentage of the outsiders is defined as:

$$outsiders = \frac{|I|}{|N|} \cdot 100, \tag{2.16}$$

in which $|I|$ and $|N|$ are the cardinality of the sets 2.14 and 2.15.

The data has been collected in different days at different hours and in Table 5.1 the discussed parameters of some performed experiments are reported. The data collected of Table 5.1 is obtained with an average window with a radius $r = 5$.

Day of observation	Minutes of monitoring	3σ	Outsiders	Start time
01/12/2011	24.87	0.093	1.05 %	14:00
01/12/2011	19.35	0.086	1.05 %	14:30
06/12/2011	17.48	0.077	1.11 %	15:00
06/12/2011	41.27	0.081	1.07 %	16:00
09/05/2012	24.82	0.084	0.75 %	08:45
09/05/2012	27.86	0.07	0.94 %	09:15
09/05/2012	34.07	0.071	0.92 %	13:00
14/05/2012	22:75	0.061	0.79 %	19:00

Table 2.1: *Data of voltage measurements.*

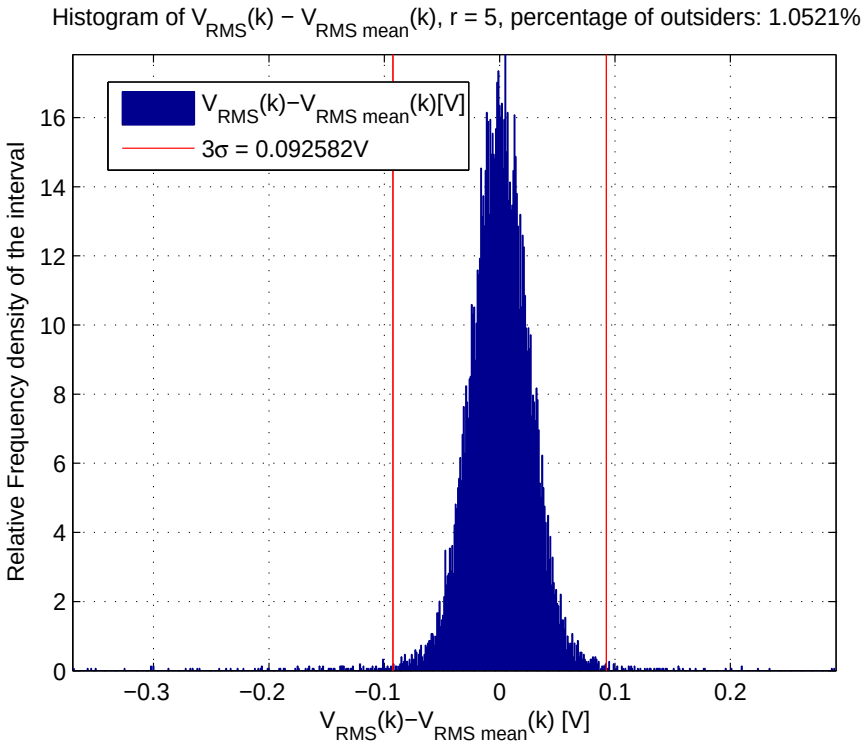

Figure 2.7: *Histogram of the noise $n(k)$ with $r = 5$. Experiment 1.*

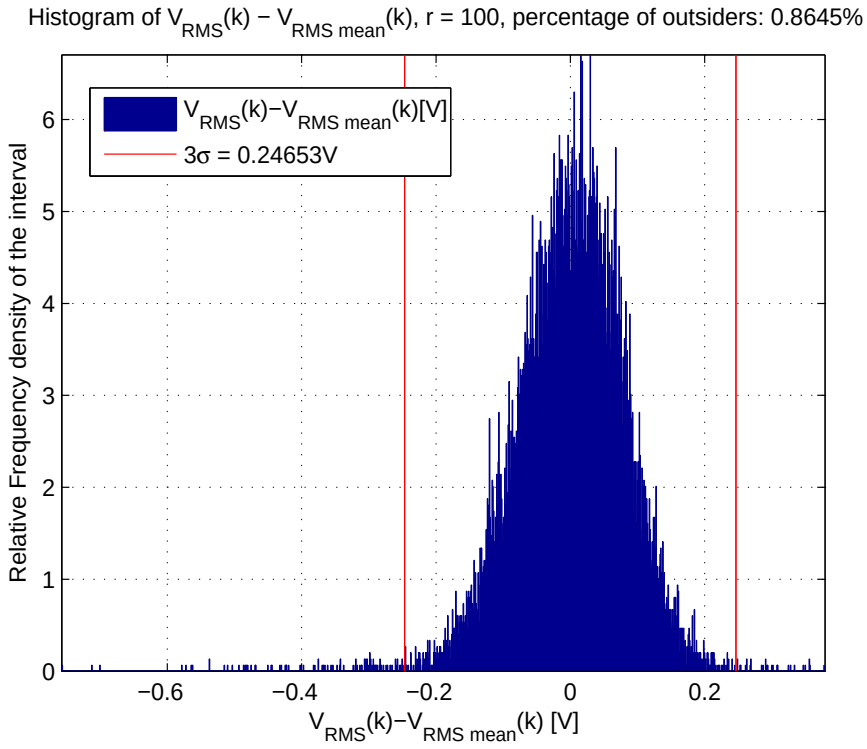

Figure 2.8: *Histogram of the noise $n(k)$ with $r = 100$. Experiment 1.*

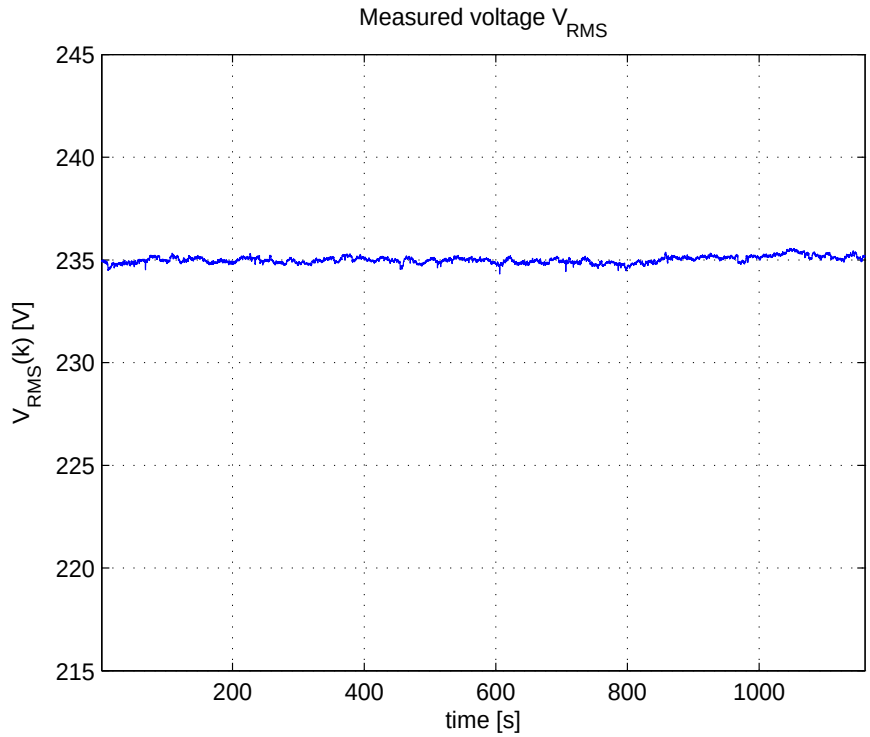

Figure 2.9: *RMS voltage recorded with no loads on. Experiment 2.*

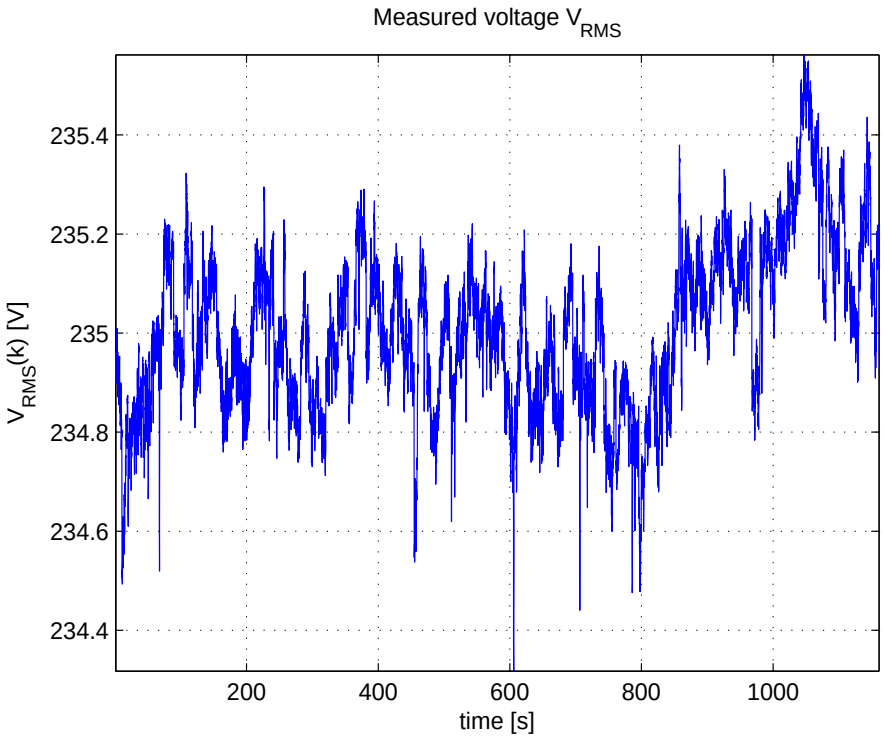

Figure 2.10: *RMS voltage recorded with no loads on. Experiment 2.*

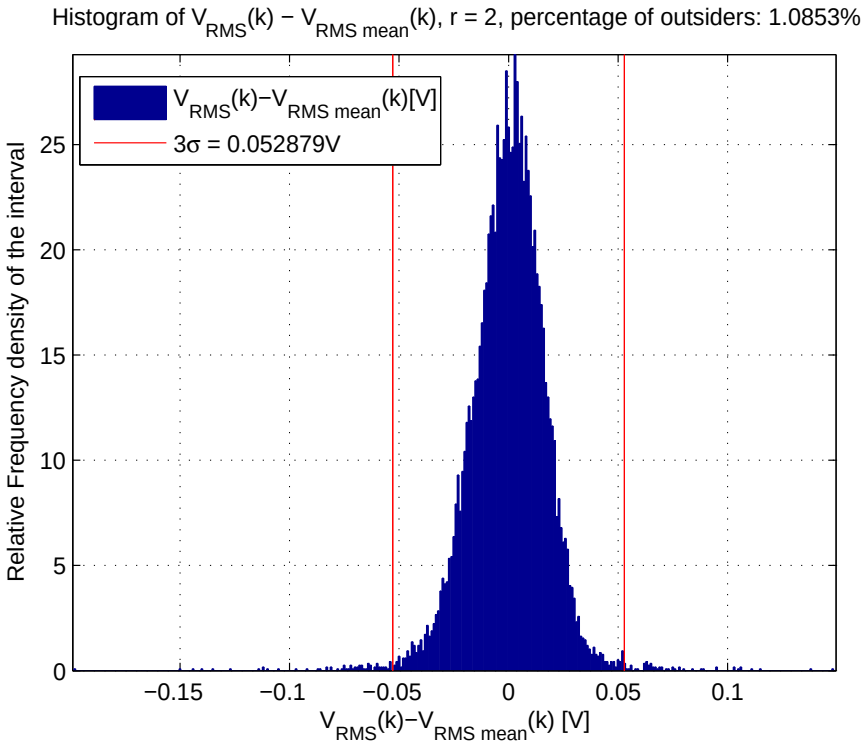

Figure 2.11: *Histogram of the noise $n(k)$ with $r = 2$. Experiment 2.*

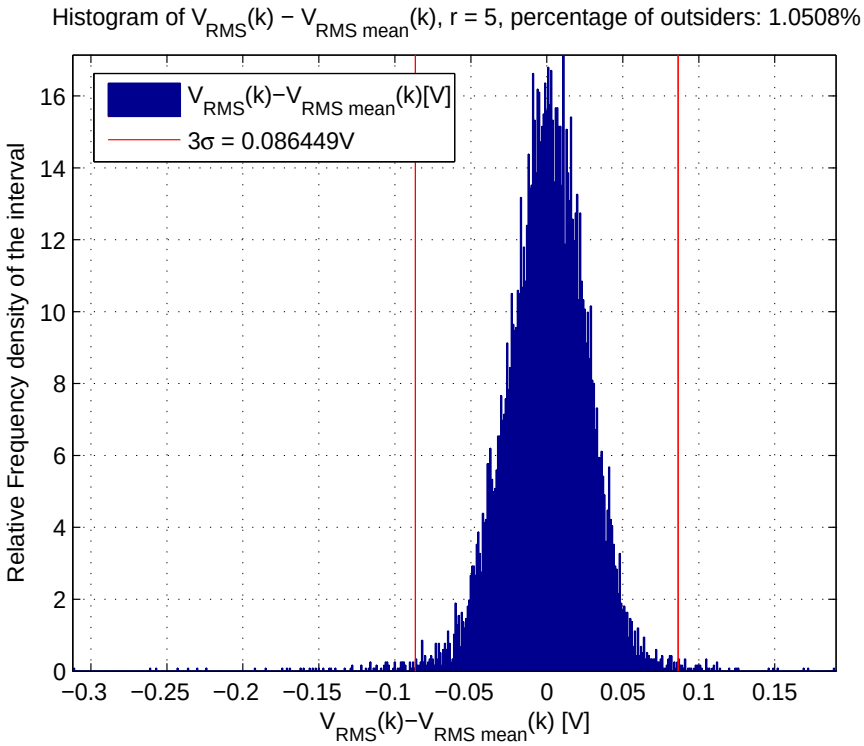

Figure 2.12: *Histogram of the noise $n(k)$ with $r = 5$. Experiment 2.*

2.6 Voltage Phase

2.6.1 Voltage Phase Model

Given the general expression of the voltage at the period k:

$$v((n+kN)T) = v_k(nT) = \sqrt{2}V_{RMS}(k)\sin\left(\omega(n+kN)T + \phi(k)\right), \tag{2.17}$$

with $n = 1...N$, $N = 200$.
The data can be processed in the following way to derive the phase of the voltage signal:

$$\begin{aligned} V_I(k) &= \frac{1}{N}\sum_{n=1}^{N} v_k(nT)\cdot\sin(2\pi n f_0 T) \\ &= \sqrt{2}\cdot V_{\text{RMS}}\cdot\sin(2\pi(n+kN)f_0T + \phi(k))\sin(2\pi n f_0 T) \\ &= \sqrt{2}\cdot V_{\text{RMS}}\left(\sin\left(2\pi(n+kN)\right)\sin\left(\phi(k)\right) + \cos\left(2\pi(n+kN)\right)\cos\left(\phi(k)\right)\right)\cdot\sin(2\pi n f_0 T), \end{aligned} \tag{2.18}$$

$$\Rightarrow V_I(k) = \sqrt{2}\cdot V_{\text{RMS}}\cdot\cos(\phi(k))\cdot\sin(2\pi n f_0 T). \tag{2.19}$$

$$\begin{aligned} V_Q(k) &= \frac{1}{N}\sum_{n=1}^{N} v_k(n(T-T/4))\cdot\sin(2\pi n f_0 T) \\ &= \sqrt{2}\cdot V_{\text{RMS}}\left(\sin\left(\frac{3}{2}\pi(n+kN)\right)\sin\left(\phi(k)\right) + \cos\left(\frac{3}{2}\pi(n+kN)\right)\cos\left(\phi(k)\right)\right)\cdot\sin(2\pi n f_0 T), \end{aligned} \tag{2.20}$$

$$\Rightarrow V_Q(k) = \sqrt{2}\cdot V_{\text{RMS}}\cdot\sin(\phi(k))\sin(2\pi n f_0 T). \tag{2.21}$$

The voltage phase is defined as:

$$\phi(k) = \phi(k-1) + \arctan({}^{V_Q}/_{V_I}). \tag{2.22}$$

The difference in phase, between two consecutive periods, is only:

$$\Delta\phi(k) = \arctan({}^{V_Q}/_{V_I}), \tag{2.23}$$

Theoretically the difference of phase between two consecutive periods (Eq. 2.23) is equal to zero when no device is on. In the reality, as already introduced, this hypothesis is not verified.
As the variability of the RMS voltage has been analysed in Section 2.5, the analysis of the phase of the voltage signal is evaluated in this Section. The phase of the voltage signal is calculated by applying (2.22) on five periods of the voltage wave ($N_S = 1000$).

2.6.2 Experimental data

For example in the experiments reported in Section 2.5 the correspondent trends of $\Delta\phi(k)$ are reported in Fig. 2.13 and 2.16.
Despite no load is on, the difference in phase of the voltage waveform is not equal to zero. The used method to recover the information about the phase is not accurate but it shows that the phase is not constant and equal to zero. The voltage phase, calculated as in (2.22), is reported in Fig. 2.14,2.17. These last figures show that a drift is present in the phase and the amplitude of the drift changes over time and it seems not predictable. The main reason for the drift in phase

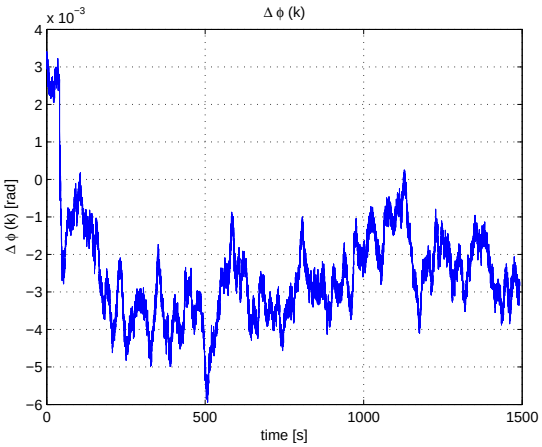

Figure 2.13: *$\Delta\phi(k)$ during the experiment 1.*

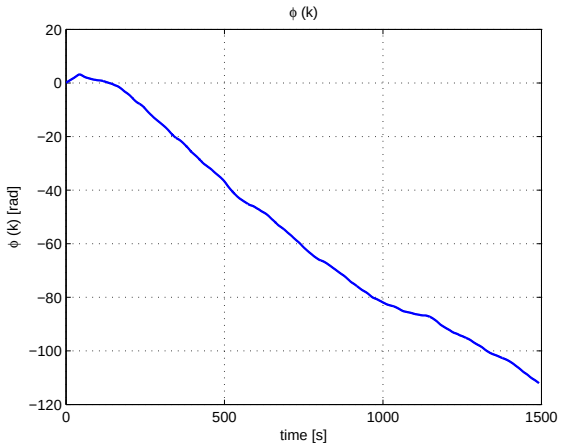

Figure 2.14: *$\phi(k)$ during the experiment 1.*

Figure 2.15: *Estimated Phase in the experiment 1*

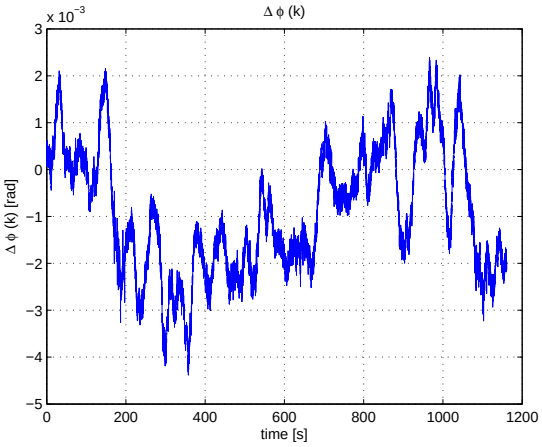

Figure 2.16: *$\Delta\phi(k)$ during the experiment 2.*

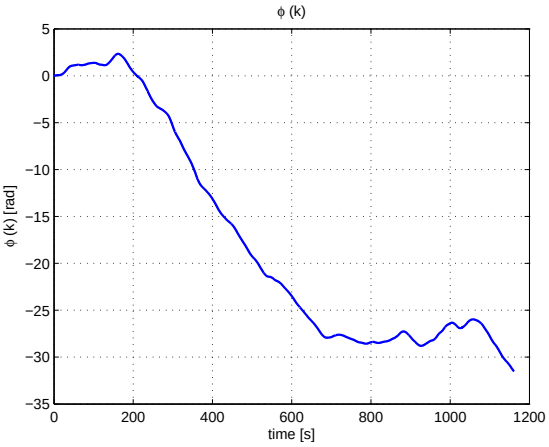

Figure 2.17: *$\phi(k)$ during the experiment 2.*

Figure 2.18: *Estimated Phase in the experiment 2.*

seems to be the variations of the fundamental frequency.

Chapter 3

Energy Disaggregation

3.1 General

The present Chapter is organized in the following way: Section 3.2 introduces the motivations and some of the possible applications that are behind the interest in energy monitoring, Section 3.3 reviews the State of the Art in the field of Appliance Load Monitoring, Section 3.4 describes the difference between techniques that are focused only on voltage signatures and techniques that uses also the current information, Section 3.5 introduces the parameters of Voltage quality, finally Section 3.6 explains our novel method.

3.2 Motivation and Applications

Saving energy and using energy more efficiently is becoming increasingly relevant because of economic and environmental reasons.
Consumers are highly aware of environmental problems and how their everyday activities are contributing to them, with a high portion already researching the better strategy to reduce the emissions CO_2. Furthermore they are more concerned about their energy consumption and the energy efficiency of their household appliances because of the will to reduce their energetic bill since the energy prices are increasing again after the 2009 economical crisis.
Recently many large consumer electronics companies, e.g. Philips, Intel and Belkin , have addressed this new user awareness by integrating sustainability as part of their management agenda. Energy management seems really a fundamental step in changing eco-systems and companies can play an important role by building an efficient interface between users and energy market. Preliminary studies [2] forecast that energy consumption could be reduced by up to 10 to 15 $\%$ by the application of energy management, through the deployment of Smart Grid [3] and home automation network [4].
For Smart Homes it is essential to know the consumption of electricity of the appliances in a household. To obtain this data Smart Meters must be installed in all households.
Various types and models of smart meters are available, one example of Smart Meter is depicted in Fig. 3.1, but all of them have the same basic functionality. Using a communications network,

Figure 3.1: *Example of Smart Meter.*

smart meter sends electricity consumption data to the utility. They can give customers control by providing accurate, real-time information on energy consumption, show how much that energy costs and the carbon dioxide it equates to but they can also provide information about gas and water consumption.
Indeed smart meters enables different applications by two-way digital communications between the utility and the customer, one of these is energy monitoring. Example of possible applications of energy monitoring (our field of interest) are:

- a transparent bill for the customers;
- an eco-feedback with also some suggestion about specific cost-effective measures to improve the energy efficiency as appliance upgrades;
- detection of malfunctioning equipment or inefficient setting (old and inefficient devices can be replaced by newer ones that consume less energy);
- detection of malfunctions in the power grid;
- smart charging of plug-in electric vehicles;
- remote meter reading, and remote customer (dis)connections;
- integration of distributed generation resources;
- new types of pricing procedure, for instance, taking into account the type of usage.

Utilities throughout Europe are now starting to roll out smart metering as part of a European mandate to have smart meters installed in 80 % of European households by 2020 (forecast plan

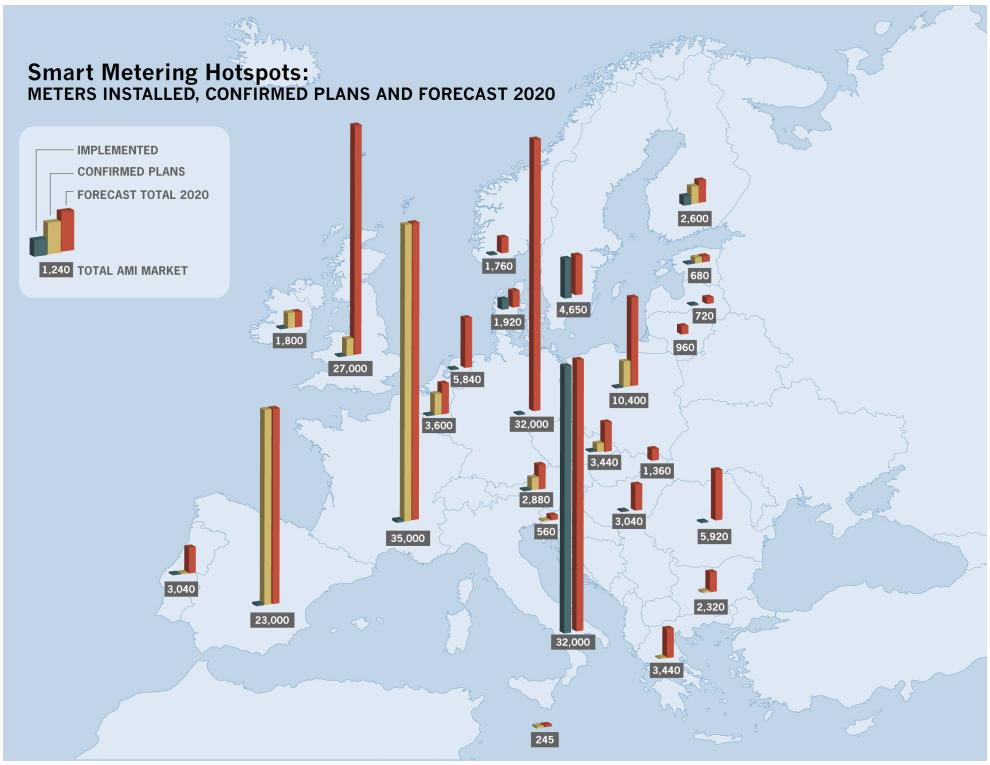

Figure 3.2: *European Smart Metering Hotspots: Meters Installed, Confirmed Plans & 2020 Forecast.*

is represented in Fig. 3.2). On the basis of ambitious plans announced by utilities and regulators in France, Spain, the U.K. and a gradual rollout in other European member states, GTM Research forecasts an additional 100 million smart meters will be installed between now and the end of 2016.

3.3 State of the Art

In this Section the main aim is the definition of **Appliance Load Monitoring** problem and the distinction between different existing approaches in this field of interest.
Our system is, indeed, an Appliance Load Monitoring System. With the term Appliance Load Monitoring (ALM) System is indicated a system that has to provide the individual consumption of the appliances existing in a generic environment.
As illustrated in Fig. 3.3 there are a lot of devices (appliances) as vacuum cleaners, lamps, hair dryers, mixers, electric whisks, washing machines, within a generic environment, that are connected in parallel through the wire cables of the environment. An ALM System, as just introduced, has the aim of providing the user with the consumption of the individual devices. For example an ALM System applied in the context of Fig. 3.3 has to continuously monitor the consumption of the washing machine, mixer, hair dryer, lamp and vacuum cleaner. The main point

Figure 3.3: *Simplified model of an environment within different devices.*

of the State of the Art is the identification of the appliance signature to provide the energy monitoring of the individual appliances.
A **Signature** can be defined as a measurable parameter of the load that gives information about its nature or its operating states.
Fig. 3.4 reports a modified version of a picture that initially appeared in [5] to organize the different possible approaches to ALM, the distinction is made by using the existing differences in

term of appliance signatures.
The signatures, as represented in Fig. 3.4, are mainly divided between intrusive or non intrusive. The first type of signature requires some form of physical or electrical intrusion in each electrical device, it is a form of direct sensing that needs a more complex hardware but a simpler software than the non-intrusive approach. This approach is also quite expensive because of the requirement of, at least, one sensor per device. The systems based on this type of signature are called Intrusive Appliance Load Monitoring (IALM). Referred to environment of Fig. 3.3, an IALM System implies, at least, 5 sensors (one sensor inside every represented device).
One example of intrusive methods is based on Physically Intrusive Signature. It is a technique, requiring a brief physical intrusion, called tag. Various devices can be constructed which are attached to an appliance during a single initial intrusion and then generate a signal whenever it operates. For example, a device can be designed which generates a certain current harmonic, or which injects a radio frequency signal on the power line whenever the appliance consumes power.
The non-intrusive methods do not require any modification of the electrical devices. This type of system are indicated with the term Non Intrusive Appliance Load Monitoring and in literature both NILM and NALM terms are used to call this kind of approach. These systems gather data by passively monitoring the normal operation of the total load.
In Fig. 3.3, to create a NILM System, a single sensor unit has to be added in parallel to the devices. The sigle sensor unit is located at a central measurement point and monitors the total consumption of the appliances in the environment.
The main distinction between Non Intrusive and Intrusive signatures is really important because in the first case only a single point of measurement is required and the signatures are referred to the total load measured in this point, in the second case of Intrusive signatures a lot of point of measurements (at least the same number of the existing devices) are required and the signatures are extracted features of the individual device.
The first NILM (Non Intrusive Load Monitoring) system was developed by George Hart at the MIT during 1980s, he patented the system in 1989 and wrote a paper [5] with the main principles of NILM in 1992 (starting point of NILM technology).
In the case of NILM System the signatures assume an important meaning because they are the features that different methods use to enable the detection of different loads by looking only at the total load.
Usually NILM methods have available the total current and voltage, so, the raw current and voltage waveforms are transformed into a feature vector (signature vector), a more compact and meaningful representation that may include real power, reactive power, and harmonics.
Indeed NILM systems look at particular signature of the total load and then they perform **Energy Disaggregation**.
Energy Disaggregation allows to take a whole building (aggregate) energy signal, and separate it into appliance specific data (monitoring of energy consumption of individual appliances).
There are different methods within the non-intrusive approach, some of them look at the steady state signatures that means they look at the appliance state change that is continuously present in the load as it operates, other at the features during the brief time of state transition (transient signatures).

The transient-based algorithms consider the electrical transient of the device as signature [6, 7, 8, 9, 10].
The term electrical transient refers to the momentary event preceding the steady state, it happens during a sudden change of the state of the device. Indeed when a device is turned on or off, characteristic oscillations in term of voltage and current signal may occur, they depend on the inner structure and the operation mode of the device so they permit to provide energy disaggregation.
The problem of this type of approach is that, in a lot of cases, the electrical transient exists only when a device is switched on, and does not occur when is switched off.
On the other side, the steady state approach focuses on the analysis of the steady state condition. With the term steady state is indicated the equilibrium condition of a device in term of voltage and current that occurs after the end of the transient. This type of signatures enables the estimation of power consumption by looking at the difference between steady-state properties of operating states. An important distinction between transient and steady-state signatures is that the second are additive while the first are not.
The steady-state approach includes methods using different signatures (Fig. 3.4), the majority of these methods consider the complex admittance ([5, 11, 12, 13, 14, 15]). As signature, the admittance is preferred to power and current because it is a voltage-indipendent property of a linear device and, also, an additive property when appliances are connected in parallel. We also focus on this type of approach (Section 3.6) because it seems to be more stable and much easier to detect than momentary indications of the transient, also because the processing requirements are far less demanding.
There are a lot of relevant publications on energy disaggregation. Two interesting papers about the State of the Art of NILM are [16] and [17] that present the most important works on this field in the last years.

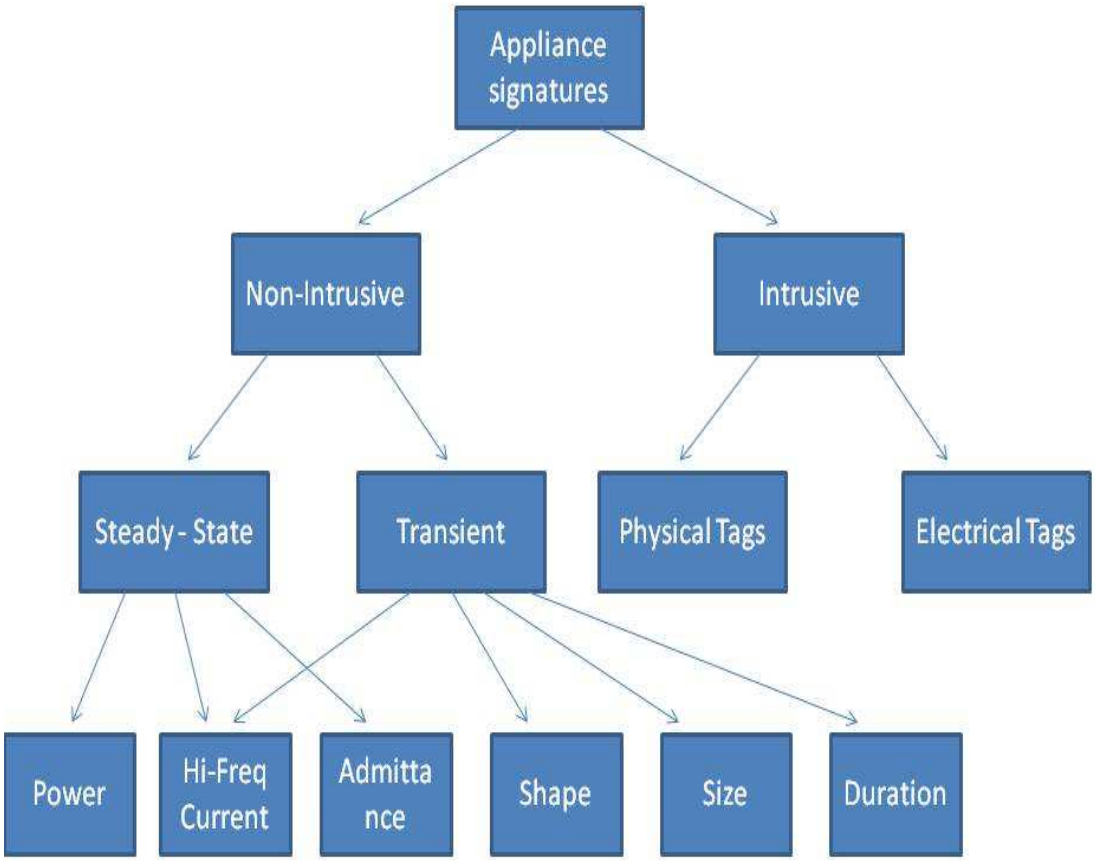

Figure 3.4: *Signature Taxonomy. Classification of energy disaggregation algorithms.*

3.4 Voltage based techniques and Current based techniques

State of the art most of centralized NILM methods for disaggregating the consumed electrical energy involve both a current meter, which measures the total current, and a voltage meter, which measures the mains voltage.
Indeed most of NILM methods reported in Section 3.3 have available both current and voltage signals and they use as signature the admittance of steady-state. They divide the overall current by the overall voltage and they obtain the complex admittance of the system. After that the power can be expressed as:

$$P(k) = V_{ref}^2 \sum_{n=1}^{N} Y_n(k), \tag{3.1}$$

where $Y_n(k), n = 1...N$ are the admittance of the N appliances ON at the period k and $V_{ref} = 230V$ is the nominal value of the voltage in the EU.
The installation of the current meter is not a trivial task, usually the process to install the current probe requires to dismantling the breaker box and clamp the probe around the main power feed conductors, for this reason building codes typically requires that the current probes have to be installed by a licensed electrician.
The technical intervention is required to install a current clamp: a current clamp is an electrical device having two jaws which open to allow clamping around an electrical conductor. This allows properties of the electric current in the conductor to be measured, without having to make physical contact with it, or to disconnect it for insertion through the probe.
At the state of the Art there are some approaches that use only the analysis of the voltage signal to avoid the use of the current clamp. In particular [18], [19] analyse a different way to detect different devices through the electrical voltage noise.
These works are based on the possibility to recognize, when a device is turned on, different type of voltage noise at different frequencies.
Indeed, in [18], Patel et al. have proposed an innovative way in the field on NILM. The approach presented in [18] uses only a single plug-in sensor to detect the electrical noise created by abrupt switching of electrical devices, the system needs to perform the FFT of the voltage noise to use it as signature. The main problem of this type of approach, as also Patel has underlined in his recent work [19], is that is based on the analysis of the transient noise that is not easy to detect unambiguously and the computational complexity is expensive. The transient events do not occur always and the signature seem to depend on the household wiring.
The last work of Patel [19] proposes a different approach but anyway based on the voltage analysis.
The approach takes into account that there are mainly three class of devices in the household:

1. Purely resistive loads, such as a lamp or an electric stove, that don not create detectable amounts of electrical noise;

2. Inductive loads as motors that create voltage noise synchronous to the AC power of 50 Hz (Europe);

3. Solid state switching devices, such as MOSFETs found in computer power supplies, that emit noise synchronous to an internal oscillator;

The last article [19] proposes a new solution to automatically detecting and classifying the use of electronic devices that emit noise synchronous to an internal oscillator (third category) by using a system called ElectriSense. This system senses the electromagnetic interference (EMI) created by switched-mode power supply (SMPS) oscillators.
SMPSs are electronic power supplies that incorporate a switching regulator to convert electrical power efficiently, these power supplies continuously generate high frequency electromagnetic interference (EMI) during operation. [19] shows that EMI signals are stable and predictable based on the device's switching frequency characteristics, so they can be considered as a signature that can be sensed and identified throughout a typical home during device operation.
The relevant part of [19] consists in the discovery that these signatures are largely specific to a device's circuit design and maintain consistent properties across homes. Moreover, they use the *continuous noise* signature so they can identify devices that don not generate transients such as those with " soft switches" and transient suppressors. With this work they have found a complementary approach to the previous [18], it is supposed to be not in competition because they are regarding different type of loads (inductive loads [18]/ solid state switching devices [19]).
This system represents an innovation point in NILM's field but it lets several questions open that I will analyse in the Chapter 6 of this Master's Thesis. Indeed we have also performed an investigation about high frequency signatures of the voltage (Chapter 6) that seems to confirm the perplexities that, for instance [17], has already exposed.

3.5 Voltage Regulation

3.5.1 Voltage quality

Section 3.4 argues about methods that consider available only the voltage information. Also our method enables energy disaggregation by using only the voltage signal.
For this reason, before to provide a detailed description of our method, some parameters that characterize the quality of the voltage signal are reported in this Section. Voltage quality (VQ) parameters are listed and defined in the European standard EN 50160, which is applicable in all EU member states for low and medium voltage networks (i.e. up to 35 kV).
Usually the important parameter of VG are the following:

1. Supply voltage variations;
2. Rapid voltage changes;
3. Flicker severity;
4. Supply voltage unbalance;
5. Harmonic voltages;

6. Interharmonic voltages;
7. Main signalling voltage on the supply voltage,
8. Supply voltage dips;
9. Supply voltage swells;
10. Transient overvoltages;
11. Frequency variation limits.

The first seven disturbances are mainly caused by the characteristic of the customers' appliance. Voltage quality disturbances can be grouped in two types (distinction made in the textbook [25]):

- *Voltage variations*, i.e. small deviations from the nominal or desired value that occur continuously over time. Voltage variations are mainly due to load pattern, changes of load or nonlinear loads. Supply voltage variations, voltage fluctuations leading to flicker, voltage unbalance, harmonic and interharmonic voltages are all examples of voltage variations.
- *Voltage events*, i.e. sudden and significant deviations from normal or desired wave shapes. Rapid voltage changes, supply voltage dips, swells and transient over voltages are among the most important voltage events, apart from interruptions that are the best-known example of a voltage event. Opposite to voltage variations that occur continuously over time, voltage events only happen every once in a while. They have to be identified through continuous monitoring. Monitoring of events takes place by using a "trigger" that starts when voltage exceeds a given threshold. For instance, voltage dips are identified when the voltage (RMS value) goes below the "dip threshold" that is currently set at -10 % of nominal or declared voltage level.

The distinction between voltage variations and voltage events is very relevant from the regulatory viewpoint:

- Voltage variations are the "physiology" of the network functioning, in fact they are part of the normal functioning of the network. Since electrical equipments are designed to work optimally at the nominal value and with an ideal sine wave, voltage variations have to be kept as small as possible. For instance, keeping voltage magnitude close to nominal value with power factor close to unity is strictly related to having less electricity losses. Voltage variations outside predefined limits may lead to severe problems for customers;
- Voltage events represent the "pathology" of the network functioning and are of large concern for end-use equipment. Voltage events are to be treated with stochastic approaches because they are considered as undesired accidents.

In particular we are interested in the impact of the Voltage variations on the execution of the algorithm because these are continuously present in the network and their presence can influence the sensitivity of the method.
A deep explanation of these parameters can be found in [2o], and the paper [21] provides an interesting overview of the regulation of Voltage quality.

3.5.2 Voltage frequency

The fundamental frequency, or utility frequency, is the frequency at which alternating current (AC) is transmitted from a power plant to the end user.
The fundamental frequency in Europe is 50 Hz, in the North America and in some area of Japan is 60 Hz. There are several reasons to keep the frequency stable and to make this happens it is necessary a perfect balance between produced and consumed electric power. The frequency grows up if the consumed electric power is less than that produced because the power supply works faster when the consumption of power is lower [22].
The synchronous time is the measured time when the network works at the fundamental frequency. 50 oscillations of the current AC correspond to 1 s of synchronous time. If the frequency is lower than 50 Hz the 50 oscillations take more time. One second of synchronous time always correspond to 50 oscillations and so it can be longer or shorter in function of the variation of the fundamental frequency. Usually the drift of the synchronous time is monitored by evaluating the difference between itself and the universal time. Each drift of the synchronous time is balanced, if the duration of the drift is longer than 20 s it is changed the fundamental frequency of the network as following:

- 49.99 Hz if the synchronous time is bigger than the universal time;
- 50.01 Hz if the synchronous time is smaller than the universal time.

The previous considerations are reported because when for the first time we have tried to look at the phase component of the supplied voltage a drift in the phase come out as explained in Section 2.5.

3.5.3 Today's voltage quality limits and values in Europe

This subsection assesses the progress made in Europe and in particular in Italy and in the Netherlands with regard to voltage quality regulation. The already cited EN 56160 gives the main definitions and characteristics of the supply voltage at the customer's terminals in public low and medium voltage networks. It is the main technical norm for the voltage quality in Europe while, there are other norms and reports as reported in IEC 61000. This last example includes limits for voltage disturbances, immunity and emission limit for electrical equipment (user's side explained in Section 2.3).
The voltage quality is defined in EN 61000-2-2 (VDE 0839 part 2-2) in public low voltage systems. The valid compatibility levels for industrial systems are given in EN 61000-2-4 (VDE 0839 parts 2-4).
In Italy the energy regulator or authority only set in place minimum quality standards. There is (currently) no regulation for voltage quality but the authority undertake steps to establish such a system in future. To this end the regulator's strategy is to first get a better understanding of existing voltage quantity levels and to collect reliable data. With this aim, at the beginning of 2006, the authority launched a voltage quality measurement action by the installation of voltage quality meters at strategic locations.

In Italy, Norway, Portugal and Czech Republic there are voltage quality monitoring systems at both transmission and distribution level and Hungary only in the distribution system. Spain and Sweden are at a proposal stage for continuously monitoring system for voltage quality.
Even if these monitoring systems are different from each other in many respects, a common point is that at least short and long interruptions, voltage magnitude, voltage dips and harmonic distortion of the voltage waveform are monitored. The number and location of voltage recorders is quite different from one country to another.
The availability, in coming years, of voltage quality data on both transmission and distribution grids will not only allow a deeper knowledge of actual voltage quality levels, but is also likely to enable regulators to define action plans to improve voltage quality and to set standards in the interest of consumer protection.
To understand better the actual limits in term of quality voltage in the different European countries [23] is suggested.

3.6 Novel method at 50 Hz

The reasons behind our work are, on one side, the increasing interest in energy consumption (Section 3.2), on the other, the will of providing the users with energy disaggregation in the easiest way.
In our research project, we have developed a novel technology that enables insight the electricity consumption on an appliance level via an extremely simple installation. The energy monitoring is achieved by a single point of measurement of the voltage in every electrical branch circuit of an environment.
The novel method presented in this Master's Thesis is innovative, because it is based only on the evaluation of the voltage signal at 50 Hz.
This method mainly differs from [19] because [19] works on high frequency components of the voltage signal, and these are used only to identify the switching on/off of the devices. Our method permits to measure the energy consumption of the different individuals appliances and it does not require high sampling rates like [19].
Ideally the voltage signal should be constant, the idea of using voltage-signal to provide energy monitoring seems counter-intuitive. Instead of this, the voltage signal changes in function of the total load on in the network. When a new device is switching on a drop in term of voltage happens; the steps depend on the electrical equivalent network and on the power of the appliance that is turned on.
So the novel method is based on the idea that when a load is switching on this leads a voltage drop that allows, knowing the relation between the delivered voltage and the impedance of the network, to determine which appliance is switching on and quantify the appliance's real power.
The method works with the assumption that it is possible to estimate the ratio between the delivered voltage and the impedance of the network, for this purpose a load of known impedance is used as additional information. Indeed, when a step in term of voltage is recognized, by turning on/off the reference load it is possible to establish the link between change in admittance (known parameter) and change in voltage (measured parameter).

Table 3.1 reports a summary about different approaches (modified version of a table in [19]). The last column is referred to our method, advantages and limitations are not reported because there will be discussed in Chapter 7.

3.7 Detail Description of Voltage Disaggregation Method

Our method requires the following elements:

- a voltage probe, to measure the mains voltage at regular time intervals;
- buffer memory, to store a few values of the measured voltage;
- a means to send the measurement result to the buffer memory;
- signal process unit, to perform energy disaggregation;
- a switchable device of known impedance with mainly resistive behaviour;
- a controller for switching on/off that switch load, either at regular intervals, or when asked for by the processing unit.

The following explanation of the method assumes to use the phasor notation for the voltage signal.
A basic ideal model of the system, is depicted in Fig. 3.5. In this model it is assumed that the losses in the network between different appliances are negligible, so that all the appliances have the same mains voltage. Devices numbered 1 through N are connected in parallel. Each device is represented by its admittance Y_n, $n = 1 \ldots N$ and may be switched on or off.

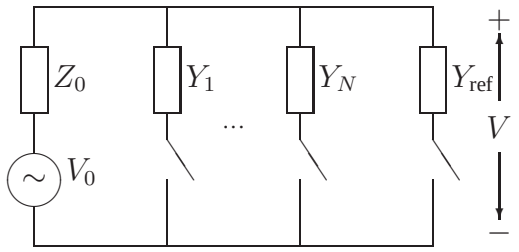

Figure 3.5: *The basic electrical network model.*

Notation:

- V_0: delivered voltage;
- Z_0: internal impedance of the network;
- $Y_{\text{i}}, i = 1, .., N$: admittance of the unknown devices;

Extractable features	Real/Reactive Power	Apparent Power from $\|I_{AC}\|$	Harmonics of $\|I_{AC}\|$	Startup of $\|I_{AC}\|$	$\|V_{AC}\|$	Transient voltage noise signature	Continuous voltage noise signature	Our method
Sensing hardware	smart meters capable of medium-rate sampling	Current clamps or inductive sensors	Current clamps or ammeters	Current clamps or ammeters	Voltmeter rate voltmeter	High-sampling rate voltmeter	Medium sampling	Voltmeter
Disaggregation level	Device category	Large load category	Large load category	Large load startup detection	Large load with mechanical switches	Individual devices utilizing SMPS	Individual devices category	Large load
Installation	Breaker or meter inline ammeter with voltmeter	Breaker with voltmeter inline ammeter or affixed outside	Breaker or meter in line, or affixed outside	Breaker or meter in line, or affixed outside	Plug-in anywhere	Plug-in anywhere	Plug-in anywhere	Plug-in anywhere
Ease of physical installation excluding calibration	Very Difficult	Current clamps: Difficult Inductive sensors: Easy	Difficult	Difficult	Very Easy	Very Easy	Very Easy	Very Easy
Ease of calibration	Very Easy	Difficult	Difficult	Easy	Very Difficult	Easy	Very Easy	Very Easy
Cost	Very high	Low	Medium	Medium	Very low	Very high	High	Low
Advantages	Automatic categorization of certain loads, loads, works well for appliances	Simple, enables central database of signatures, reduce per-home calibration	Discriminates among devices with similar current draw	Discriminates among devices with similar current draw and startup characteristics	Simplicity and cost signature, independent of load characteristics	Nearly every device has observable independent of load	Stable signatures among homes and devices	
Limitations	I and V must be sampled synchronously	Few devices with diverse power draws	Limited to large inductive loads that distort AC line, loads must be synchronous to 60 Hz	Limited to loads with diverse, long duration startup characteristics like motors and some CFLs	Few devices affect VAC line, susceptible to line variations	Requires per-home calibration, requires fast sampling (1-100 MHz)	Requires medium sampling rate (50 - 500 kHz)	

Table 3.1: *Summary of the different technologies*

- Y_{ref}: known admittance of the switchable reference device (main resistive device under our control).

The voltage V is equals to:

$$V = \frac{V_0}{1 + Z_0 Y}, \tag{3.2}$$

where Y is the sum of the admittances of the active devices. Assuming that the network parameters V_0 and Z_0 are stable, a change in the observed voltage V can be attributed to a change in the total admittance. From (3.2) it follows that the change in V^{-1} is directly proportional to the change in total admittance:

$$\Delta \left(\frac{1}{V} \right) = \frac{Z_0}{V_0} \Delta Y. \tag{3.3}$$

In order to determine the coefficient of proportionality the method switches the known admittance on or off and measures the corresponding change in inverse voltage $(\Delta V^{-1})_{\text{ref. on}}$ or $(\Delta V^{-1})_{\text{ref. off}}$. Then Z_0/V_0 is estimated as

$$\frac{V_0}{Z_0} = \frac{Y_{\text{ref}}}{(\Delta V^{-1})_{\text{ref. on}}} \text{ or } -\frac{Y_{\text{ref}}}{(\Delta V^{-1})_{\text{ref. off}}}. \tag{3.4}$$

The admittance Y_{L} of the load switching on and generating the change in total admittance ΔY can be then estimated as

$$\hat{Y_{\text{L}}} = \Delta Y = Y_{\text{ref}} \frac{(\Delta V^{-1})_{\text{Y}}}{(\Delta V^{-1})_{\text{ref}}}. \tag{3.5}$$

with $(\Delta V^{-1})_{\text{Y}_{\text{L}}}$ the variation in inverse voltage due to the new load.
In our method the estimated changes in admittance ΔY (4.23) are available and it is possible to estimate the total complex power at the period k as:

$$P(k) = V_{RMS}^2(k) \sum_{n=1}^{N} \Delta Y, \tag{3.6}$$

where V_{RMS} is the actual value of the voltage (non the reference voltage) and $\Delta Y, n = 1, ..., N$ are the estimated change in term of complex admittance until the period k.
The actual value of the voltage signal is the value that corresponds to the load turned on, in the case of the switching on of the device the V_{RMS} value is the RMS value after the switching, in the case of the switching off of the device the V_{RMS} value is the RMS value before the switching.
We can also provide Power Disaggregation because we can disaggregate the total power consumption into different contributes. By checking the single step it is possible to estimate the change in term of power due to the turning on of a device m (with admittance Y_{m}) as:

$$P_{\text{m}} = V_{RMS}^2(k) Y_{\text{m}}. \tag{3.7}$$

The energy consumed by the generic appliance m can be finally estimate as:

$$E_{\text{m}} = \sum_{k=switch\,on}^{switch\,off} P_{\text{m}}. \tag{3.8}$$

In Fig.3.6 a simplified electrical network, with only one switchable unknown device Y_{x}, is represented. In the following part the step in term of measured voltage are reported to understand better the voltage method. As an initial hypothesis is assumed that the voltage probe senses the

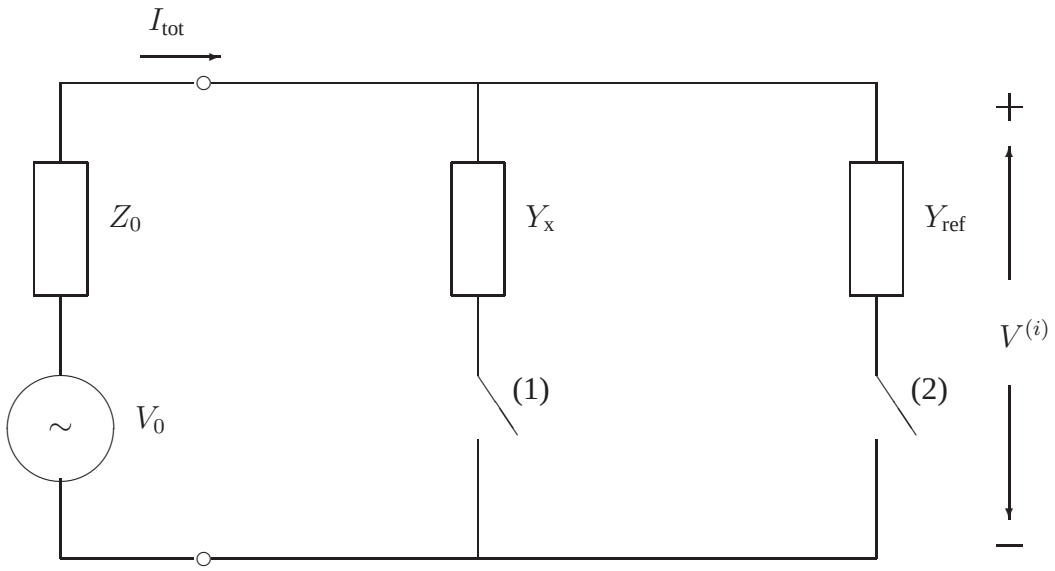

Figure 3.6: *A basic electrical network model.*

voltage across the reference load because the important part of the novel method is the estimation of the existing equivalent electrical network. This estimation takes place by turning on/off the reference load so it makes sense to put the voltage sensor in parallel with the reference load. In view of a real application for energy monitoring, we envision a device that includes the reference load and the voltage probe in a single unit. This unit could be placed in any electrical socket.
The steps of the voltage method are composed of measurements of the voltage in three different situations:

- $V^{(0)}$: measured voltage when both switch (1) and switch (2) are open that corresponds to the situation no load is on
$$V^{(0)} = V_0; \tag{3.9}$$
- $V^{(1)}$: measured voltage when switch (1) is closed and switch (2) is open that corresponds to the situation in which a new unknown device is turned on
$$V^{(1)} = V_0 - Z_0 I_{\text{tot}} = V_0 - Z_0(V^{(1)} Y_{\text{x}}) \tag{3.10}$$
$$\Rightarrow\ V^{(1)} = \frac{V_0}{(1 + Z_0 Y_{\text{x}})}; \tag{3.11}$$
- $V^{(2)}$: measured voltage when both switch (1) and switch (2) are closed that corresponds to the situation both reference load and unknown device on
$$V^{(2)} = V_0 - Z_0(V^{(2)} Y_{\text{x}}) - Z_0(V^{(2)} Y_{\text{ref}})$$

$$\Rightarrow\ V^{(2)} = \frac{V_0}{(1 + Z_0\,(Y_{\text{x}} + Y_{\text{ref}}))}. \tag{3.12}$$

When the measurements regarding the three different conditions are available, the algorithm can estimate the network parameters by evaluating:

$$I_0 \triangleq \frac{V_0}{Z_0} = \frac{Y_{\text{ref}}}{\left(\frac{1}{V^{(2)}} - \frac{1}{V^{(1)}}\right)}. \tag{3.13}$$

After the estimation of the ratio $\frac{V_0}{Z_0}$ that models the existing equivalent electrical network, it is possible to estimate the unknown load as:

$$Y_{\text{x}} = \frac{V_0}{Z_0} \cdot \left(\frac{1}{V^{(1)}} - \frac{1}{V^{(0)}}\right). \tag{3.14}$$

The method monitors the voltage signal, maps voltage changes in admittance changes, from the change in admittance derives the changes in term of power and so it estimates the energy consumption of the different devices of the environment.

Chapter 4

System Design

4.1 General

Chapter 4 defines the design of the system by keeping into account different types of losses: on one side the losses given by cable, on the other the losses given by the noise that afflicts all the measurements.
This Chapter has as aim the research of the optimal position of the voltage sensor, reference load and unknown devices and also the research of the best value of the reference device and the range of possible appliances that the method can correctly estimate. After the determination of all these requirements the Chapter includes a possible implementation of the different steps of the method.
Chapter 4 is organized as follows: Section 4.2 discusses the optimal position of the voltage sensor by also keeping into account the possible losses and their influence in the execution of the algorithm, Section 4.3 develops our method in a generic network, Section 4.4 reports an analysis about the influence of the crosstalk in our system, Section 4.5 evaluates theoretically how the voltage noise introduces, in first approximation, error in the estimation, Section 4.6 defines the range of detectable appliances and also includes some suggestions for the design of the reference device, Section 4.7 focuses on the monitoring phase (how the voltage is monitored) and the initialization phase (estimation of the equivalent network) of the algorithm, Section 4.8 argues about the detection of jumps in term of RMS value and phase information, Section 4.9 explains the overall solution implemented in our DEMO and the possible implementation of our technology in a practical environment, finally Section **??** reports the proposed final solution that includes a voltage sensor for every electrical branch circuit of an household (MIMO system).

4.2 Sensor Position

In the present Section the goal is finding the best position for the voltage sensor, that is also the reference's position, in a practical context.
In the following analysis I introduce the possible losses of the cables, that exist in a generic environment, are taken into account and argued. It is necessary to take into account these losses,

as shown in Fig. 4.1, and estimate how they affect the performance of this NALM approach. The

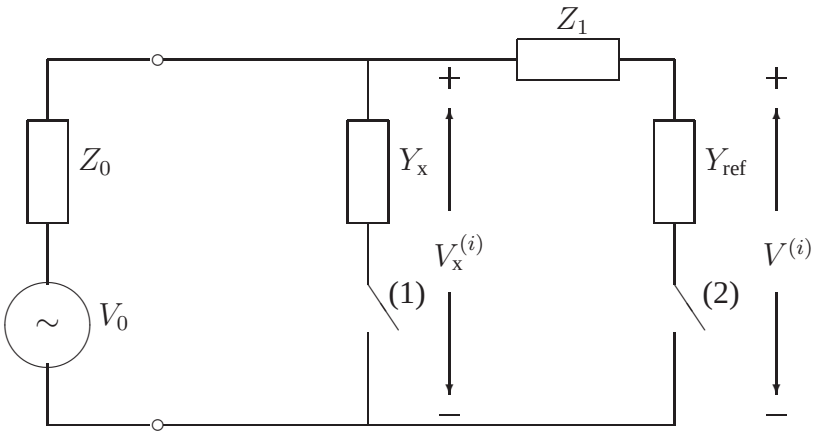

Figure 4.1: *Network model with cable losses. Configuration 1: the reference load is placed after the unknown load(s).*

mathematical expression of a generic impedance of a copper cable has been already discussed in Section 2.3.
We have analysed two different configurations:

- Configuration 1: Reference load is placed after the unknown load(s) (Fig. 4.1);
- Configuration 2: Reference load is placed before the unknown load(s) (Fig. 4.2).

We start with the theoretical analysis of Configuration 1. In this first analysis a wire cable, placed between reference and unknown device, has been considered and represented with an impedance Z_1 (2.5) (see Fig. 4.1).
The voltage $V^{(0)}$ of (3.9) and $V^{(1)}$ of (3.10) does not depend on Z_1.
The wire impedance Z_1 affects the measured voltage $V^{(2)}$ of (3.12) because the copper line and the reference load in series creates a voltage divider. Applying the Ohm's Law it is found that:

$$V^{(2)} = \frac{Z_{\text{ref}}}{Z_{\text{ref}} + Z_1} \cdot V_{\text{x}}^{(2)} \tag{4.1}$$

in which:

$$V_{\text{x}}^{(2)} = \frac{V_0}{(1 + Z_0(Y_{\text{x}} + Y))}, \tag{4.2}$$

where $Y = \frac{Y_{\text{ref}}}{1+Z_1 Y_{\text{ref}}}$.
Finally $V^{(2)}$ can be expressed as:

$$V^{(2)} = \frac{Z_{\text{ref}}}{Z_{\text{ref}} + Z_1} \cdot \frac{V_0}{(1 + Z_0(Y_{\text{x}} + Y))}. \tag{4.3}$$

It is interesting to consider how the equivalent estimated network is conditioned by the change of $V^{(2)}$:

$$\widehat{\left(\frac{V_0}{Z_0}\right)} = \frac{Y_{\text{ref}}}{\left(\frac{1}{V^{(2)}} - \frac{1}{V^{(1)}}\right)}. \tag{4.4}$$

Focusing on the denominator:

$$\left(\frac{1}{V^{(2)}} - \frac{1}{V^{(1)}}\right) = \left(\frac{Z_1}{Z_{\text{ref}}}\frac{(1+Z_0Y_{\text{x}})}{V_0} + \frac{Z_{\text{ref}}+Z_1}{Z_{\text{ref}}} \cdot \frac{Z_0 Y}{V_0}\right). \tag{4.5}$$

The copper line impedance, instead of being irrelevant, can leads to a significant change in the ratio concerning the estimated network:

$$\widehat{\left(\frac{V_0}{Z_0}\right)} = \frac{1}{\left(\frac{Z_1}{Z_0}(1+Z_0Y_{\text{x}}) + \frac{Z_{\text{ref}}+Z_1}{Z_{\text{ref}}}\frac{1}{1+Z_1Y_{\text{ref}}}\right)}\frac{V_0}{Z_0}. \tag{4.6}$$

Since $\frac{Z_{\text{ref}}+Z_1}{Z_{\text{ref}}}\ \frac{1}{1+Z_1Y_{\text{ref}}} = 1$, this permits to write:

$$\widehat{\left(\frac{V_0}{Z_0}\right)} = \frac{1}{\left(1 + \frac{Z_1}{Z_0}(1+Z_0Y_{\text{x}})\right)}\frac{V_0}{Z_0}\ . \tag{4.7}$$

The denominator results relevant and it changes the estimated admittance in the following way:

$$\widehat{Y}_{\text{x1}} = \frac{Y_{\text{x}}}{(1+\frac{Z_1}{Z_0}(1+Z_0Y_{\text{x}}))} \tag{4.8}$$

The analysis proceeds with Configuration 2: the reference load is placed, and therefore the voltmeter, before the unknown load as shown in Fig. 4.2. The measured voltage changes as follows:

$$V^{(0)} = V_0, \tag{4.9}$$

$$V^{(1)} = \frac{V_0}{(1+Z_0Y)} \tag{4.10}$$

where $Y = \frac{Y_{\text{x}}}{1+Z_1Y_{\text{x}}}$,

$$V^{(2)} = \frac{V_0}{(1+Z_0(Y_{\text{ref}}+Y))}. \tag{4.11}$$

This type of network enables to correctly estimate the ratio $\frac{V_0}{Z_0}$ and determines the following estimation of the unknown load:

$$\widehat{Y}_{\text{x2}} = \frac{Y_{\text{x}}}{(1+Z_1Y_{\text{x}})}. \tag{4.12}$$

Looking for the relative error:

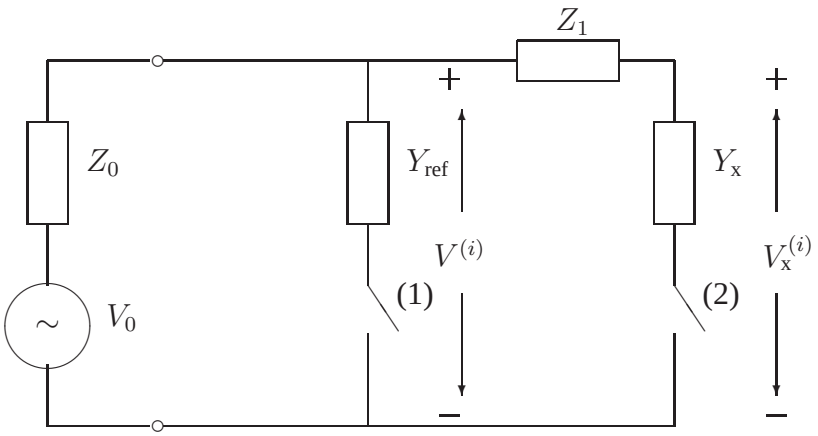

Figure 4.2: *Network model with cable losses. Configuration 2: the reference load is placed before the unknown load(s).*

- Z_0 does not appear in the estimated admittance of Configuration 2 (see (4.12)). This is definitely a positive point of this configuration that makes it more desirable than Configuration 1 (see (4.8)). In particular because usually Z_0 is a small number, for example in the performed experiments we have found an estimated value of Z_0 equals to 0.5 Ω, easily it could be comparable with the impedance of the wire cable if this last one has also a limited length (for instance a wire cable of twenty meters).
  Usually Z_0 and Z_1, in real context, could be comparable and so they lead to a wrong estimation in Configuration 1 (see (4.8));

- $Z_1 Y_{\text{x}}$: this error term is present in both the settings.
  This suggests that, with cables of the same length, better performances will be obtained in the estimation of loads with the largest impedance.
  However, the error can be limited by using cables of limited length (below fifty meters they don't give relevant problem) because usually the total admittance multiplied by the impedance of the cables is a small number that can be considered irrelevant for the performances.

Comparing the estimated admittance (4.8) with (4.12):

$$\frac{Y_{\text{x}}}{\left(1+\frac{Z_1}{Z_0}(1+Z_0 Y_{\text{x}})\right)} < \frac{Y_{\mathbf{x}}}{(1+Z_1 Y_{\text{x}})}, \tag{4.13}$$

the admittance of Configuration 1 is underestimated compared to the resultant admittance of Configuration 2.

Definition 3 (Absolute Error) *The absolute error is the magnitude of the difference between the exact value and the approximation. Given some value v and its approximation v_{approx}, the absolute error is*

$$\epsilon = |v - v_{approx}|. \tag{4.14}$$

Definition 4 (Relative Error) *If $v \neq 0$ the relative error is*

$$\eta = \frac{|v - v_{approx}|}{|v|} = \left| \frac{v - v_{approx}}{v} \right|. \tag{4.15}$$

The relative error of Configuration 1 (calculated by using the Def. 4) is definitely bigger that the relative error of Configuration 2 (the comparison is reported in (4.16)). Furthermore, in real cases of interest, Configuration 1 could underestimate the load if Z_1 assumes values comparable with Z_0, this could lead to a completely wrong estimation of the appliance.
After this analysis we propose as solution for the system design to locate a single device including reference load and measuring instruments as close as possible to the voltage source to sense all the appliances placed after the sense unit.
The relative error of the two configuration is composed as follows:

$$\eta_1 = \frac{\left(\frac{Z_1}{Z_0}(1 + Z_0 Y_L)\right)}{\left(1 + \frac{Z_1}{Z_0}(1 + Z_0 Y_L)\right)} > \frac{Z_1 Y_L}{(1 + Z_1 Y_L)} = \eta_2. \tag{4.16}$$

4.3 Voltage Disaggregation in a Generic Network

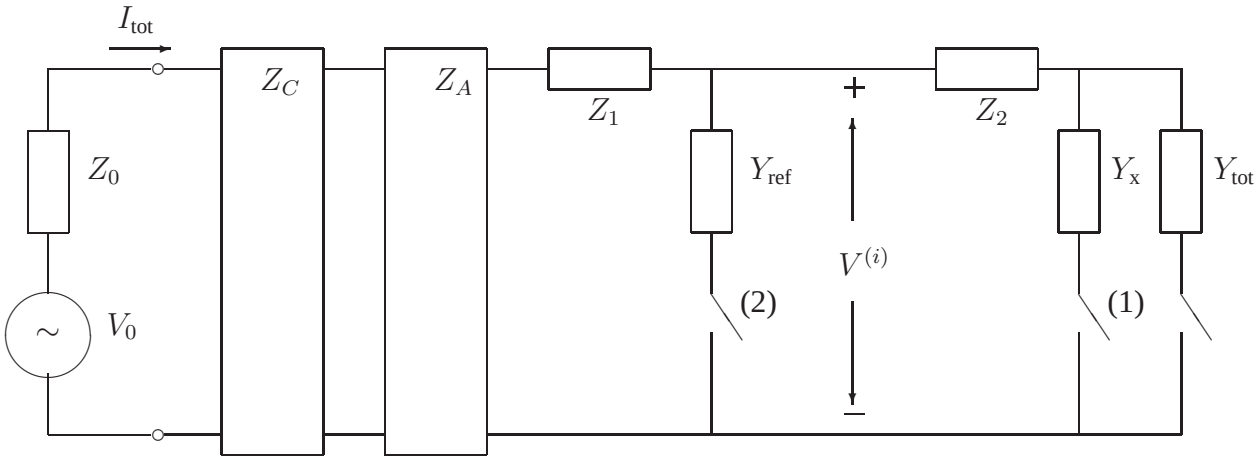

Figure 4.3: *Model of the network within circuit breakers. Focus on a single electrical branch circuit.*

In the following part the different steps of the algorithm are reported as in Section 2.2, in this case they keep into account the presence of the circuit breakers, of more than one appliance active in the electrical branch circuit, and of cables between different appliances.
The steps are developed by assuming to work on the optimal configuration of Section 4.2 with the reference load as close as possible to the voltage source.
The following analysis considers:

- only a reserved electrical branch circuit;
- the Configuration 2 (best configuration for the execution of the method);
- the presence of the miniature circuit breakers;
- more than one device active in the electrical branch circuit;
- wire cables between different devices.

(3.9),(3.10),(3.12), in the explained context, change in the following way:

$$V^{(0)} = \frac{V_0}{(1 + (Z_0 + Z_C + Z_A + Z_1)Y^{(0)})}, \tag{4.17}$$

$$Y^{(0)} = \frac{Y_{\text{tot}}}{1 + Z_2 Y_{\text{tot}}} \tag{4.18}$$

Y_{tot} is the total admittance that the instrument detects on its right (it includes also the impedances of the cables between different appliances).

$$V^{(1)} = \frac{V_0}{1 + (Z_0 + Z_C + Z_A + Z_1)Y^{(1)}}\ , \tag{4.19}$$

where:

$$Y^{(1)} = \frac{Y_{\text{tot}} + Y_{\text{x}}}{1 + Z_2(Y_{\text{tot}} + Y_{\text{x}})}, \tag{4.20}$$

and finally

$$V^{(2)} = \frac{V_0}{1 + (Z_0 + Z_C + Z_A + Z_1)(Y_{\text{ref}} + Y^{(1)})}. \tag{4.21}$$

The ratio concerning the estimation of the network is correctly determined in this way and the estimation of the admittance of the new load switched on can be expressed as:

$$\widehat{Y_{\text{x}}} = Y^{(1)} - Y^{(0)} = \tag{4.22}$$

$$= \frac{Y_{\text{x}}}{(1 + Z_2(Y_{\text{tot}} + Y_{\text{x}}))(1 + Z_2 Y_{\text{tot}})}. \tag{4.23}$$

So the relative error is:

$$\eta = \frac{Z_2(2Y_{\text{tot}} + Y_{\text{x}} + Z_2 Y_{\text{tot}}(Y_{\text{tot}} + Y_{\text{x}}))}{(1 + Z_2(Y_{\text{tot}} + Y_{\text{x}}))(1 + Z_2 Y_{\text{tot}})}. \tag{4.24}$$

(4.24) shows that the relative error depends on the interconnections lines in a decreasing ways in the sense that the line closer to the reference is the one that affects the most the estimation. The line more distant from the reference is the one influencing the less. The relative error always depends on the value of the unknown load and on the equivalent admittance in a way proportional to the length of the line.
Summarizing:

- Y_{tot}: performances of the voltage method depend on the available network. Indeed when one appliance is switched on if the equivalent admittance and the impedance of the cable are high their product can not be neglected in the analysis, this usually does not happen. This term implies that measurements of the same admittance in two different contexts (with different active applications and different distance) could leads to different results;

- Z_2: the first cable is the more relevant in the error. Lowering this value, thereby reducing the length of the cable between reference and unknown load it reduces the error and the influence of the other active appliances in the process of the determination of the appliance. As it is explained in the following example, a cable with quite usual length does not influence the performances.

Let us to impose a relative error, estimated as in (4.24), less than 0.04. We want to compute the maximum length of the cable that allows to achieve this performance in terms of prediction accuracy of the unknown load.
The maximum length corresponds to the maximum value that the impedance Z_2 of (2.5) can assume to guarantee a certain value of the relative error (4.24). The relation between length of the cable and impedance of the cable is reported in (2.5).
In the graph in Fig. 4.4 l_{max} is the maximum length of the cable that yield a relative error less than 0.04. This parameter, as it can seen in (4.24), is function of Y_{x} and of Y_{tot}, for this reason the graphs are reported for different values of P_{tot} and the value of l_{max} is elaborated in function of different values of P_{x} (x-axis values). The values of P_{tot} and P_{x} are calculated by multiplying the correspondents admittances per a fixed value of voltage (235 V as fixed value to only have an idea of the possible performances).

4.4 Influence of the Crosstalk on the System Design

In Section 2.3.1 the Crosstalk Problem has been recalled because, in a practical implementation of the voltage method, it can afflict the performances and so it is appropriate to assess its influence.
In our case study the transmitted signal is the voltage drop and the crosstalk problem happens when a voltage drop in a electric circuit interferes with the working of the voltage algorithm in another branch circuit. The entity of the undesired reciprocal influence between electric branch circuits depends on the presence of the circuit breakers (their technical description is reported in [24]).
All the circuit breakers are included in the same electrical cabinet. There is a main circuit breakers and a lot of others breakers within this circuit breaker box enclosure.
The following analysis estimates the factor of attenuation between different branch circuits in term of measured voltage drops and also the correspondent attenuation in term of estimated admittances.
Notation:

- V_0: delivered voltage;

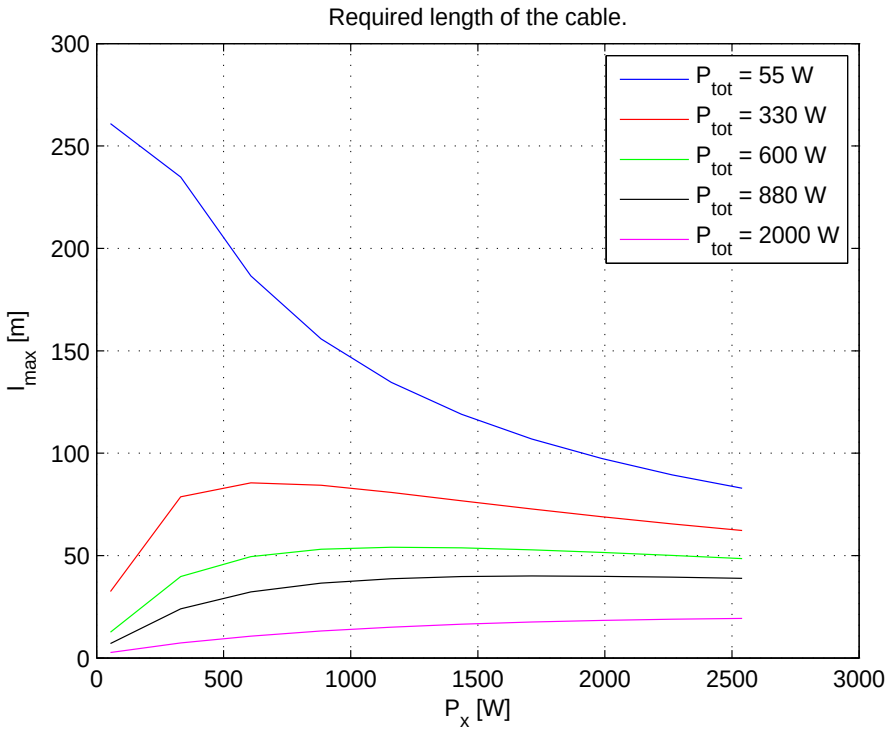

Figure 4.4: *Theoretical example of possible performances with different appliances and cables of different lengths.*

- $Z_0{}' = Z_0 + Z_1$: equivalent common impedance of the network;
- $Z_1 = 0.9$ mΩ is the internal resistance per pole of the main common circuit breaker (as specified in [5]);
- Y: admittance of the unknown load;
- Z_A: impedance of the circuit breaker of the branch circuit A;
- Z_B: impedance of the circuit breaker of the branch circuit B;
- Z_A = Z_B = 7 mΩ in the considered network (as specified in [5]).

As already explained, circuits, designed to operate independently, influence each other because of the common impedance of the network that they share.
Ideally if an appliance is turned on in one electrical branch circuit it should not affect the adjacent circuits.
A basic model for the analysis of the crosstalk (of Fig. 2.3) includes a voltage sensor in the branch circuit B, placed after the switching of this circuit. In this way the voltage probe can sense the crosstalk due to a load in the branch circuit A by the common impedance (series of the network impedance and the impedance of the main switch).
It is relevant to assess the voltage drop in two different situations:

- CASE A: a heavy load is switched on in branch circuit B, the probe measures the following voltage:
$$V_{(1)} = \frac{1}{1 + (Z_0{}' + Z_B)Y} V_0. \tag{4.25}$$
- CASE B: the same load is switched on in branch circuit A, the measuring instrument placed in branch circuit B records the following voltage:
$$V_{(2)} = \frac{1 + Z_A Y}{1 + (Z_0{}' + Z_A)Y} V_0. \tag{4.26}$$

Ideally the measuring instrument, placed in branch circuit B, should sense the open circuit voltage of the network, since there are no active devices in branch circuit B, instead of this it records a voltage drop because of the presence of a load in branch circuit A (4.26).
If we look at the entity of the voltage drop in the two different cases:

- CASE A
$$\Delta V_{(1)} = (Z_0{}' + Z_A) \frac{Y V_0}{1 + (Z_0{}' + Z_A)Y} \; ; \tag{4.27}$$
- CASE B
$$\Delta V_{(2)} = Z_0{}' \frac{Y V_0}{1 + (Z_0{}' + Z_A)Y} \; . \tag{4.28}$$

The attenuation factor that afflicts the recognized voltage drop is:

$$\alpha_{\Delta V} = \frac{Z_0{}' + Z_A}{Z_0{}'}. \tag{4.29}$$

In the simplified model of Section 2.2 Z_0 represents the equivalent impedance of the entire network before the voltage sensor, in that case it assumes small values that can be of the order of 0.5Ω. In the case reported in this Section Z_0 is the impedance of the equivalent electrical network before the circuit breakers. We do not know exactly its value because we have not tested but we can suppose that it corresponds to a really small value with an order of magnitude less than $m\Omega$. Since $Z_0 \ll Z_1$ the resultant attenuation factor α is equal to 8.78 in the considered network (this assumption has been tested and validated).
From (4.29) we do the following considerations:

- The voltage method can not be implemented if the reference and the unknown loads are not placed in the same electrical branch circuit. Indeed the starting point of the algorithm is the detection of the voltage drops and voltage drops due to devices in other branch circuits could be not recognized if their real power is not enough high.
- Even if the voltage jumps of appliances placed in a different electrical branch circuit are detected they can be roughly quantified. Indeed the power of the device that is switched on, as already explained, is underestimated and this lead to a wrong estimation of the application used by the users.

Regarding the last consideration the correspondent estimated admittance in the case of the configuration of (4.26) is:

$$\widehat{Y} = \frac{Z_0{}'}{Z_0{}' + Z_B} \cdot \frac{Y}{1 + Z_A Y}. \tag{4.30}$$

Since $\frac{Y}{1+Z_A Y} \approx 1$ the attenuation in term of estimated admittance is:

$$\alpha_{\Delta Y} \approx \frac{Z_0{}' + Z_B}{Z_0{}'}. \tag{4.31}$$

The correspondent relative error in the estimation of the detected appliances is:

$$\eta_{crosstalk} = \frac{Z_B}{Z_0{}' + Z_B}. \tag{4.32}$$

The attenuation in term of voltage jumps (4.29) is the same of the attenuation that afflicts the estimation of the appliances (4.31) because of the same value of the circuit breakers admittances. After these considerations it appears clear that it is necessary to keep into account the possible interferences due to the presence of other devices in the other branch circuits.
It is very important to carefully choose the threshold for the event detector of the voltage algorithm to try to limit the false positive in the detection and this consideration conducts us to study also the variability of the measured RMS voltage of our testing Lab in Chapter 3.
As conclusion of the analysis of the crosstalk it is suggested to put at least one voltage sensor for each electrical branch circuit to identify in which electrical branch circuit a device is switched on/off and to correctly estimate the power consumption of the devices.

4.5 Effects of the voltage noise on the estimation of the appliances

In Section 2.5 the noise that afflicts the signal during short intervals of time has been evaluated. After the estimation of the noise statistical it is possible to analyse the impact of noise on the estimation of the appliances.
Indeed in the real execution of the algorithm we need to take into account the error propagation due to the noise that affects all the measurements. The propagation of uncertainty is the effect of variables' errors on the uncertainty of a function based on them. When the variables are the values of experimental measurements they have uncertainties which propagate to the combination of variables in the function.
The theoretical analysis takes place by assuming to look at the ideal case (without considering possible interferences and losses and with an ideal reference load) represented in Fig. 2.1.
In following analysis we suppose to switch on/off only one device at a time (first unknown device and then reference device) because we want to underline the effect of the voltage noise in the simpler case. The analysis refers to the following voltages:

- $V^{(0)}$ is the measured voltage with an existing total admittance $Y^{(0)}$:

$$V^{(0)} = \frac{V_0}{(1 + Z_0 Y^{(0)})}. \tag{4.33}$$

- $V^{(1)}$ is the measured voltage when the unknown load is switched on and the total admittance is equal to $Y^{(0)} + Y_{\text{x}}$;

$$V^{(1)} = \frac{V_0}{(1 + Z_0 \left(Y_{\text{x}} + Y^{(0)}\right))}. \tag{4.34}$$

- $V^{(2)}$ is the measured voltage when the reference load is switched on (unknown load is disconnected) and the total admittance is equal to $Y^{(0)} + Y_{\text{ref}}$:

$$V^{(2)} = \frac{V_0}{(1 + Z_0 \left(Y_{\text{ref}} + Y^{(0)}\right))}. \tag{4.35}$$

The estimated network of the formula 3.13 becomes:

$$I_0 \triangleq \frac{V_0}{Z_0} = \frac{Y_{\text{ref}}}{(\frac{1}{V^{(2)}} - \frac{1}{V^{(0)}})}; \tag{4.36}$$

and the unknown admittance is calculated in the following way:

$$Y_{\text{x}} = \frac{Y_{\text{ref}}}{\left(\frac{1}{V^{(2)}} - \frac{1}{V^{(0)}}\right)} \left(\frac{1}{V^{(1)}} - \frac{1}{V^{(0)}}\right). \tag{4.37}$$

The estimated admittance (4.37) is an indirect measure and as such it is affected by the error of the direct measurements, these last ones are affected from the noise $n(k)$:

- $\hat{V}^{(0)}(k_0) = V^{(0)}_{RMSmean}(k_0) + n_0(k_0)$,
- $\hat{V}^{(1)}(k_1) = V^{(1)}_{RMSmean}(k_1) + n_1(k_1)$,
- $\hat{V}^{(2)}(k_2) = V^{(2)}_{RMSmean}(k_2) + n_2(k_2)$;
- $\{n_i\} \in N(0, \sigma_i^2)$ (from Section 2.5).

(4.37) includes in itself the measurements of the voltage affected by error and for this reason the estimation of Y_{x} is affected by the noise of the voltage as it is reported in the following expression:

$$\hat{Y}_{\text{x}} = \frac{Y_{\text{ref}}}{\left(\frac{1}{\hat{V}^{(2)}} - \frac{1}{\hat{V}^{(0)}}\right)} \left(\frac{1}{\hat{V}^{(1)}} - \frac{1}{\hat{V}^{(0)}}\right) \tag{4.38}$$

Because of the presence of noise in the measurements it is possible to evaluate the noisy estimation of Y_L as:

$$\Rightarrow \hat{Y}_{\text{x}} = Y_{\text{x}} + \sum_{i=0}^{2} \frac{\partial Y_{\text{x}}}{\partial V^{(i)}} n_i \ , \tag{4.39}$$

by considering only the first order in the noise. To this analysis it is used that $n_i, i = 0, 1, 2$ are supposed to be independent, Gaussian random with the same variance σ_V^2 because we have proved in the previous Section 2.5 that it can be a good assumption. The partial derivatives are:

$$\frac{\partial Y_{\text{x}}}{\partial V^{(2)}} = \frac{Y_{\text{ref}}}{\left(\frac{1}{V^{(2)}} - \frac{1}{V^{(0)}}\right)^2} \left(\frac{1}{(V^{(2)})^2}\right) \left(\frac{1}{V^{(1)}} - \frac{1}{V^{(0)}}\right), \tag{4.40}$$

$$\frac{\partial Y_{\text{x}}}{\partial V^{(1)}} = \frac{Y_{\text{ref}}}{\left(\frac{1}{V^{(2)}} - \frac{1}{V^{(0)}}\right)} \left(\frac{-1}{(V^{(1)})^2}\right), \tag{4.41}$$

$$\frac{\partial Y_{\text{x}}}{\partial V^{(0)}} = \frac{Y_{\text{ref}}}{\left(\frac{1}{V^{(2)}} - \frac{1}{V^{(0)}}\right)^2} \left(\frac{1}{(V^{(0)})^2}\right) \left(\frac{1}{V^{(2)}} - \frac{1}{V^{(1)}}\right). \tag{4.42}$$

So (4.39) can be written as

$$\Rightarrow \hat{Y}_{\text{x}} = Y_{\text{x}} + n_Y, \tag{4.43}$$

where n_Y is a Gaussian variable with variance:

$$\sigma_Y^2 = \sum_{i=0}^{2} \left(\frac{\partial \hat{Y}_{\text{x}}}{\partial V^{(i)}}\right)^2 \sigma_V^2. \tag{4.44}$$

So:

$$\sigma_Y^2 = \frac{Y_{\text{ref}}^2 \sigma^2{}_V}{\left(\frac{1}{V^{(2)}} - \frac{1}{V^{(0)}}\right)^4} \Bigg[\left(\frac{1}{V^{(0)}}\right)^4 \left(\frac{1}{V^{(2)}} - \frac{1}{V^{(1)}}\right)^2 + \\ + \left(\frac{1}{V^{(1)}}\right)^4 \left(\frac{1}{V^{(2)}} - \frac{1}{V^{(0)}}\right)^2 + \left(\frac{1}{V^{(2)}}\right)^4 \left(\frac{1}{V^{(1)}} - \frac{1}{V^{(0)}}\right)^2 \Bigg] \tag{4.45}$$

By replacing voltage $V^{(i)}, i = 0, 1, 2$ with the definitions (4.33), (4.34) and (4.35) can be derived the following expression of the variance of the relative error:

$$\frac{\sigma_Y^2}{Y_{\text{x}}^2} = \left(\frac{\sigma_V}{V_0}\right)^2 \frac{1}{\left(Z_0 Y_{\text{x}} Y_{\text{ref}}\right)^2}\Bigg[\left(1 + Z_0 Y^{(0)}\right)^4 \left(Y_{\text{ref}} - Y_{\text{x}}\right)^2 + \\ + \left(1 + Z_0\left(Y^{(0)} + Y\text{x}\right)\right)^4 Y_{\text{ref}}^2 + \left(1 + Z_0\left(Y^{(0)} + Y_{\text{ref}}\right)\right)^4 Y_{\text{x}}^2\Bigg] \quad (4.46)$$

(4.46) shows that the relative load estimation variance is proportional to the ratio σ_V / V_0, and it also depends on the value of the admittances of reference and unknown load and finally it is conditioned from the impedance of the network.

4.6 Choice of reference load and Definition of the Range of detectable loads

4.6.1 Optimum Case: best choice of the reference load, unknown load in term of relative error performance

The relative load estimation variance, reported in (4.46), is function of more than one variable. This section is developed to show the best configuration for the execution of the algorithm in term of choice of reference and unknown load(s). To understand the optimum working condition, it is necessary to consider both the first and the second partial derivatives as to Y_{ref} and to Y_{x}. The optimum condition can be derived by setting to zero the first partial derivatives:

$$\begin{cases} \frac{\partial\left(\sigma_Y^2 / Y_{\text{x}}^2\right)}{\partial Y_{\text{ref}}} = 0 \\ \frac{\partial\left(\sigma_Y^2 / Y_{\text{x}}^2\right)}{\partial Y_{\text{x}}} = 0 \end{cases} \quad (4.47)$$

The system (4.47) can be written in the following way by solving the partial derivatives (in which $Y_{\text{x}} = \Delta Y$ is the detected change in the admittance):

$$\begin{cases} Y_{\text{x}}\left(1 + Z_0 Y_{\text{ref}}\right)^3 \left(-1 + Z_0 Y_{\text{ref}}\right) + Y_{\text{ref}} - Y_{\text{x}} = 0 & (4.48) \\ -Y_{\text{ref}}\left(1 + Z_0 Y_{\text{x}}\right)^3 \left(1 - Z_0 Y_{\text{x}}\right) - Y_{\text{ref}} + Y_{\text{x}} = 0 & (4.49) \end{cases}$$

The following equation is the result of the difference between (4.48) and (4.49):

$$Y_{\text{x}}\left(Z_0^4 Y_{\text{ref}}^4 + 2Z_0^3 Y_{\text{ref}}^3 - 2Z_0 Y_{\text{ref}} - 1\right) + Y_{\text{ref}}\left(-Z_0^4 Y_{\text{x}}^4 - 2Z_0^3 Y_{\text{x}}^3 + 2Z_0 Y_{\text{x}} + 1\right) + 2Y_{\text{ref}} - 2Y_{\text{x}} = 0, \quad (4.50)$$

and it is equal to zero when $Y_{\text{ref}} = Y_{\text{x}}$, as can be seen also from the symmetry between (4.48) and (4.49).

The optimal solution occurs when the admittances assume the same optimum value. For this reason the optimum value is derived by solving (4.48) and keeping into account that it is assumed

$Y_{\text{ref}} = Y_{\text{x}}$ in the optimum case.
(4.48) can be factorized in the following way (by using Ruffini's rule):

$$Z_0^2 \left(Y_{\text{ref}} - {}^1/_{Z_0}\right) \left(Z_0^2 Y_{\text{ref}}^2 - 1\right) = 0 \; ; \tag{4.51}$$

and a possible solution is the following condition:

$$Y_{\text{ref}} = Y_{\text{x}} = {}^1/_{Z_0} \; . \tag{4.52}$$

To demonstrate that (4.52) is the best condition it is also necessary to prove that it corresponds to a relative minimum of (4.46). This can be infer from the application of the second derivative test.
The second derivative test discriminant is defined as:

$$D = \frac{\partial}{\partial Y_{\text{ref}}} \frac{\partial \left({}^{\sigma_Y^2}/_{Y_{\text{x}}^2}\right)}{\partial Y_{\text{ref}}} \cdot \frac{\partial}{\partial Y_{\text{x}}} \frac{\partial \left({}^{\sigma_Y^2}/_{Y_{\text{x}}^2}\right)}{\partial Y_{\text{x}}} - \frac{\partial}{\partial Y_{\text{ref}}} \frac{\partial \left({}^{\sigma_Y^2}/_{Y_{\text{x}}^2}\right)}{\partial Y_{\text{x}}} \cdot \frac{\partial}{\partial Y_{\text{x}}} \frac{\partial \left({}^{\sigma_Y^2}/_{Y_{\text{x}}^2}\right)}{\partial Y_{\text{ref}}} \tag{4.53}$$

(4.53) in the condition of (4.52) assumes a positive value and this proves that (4.52) is a relative minimum of the variance of the relative error and this proves that (4.52) corresponds to the best configuration in term of variance of the relative error.
In the reality Z_0 usually assumes small values. Small value of the impedance network corresponds, in the best configuration, to big value of the admittances (following the rule of (4.52)).
For example with a value of Z_0 equal to $0.5\ \Omega$ the necessary admittances to obtain the best performances have a real power of about 378000 W.
The value of the variance, that is obtained in the optimum case, is very low but this case is not useful because in practise the network doesn't allow to use device of such high real power.

4.6.2 Range of detectable loads

The analysis of the voltage of Section 2.5 enables to estimate the threshold for detectable voltage jumps, and thus the range of appliances that the method can correctly estimate. The analysis of Section 4.5 gives an idea of the relative error that the method commits in the estimation of loads with different real power (performances in the range of detectable loads that depend also on the choice of the reference device).
In particular in this first part some considerations are reported with the aim to establish the minimum voltage jump detectable with a certain accuracy, that corresponds to a lower limit in term of power of the detectable appliances (link between changes in voltage and changes in power see Section 2.4).
The analysis of voltage RMS of Section 2.5 permits to estimate the minimum jump in term of voltage that we want to detect, and also, for different possible thresholds, evaluate the ratio between false and true positive that depends on the variance of the voltage.
From considerations reported in Section 2.5 it can be supposed to choose as threshold for the voltage method a value equal to $3\sigma_V$.
Indeed from that analysis it has been seen that the percentage of outsiders (that will correspond to false positive in the execution of the algorithm) is very low in the real experiments.
The threshold for sure can not be reduced because of:

- increasing of the percentage of false positive;
- increasing of the variance of the relative error (according to the analysis of section 4.5).

So the choice of the threshold for detecting voltage variations as a new device:

$$\text{THR} = 3\sigma_{\text{V}}. \tag{4.54}$$

In this way it is possible to estimate the minimum load recognizable through the execution of the algorithm by using the link between change in voltage and change in admittance. Indeed the link is:

$$\Delta V = Z_0 Y_{\text{x}} V_0, \tag{4.55}$$

that is the difference between (4.33) and (4.34). The minimum detectable change in admittance can find by imposing the chosen threshold in term of voltage jumps, so the minimum detectable admittance is:

$$Y_{\text{xmin}} \approx \frac{\text{THR}}{Z_0 V_0}. \tag{4.56}$$

For example in the case of the analysis can be the follower:

- $Z_0 \approx 0.5\Omega$;
- $V_0 = 235$ V;
- $\sigma_V \approx 5.5 \cdot 10^{-2}$ V ($r = 2$) .

So the minimum load, according with the analysis of Section 2.5 and 4.5, is approximately equal to $P_{\text{x}} = V_0^2 Y_{\text{x}} \approx 80$ W.
This minimum in term of detectable real power makes sense if the solution includes a single unit for each branch circuit for taking into account the presence of the crosstalk between different electrical branch circuits (Section 2.3.1).
The threshold should be higher in function of the implementation of the event detector for the voltage variations (Section 4.8.1).
On the other side the maximum power that can be detected and estimated is the limit in term of power that the network allows.

4.6.3 Design of the Reference load

This section is developed with the aim of finding the value of the preferable reference load to estimate a given appliance of interest. This method is designed to estimate device with an high power consumption in the range between 80 W and 2000 W.
The expression of the variance of the relative error (4.46) can be written 4.57 by using the assumption that usually $|Z_0 Y^{(i)}| \ll 1$ as:

$$\left(\frac{\sigma_Y}{Y_{\text{x}}}\right)^2 \approx \left(\frac{\sigma_V}{V_0}\right)^2 \frac{2}{\left(Z_0 Y_{\text{x}} Y_{\text{ref}}\right)^2} \left(Y_{\text{ref}}^2 + Y_{\text{x}}^2 - Y_{\text{ref}} Y_{\text{x}}\right). \tag{4.57}$$

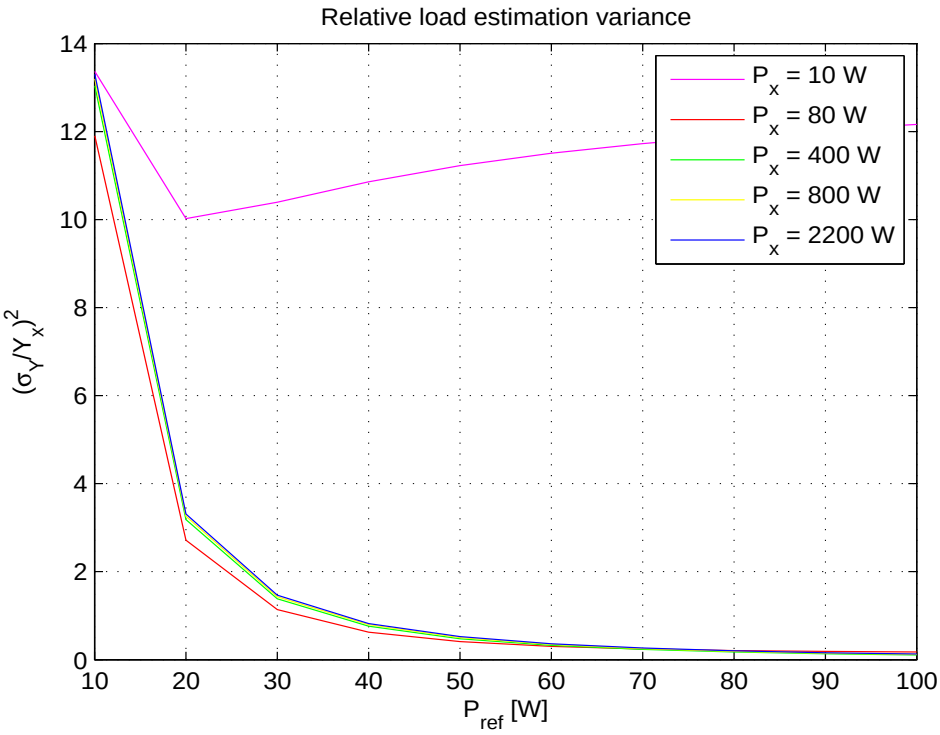

Figure 4.5: *Relative load estimation with different P_x and different reference load (range 10 W - 100 W).*

It can be reasonable to consider, as starting point of the analysis, a reference load with a real power between 10 W and 3000 W. In Fig. 4.5 and 4.6 different trends pattern of (4.57) are reported. In Fig. 4.5 the range of range of real power for the reference load is from 10 W to 100 W, in Fig. 4.6 is 100-1000 W.
In Fig. 4.6 the different trends correspond to different values of power of the unknown component. The figure shows that in the estimation of loads with small power (such as $P_{\text{x}} = 10$W) the variance of the relative error increases a lot. This represents another motivation for which the minimum detectable load can not have a real power less than 100 W. From the comparison between Fig. 4.5 and Fig. 4.6 can be also inferred that the variance of the relative error is higher for reference load with small real power, so the reference load should not have a real power less than 100 W. Fig. 4.6 shows that the theoretical performance is really good by using a reference load with a real power bigger than 300-400 W, indeed the variance of the relative error converges to the same small value for all the devices of interest. These considerations can be explained by looking at the expression (4.46) and at Fig. 4.7. Fig. 4.6 shows the trend of (4.46) in the case $P_{\text{x}} = 80$ W (minimum detectable load). We can clearly see that it is minimized when the condition $Y_{\text{ref}} \approx Y_L$ is verified, furthermore if $Y_{\text{ref}} > Y_L$ the relative estimation error is less than $2\sigma_V^2/(V_0 Z_0 Y_L)^2$. For the minimum detectable load the relative estimation error is 0.22, and it decreases for higher loads.
As conclusion of this Section, it is suggested, for the implementation of this novel technology, a

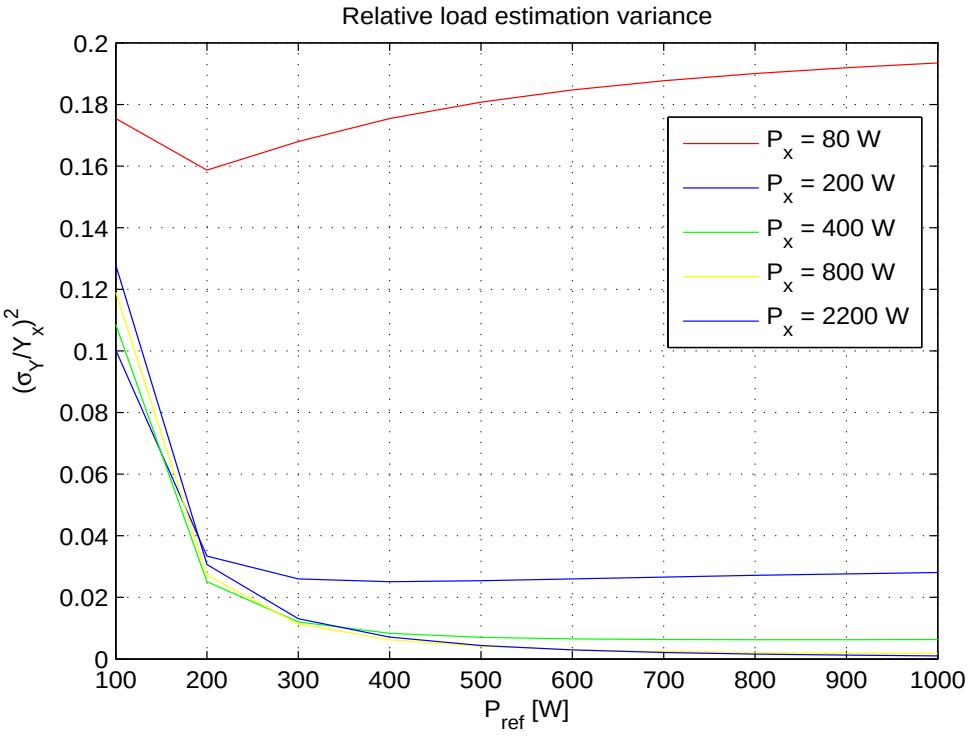

Figure 4.6: *Relative load estimation with different P_x and different P_{ref} (range P_{ref} 100 W - 1000 W).*

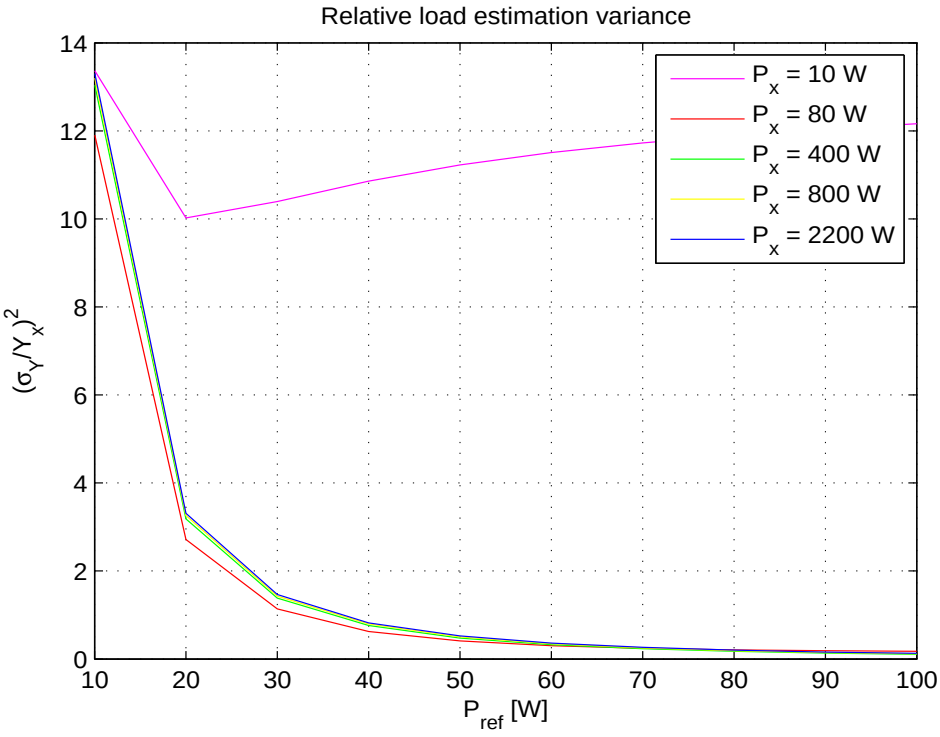

Figure 4.7: *Relative load estimation of (4.46) with $P_x = 80W$ and different P_{ref} (range 80 W - 400 W).*

reference resistive load with a real power bigger than 300/400 W, for the execution of our tests we have chosen an Halogen Lamp with a real power of 400 W.

4.7 Monitoring and Estimation of the Network

In this Section the parameters, that are continuously monitored by the system, are indicated and discussed, furthermore the Section argues about the estimation of the network that is the main point of the novel method. The term "estimation of the network" refers to the estimation of the ratio V_0/Z_0 that characterizes the equivalent electrical network.
This discussion is referred to the simple scenario of the set-up of Section 5.2.
The two important parameters to take into account, during the monitoring phase, are the RMS value of the voltage signal and its phase information.
In the implementation of our DEMO the RMS values are calculated over 5 periods of the sinusoidal wave. The phase information is also calculated over five periods of the voltage signal, as expressed in Section 2.6.1. Both (2.22),(2.23) are evaluated to keep into account both the total phase information and the change in the phase between two consecutive time intervals.
Every time in which a jump in the RMS voltage is recognized we can suppose to switch on/off the reference load and estimate the network. This seems the adequate strategy because of the variability of the network in a real context could be higher and so is better to do the update of the estimation frequently. In the experiments executed in the Lab at the High Tech Campus it

Algorithm 4.1 Monitoring

Sample 10 kHz i(t), v(t);
Calculate admittance of the reference load;
Average over five periods $V_{RMS}(k)$
Evaluate $\phi(k)$, $\Delta\phi(k)$ with 5 periods of the voltage signal;

is necessary to remind that the network is more robust than a domestic house (Section 2.5), this implies that the quantitative targets for the minimum standard of the voltage is supposedly better in our case.
For this reason in our DEMO (Section 5.4) we do not perform the estimation of the network every time in which a new load is recognized, we execute the estimation at the beginning of the execution and, after a while, we repeat the estimation.
So when the algorithm starts the first step is the initialization of the ratio V_0/Z_0, at this end, it is necessary to switch on/off the reference load.
In our particular context, with a resistive reference load with a nominal power of 400 W (Halogen lamp) and with a quite stable voltage (Section 2.5), algorithm 4.2 can be implemented by supposing to switch on/off the reference load only one time. Let's see in detail the execution of the training phase of the algorithm 4.2.
The estimation of the network takes place two times respectively with the switching on/off of the reference load ($num = 2$).

Algorithm 4.2 Initialization Phase

$n \leftarrow 0$
if $n < num$ **then**
  Event Detection based on Variance Method by using both current and voltage;
  if Event is over **then**
    Estimation of the network;
    $n \leftarrow n + 1$
  end if
end if

In our DEMO the complex power consumption, calculated by using the overall current and voltage across the reference load, is continuously monitored to detect when the reference load is on and, in this case, estimate the existing network. The estimation is executed when the power of the reference load is identified as stable through an event detector (it corresponds to the end of the event) that is based on both current and voltage. This event detector is the different from the event detector based only on the voltage signal that is discussed in Section 4.8. It is part of the previous system Coded Power developed at Philips Research that was based on current and voltage. This event detector considers the overall power consumption (calculating by using voltage and current) and it defines as an event the time window over which the overall complex power varies more than a threshold. To detect this variations the algorithm computes the complex power and a window of L periods, it estimates the average value of the complex power and the standard deviation as:

$$\mu(k) = \frac{1}{L}\sum_{l=1}^{L} \hat{P_{i,v}}(k-l) \tag{4.58}$$

$$\sigma(k) = \sqrt{\frac{1}{L-1}\sum_{l=1}^{L}\left(\hat{P_{i,v}}(k-l) - \mu(k)\right)^2} \tag{4.59}$$

The events that we analyse with our method are simple to detect (consist in simple transition between OFF/ON states) with this event detector based on the complex power with $L` = 2$.
It remains to check in a domestic environment how often is opportune to execute the Initialization phase. To evaluate how often the network changes and how this can influence the performances of the method is not sufficient the valuation of the variability of the voltage but it is also required to switch on/off the reference load in the analysed configuration, and estimate the same unknown load until when the estimation tends to diverge (the estimated value tends to a wrong value because the equivalent network is different from the estimated).
Anyway, in a domestic environment, the best suggested implementation requires to update the estimation of the network every time in which a voltage jumps is detected by the event detector.

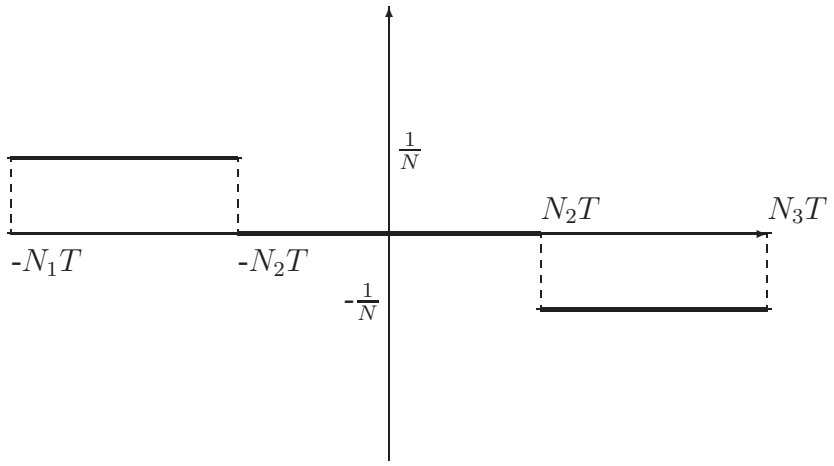

Figure 4.8: *Filter h_N*

4.8 Event detection

4.8.1 Detection voltage drop RMS

The basic idea of the event detector of our system is to look at the time evolution of the voltage RMS (2.8) calculated over 1000 samples.
This simple event detector is designed to detect when a voltage change occurs and also to identify after how long the RMS voltage returns to be stable (end of the long-term transient).
The long-term transient is different from the electrical transient. This last type of transient consists in the fact that when a device is switched on, its complex admittance changes over time until the device warms up completely. This term is relevant because devices with the same nominal admittance might have different behave with respect to the long- term transient.
The goal of the event detector is to identify the long term transient as an event, every time in which a voltage jump is recognized the event starts and it ends when the voltage gets again stability. A possible implementation of this event detector is reported in algorithm 4.3, and includes two simple filter. The parameters of the filters could change in real context with different devices. The implemented filters have the same structure of the filter of Fig. 4.8, the generic filter h_n has the following expression:

$$h_N = \begin{cases} 0, & n < -N_1T \\ 1/N, & -N_1T \leq n \leq -N_2T \\ 0, & -N_2T < n < N_2T \\ -1/N, & N_2T \leq n \leq N_3T \\ 0, & n > N_3T. \end{cases} \tag{4.60}$$

- $N_2 - N_1 = 5$;

Algorithm 4.3 Event detector voltage

ΔV_1: output filter 1;
ΔV_2: output filter 2;
if Event is ON and ($|\Delta V_1| > th_1$ or $|\Delta V_1| > th_2$) **then**
  Event is ON;
else
  if Event is ON and ($|\Delta V_1| < th_1$ and $|\Delta V_1| < th_2$) **then**
    Event is OFF;
  end if
else
  if No Event and ($|\Delta V_1| > th$) **then**
    Event is ON;
  end if
else
  No event;
end if

- $2N_2 = 10$ (in the reality it is better to set this equal to 2;
- $N_3 - N_2 = 5$;
- $th_1 = 0.15V$;
- $th_2 = 0.2V$;
- $th = 0.25V$;
- $N = 5$.

4.8.2 Detection jump in phase

The detection of the change in the phase information is a bit tricky because of the presence of the drift that afflicts the phase information in a non constant way (Section 2.6.1). A preliminary idea (for our DEMO) could be that every time an event in the voltage trend is recognized the algorithm looks at the phase information to understand if in the same moment a jump in the phase can be recognized (inductive or capacitive loads).
If also in the phase information a jump is detected we need to take into account the drift before the jump and evaluate the jump in term of phase (see algorithm 4.4).
Ideally, in a practical execution, if a PLL system (phase locked look system) is available, the phase information is recovered correctly, and an event detector for the phase information is not needed.
Indeed the event detector based on the RMS voltage recognizes the presence of new devices and after that the steps of our method could be applied to the voltage complex phasor. In this way we can correctly estimate the complex power of the unknown devices.

Algorithm 4.4 Event detector Phase

$\Delta\phi(k) \leftarrow phi(k) -$ mean(*phase before event*);
if Event is ON and ($|\Delta\phi(k)| > th_{phase}$) and Event Phase is OFF **then**
  Event Phase is ON;
  Phase event $\leftarrow \Delta\phi(k) - drift$;
else
  if Event Phase is ON **then**
    $\phi(k) = \Delta\phi(k) + \phi(k) - drift$;
  end if
else
  if Event is OFF **then**
    Event phase is OFF;
  end if
else
  No event;
end if

4.9 Overall solution

In Fig. 4.9 the flowchart of the voltage method is reported, it shows the main steps as boxes of various kinds, and it also underlines the connections with arrows. This diagrammatic representation gives the step-by-step solution of the algorithm.

1. The algorithm starts by sampling the voltage, calculating the corresponding RMS value of (2.8);

2. If it lacks the estimation of the network or the time from the last estimation is higher than THR_t it is necessary to:

   - Turn on/off the reference load for num times (in our DEMO $num = 1$);
   - Every time in which the reference is turned on wait until the end of the long-term transient (event calculated through the variance method (by using i,v));
   - When the transient is over the algorithm estimates the ratio V_0/Z_0;
   - After num valid estimations of the network the algorithm estimates I_0 as the average value of the $2\,num$ estimations (switching on/off two estimations every time in which the reference load is turned on);

3. If the algorithm recognizes a voltage jump as a new event:

   - The algorithm evaluates the jump in term of admittance until when the transient is supposed to be finish;
   - Estimation of the complex admittance of the unknown load:

Algorithm 4.5 DEMO

```
Monitoring;
n ← 0
if n < num then
    Initialization Phase;
else
    Event detection based only on the voltage;
    if Event ON then
        Evaluate Real Power;
        if Event ON phase then
            Update φ(k), Estimate Reactive power;
        end if
    end if
    if Event OFF then
        if Reference is turned ON then
            n ← 0;
        end if
        Fix real and reactive power to the estimated value;
        Evaluate jump in real and reactive power;
        Update signatures;
    end if
end if
```

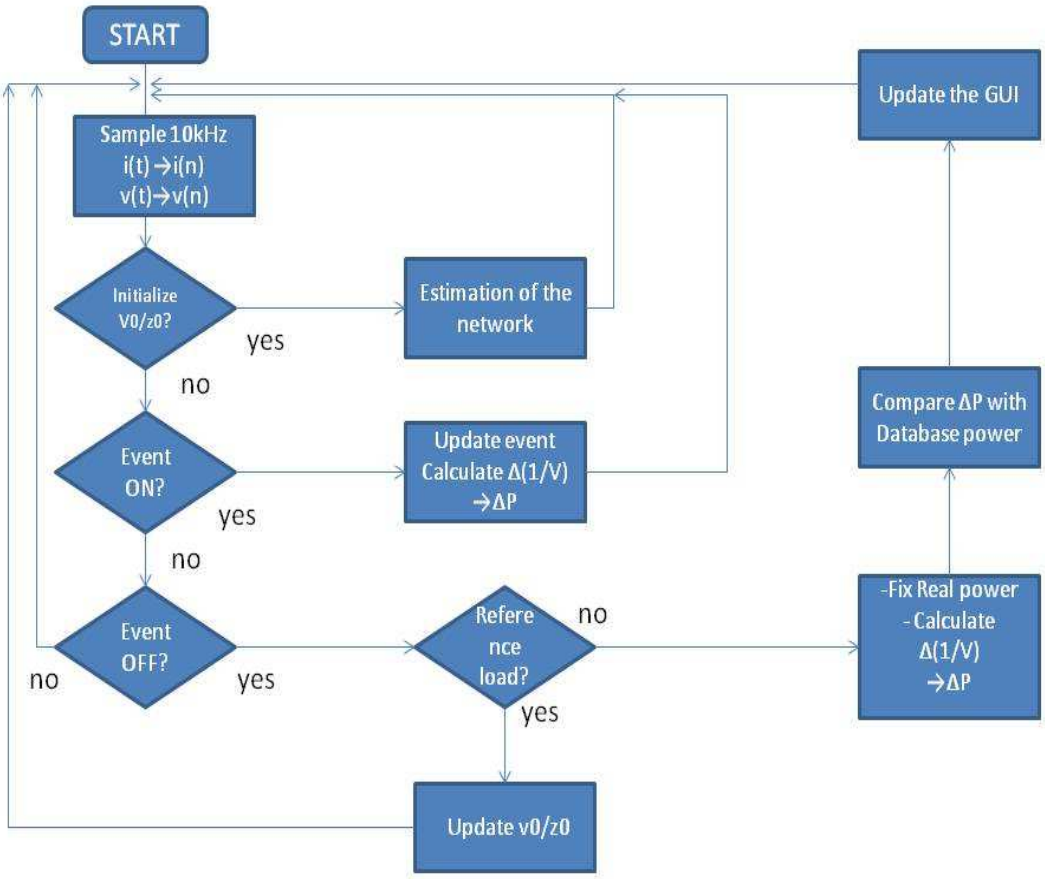

Figure 4.9: *Flow diagram of the overall voltage algorithm as it is implemented in our DEMO.*

  - $\Delta\phi < THR_\phi \Rightarrow Y_L = G_L$;
  - $\Delta\phi \geq THR_\phi \Rightarrow Y_L = G_L + iB_L$;

  where B is the susceptance of the unknown load and it has the following meaning:

  - $B > 0$ when the load is mainly capacitive ;
  - $B < 0$ when the load is an inductor;

- After the end of the event the algorithm estimates the resultant complex power (Section 2.4) and it sets the complex power to that constant value until the next event is recognized from the event detector;
- Update the signatures by detecting which device is on, at this end it is necessary to compare the jump in term of complex power with the nominal power of the devices that exist in our database.

- Update the User Interface to show the detection of the devices and the estimation of energy consumption of the environment.

In the practical execution the technology should work in a different way:

- Sample the voltage signal, calculate the corresponding RMS value of(2.8);
- If an Event is ON, evaluate $\Delta(1/V)$ (complex voltage) until when the event is finished;
- Turn on/off the reference load to estimate the electrical network;
- With the estimation of the network evaluate the jump in term of complex power associated at the previous event;
- Update the signatures and GUI with the information associated to the estimated jump.

Chapter 5

Experiments and Results

5.1 General

Chapter 5 is focused on the performed experiments to test the novel technology and validate the theoretical analysis performed in the previous Chapters.
It is divided in the following Sections: Section 5.2 explains the experimental set-up that we have used in our Lab at the High Tech Campus, Section 5.3 reports the validation of the theoretical model of the electrical system developed in Chapter 2, Section 5.4 describes the implementation of a DEMO to show the application of the voltage method in a practical context, Section 5.5 presents preliminary results about the Crosstalk between different electrical branch circuits, finally Chapter 5 ends with Section 5.6 that validates the model of the variance of the relative error.

5.2 Experimental set-up

Fig. 5.1 shows the architecture of the demonstrator that we used to emulate an environment and test the novel technology. In Fig. 5.2 a picture of the real experimental set-up used for performing the experiments is reported.
In all the experiments a dedicated electrical branch circuit is used as our own network, which delivers electricity to the reference load and the unknown loads (in Fig. 5.1 all the admittances are connected in parallel within the same electrical branch circuit).
The measuring equipment consists of a differential voltage probe sensing the voltage across the reference load and an Agilent current probe sensing the current of the reference load to estimate its power. The voltage sensor maps the voltage into 0-5 volts range to ensure safe input to the AD converter, the current probe operates at 0.1 V/Amps configuration and it is linear within a high dynamic range from milli-Amperes to tens of Amperes.
The two instruments are connected to a 24 bits National Instruments AD converter which digitizes the data at a sampling rate of 10kHz per each channel and that interfaces LabVIEW. The AD Converter with 10 Volts range provides a granularity of approximately 0.6 μV.
Labview takes the data from the AD Converter and stores them.

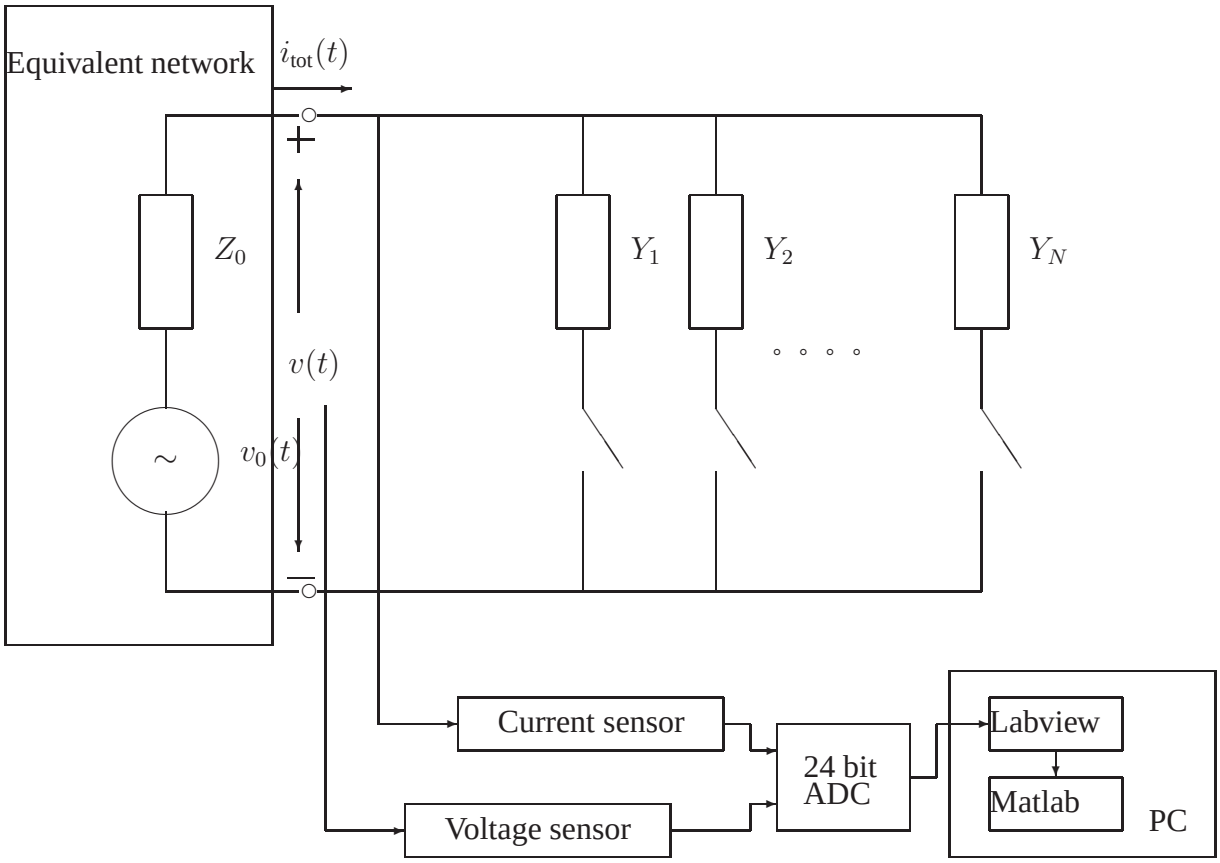

Figure 5.1: *Architecture of the demonstrator.*

The data is shared with Matlab, it is provided in batches of 1k samples and this permits to obtain a communication process faster compared to single bit transfer.
LabVIEW runs in a PC that is powered by another branch circuit, so also the power supply connects to the ADC. This decision is due to the will to isolate the measurements, to delete the effects of the crosstalk due to other appliances of the same branch circuit.

Figure 5.2: *Real Experimental Set-up.*

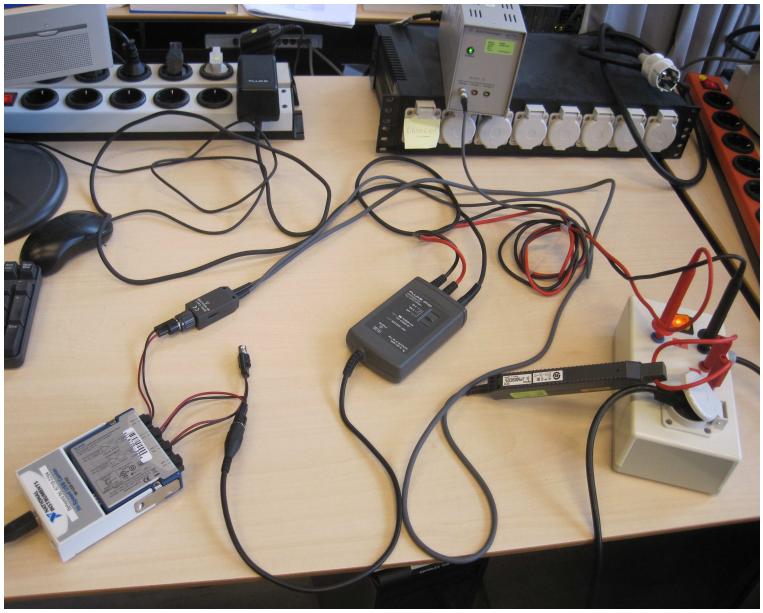

Figure 5.3: *Measurement instruments.*

Fig. 5.3 is a image of the measurement instruments. Indeed the AD Converter is on the left, and

its first two input channels are connected to the current and voltage probes. The current clamp is on the right side, so also the voltage sensor. The current clamp is required only for the estimation of the power of the reference load (Section 4.7). The estimation of the unknown devices is realized by keeping into account only the voltage signal gathered by the voltage probe.

5.3 Validation of the System Model

In this Section the results of some experiments are presented to validate the theoretical model developed in Sections 2.2 4.2. All the results are obtained with the experimental set-up of Section **??**.
In addiction the following elements are used to carry out the experiments (Notation refers to Fig. 4.1):

- As Y_{ref} a water kettle (Philips HD4649) with a nominal power of 2200 W is used. It has been chosen, in the preliminary studies, because of its behaviour mainly resistive and because of its large nominal real power;
- As Y_{x} a hair dryer (Philips Salon Dry Compact HP4960), is used at the stage 1, that is characterized by a nominal power of 720 W;
- As Z_1 a cable, long about 20 meters, is used to emulate the cable losses in a practical network.

To support the theoretical model of Section 4.2 three different sorts of experiments have been performed. In each type of experiment the position of the testing ground has been changed by implementing the following configurations:

- **Basic Configuration**: implements Fig. 3.6.
- **Configuration 1**: implements Fig. 4.1.
- **Configuration 2**: implements Fig. 4.2.

In each measurement round the steps presented above are executed: first the instruments record only the voltage of the network, then the hair dryer is switched on ($Y = Y_{\text{x}}$), followed by the switching on of the water kettle ($Y = Y_{\text{ref}} + Y_{\text{x}}$), then the switching off of the same device ($Y = Y_{\text{x}}$), and finally also the hair dryer is switched off. The measurement round is executed many times for each configuration.

5.3.1 Basic Configuration

The first basic ideal Configuration is theoretically perfect in the sense that it should get results not affected by error. The experiments are executed in a real laboratory and the results are, also in this case, affected by error. The V_{RMS} voltage recorded during one experiment (that includes several rounds) is reported in Fig. 5.4.

The V_{RMS} voltage is computed over one period of $N_{\text{s}} = 200$ samples ($T = \frac{1}{f_0} = 0.02$s, $f_0 = 50$ Hz fundamental frequency in the EU) is:

$$V_{RMS}(k) = \frac{1}{N_S} \sum_{i=kN_s}^{(k+1)N_S} V(i)^2. \tag{5.1}$$

For instance, in Fig. 5.4, the first measurement round starts at $k = 0$ and ends at around $k = 1000$. At the beginning the recorded voltage corresponds to the situation where no load is on, around $k = 600$ a first voltage drop happens that corresponds exactly to the switching on of the hair dryer, then the following large drop is the switching on of the water kettle. The round finishes with the two jumps that correspond to the switching off of water kettle and hair dryer, finally the amplitude of the RMS voltage comes back to the original level without loads on. This type of set-up correctly estimates the admittance of the unknown load and in this way estimates the real power of the unknown load like it can be observed in Fig. 5.5. In Fig. 5.5 the values (in term of change of the real power) that are estimated by our method are represented with blue dots, with red dots the values estimated by a system that uses both voltage and current are reported to understand the comparison between the different approaches. In this case the term "event" indicates every time in which the unknown load is estimated (a round of execution of the experiment). The results or our method are consistent, the error takes into account the fact that in reality each measurement is somewhat affected by uncertainty [25] and the estimation of the unknown admittance is also affected by the propagation of the error as seen in Chapter 4.
It is easier to understand the performance of the voltage disaggregation method looking at the relative error.

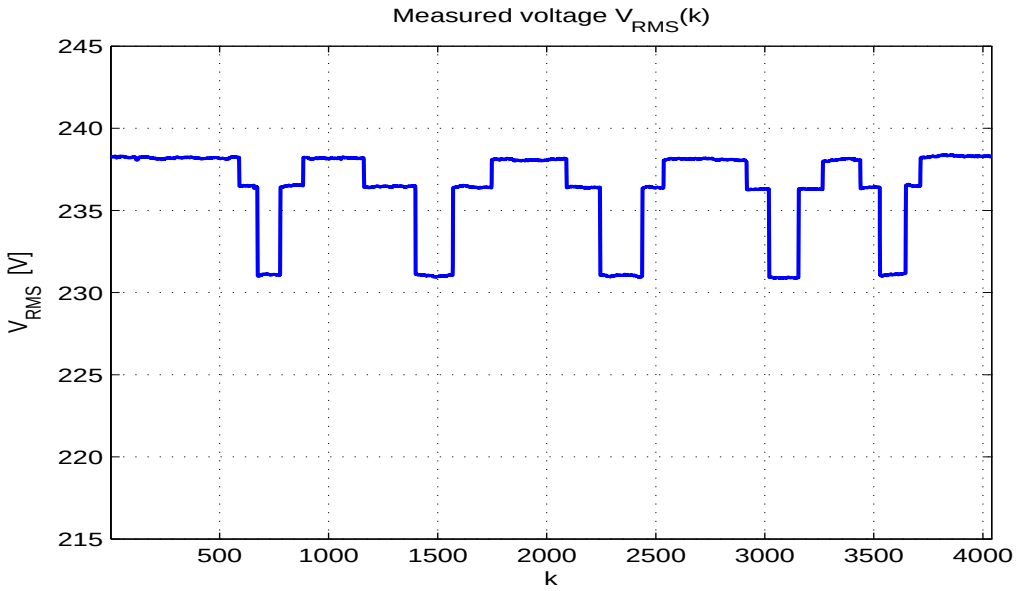

Figure 5.4: *Measured $V_{RMS}(k)$ in Basic Configuration.*

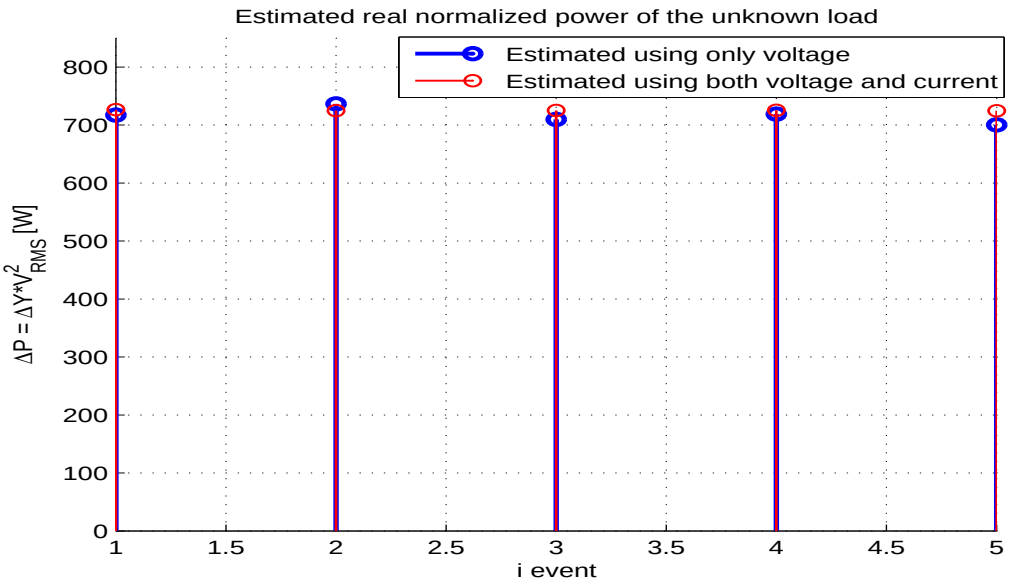

Figure 5.5: *Estimated value of the real power of the unknown load in Basic Configuration.*

In these experiments the relative error can be expressed as (considering also the sign)

$$\eta = \frac{\Delta P_{i,v} - \Delta P_v}{\Delta P_{i,v}} \tag{5.2}$$

where:

- $\Delta P_{i,v}$ is the value of the real power of the device estimated using both current and voltage signals;
- ΔP_v is the value of the real power of the device estimated using only the voltage signal.

Both these values are obtained from the estimated admittance of the load multiplied by squaring the measured V_{RMS} voltage $\Delta P = V_{RMS}^2 \cdot \Delta Y$ (Section 2.4).
In Fig. 5.6 the histogram of the relative error that we obtain by repeating the experiments on different days and different times is reported.
Data of the normalized histogram of Fig. 5.6:

- Width of the interval: 0.016;
- Number of events: 136;
- Mean Error: -0.0041 ;
- Variance Error: 0.0016;

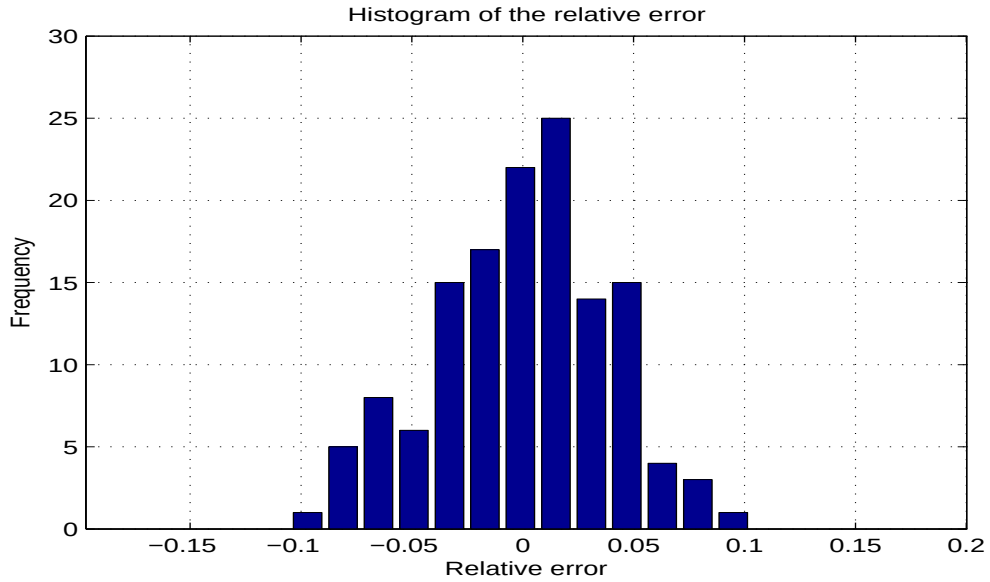

Figure 5.6: *Normalized histogram of the relative error obtained during the experiments performed with Basic Configuration.*

5.3.2 Configuration 1

The theoretical analysis of Configuration 1 (Section 4.2) gives as result that the voltage sensor can not correctly estimate loads that are placed between the equivalent network and the instrument if the impedance of the network has a value comparable with the impedance of the wire cable between unknown device and instrument.
To support this thesis, in the second type of experiments, a cable of about twenty meters is put after the unknown load and before the voltage meter (Fig. 4.1).
As we have found in the theoretical analysis, the voltage probe records a different voltage drop (when the reference load is switched on (see (4.3), and this does not permit to correctly estimate the load that is placed before the reference load (see (4.8)).
Fig. 5.8 shows the wrong estimation of the real power of the unknown load that appears to be halved.
This result is consistent with the assumption that the equivalent impedance of the electrical network is comparable with the impedance of a cable of limited length. Furthermore it gives us a limit of the algorithm in the sense that a load before the instrument can not be estimated. A correct Configuration forecasts to put the voltage sensor as close as possible to the electrical socket if it would be estimate all the loads of the electrical branch circuit.
Data of the normalized histogram of Fig. 5.9:

- Width of the interval: 0.007;
- Number of events: 98;
- Mean Error: -0.5905 ;

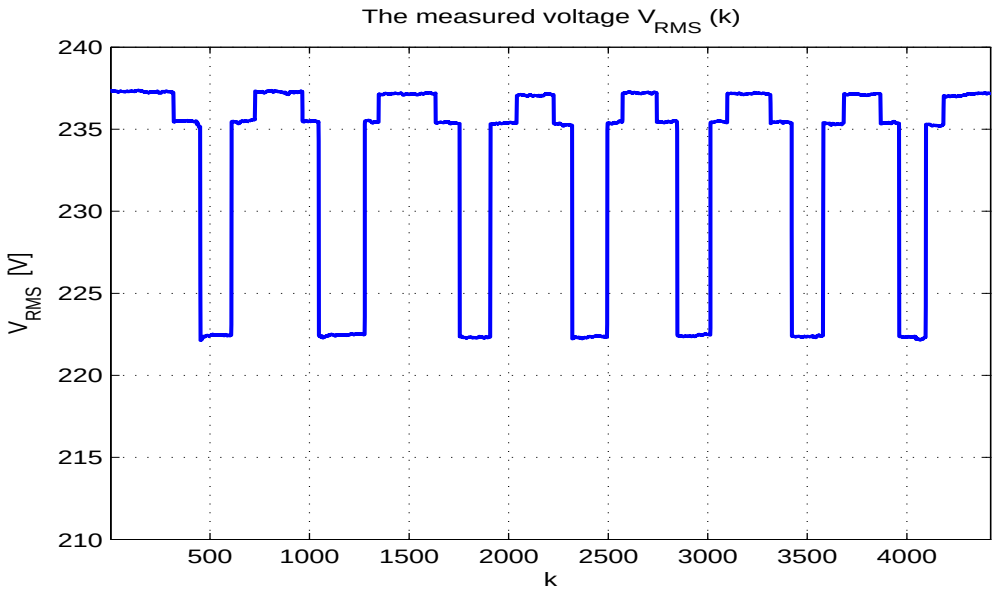

Figure 5.7: *Measured $V_{RMS}(k)$ in Configuration 1.*

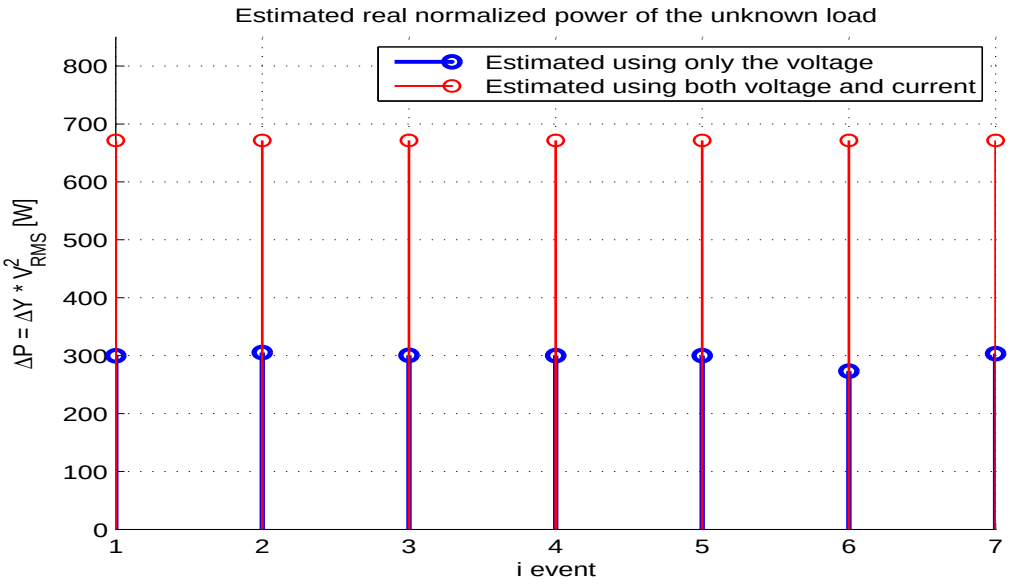

Figure 5.8: *Estimated value of the real power of the unknown load in the Configuration 1.*

- Variance Error: 1.4e-4;

5.3.3 Configuration 2

On the contrary, the third test wants to support the thesis that the presence of a cable, placed between the reference load and the unknown load, does not influence the performance of the

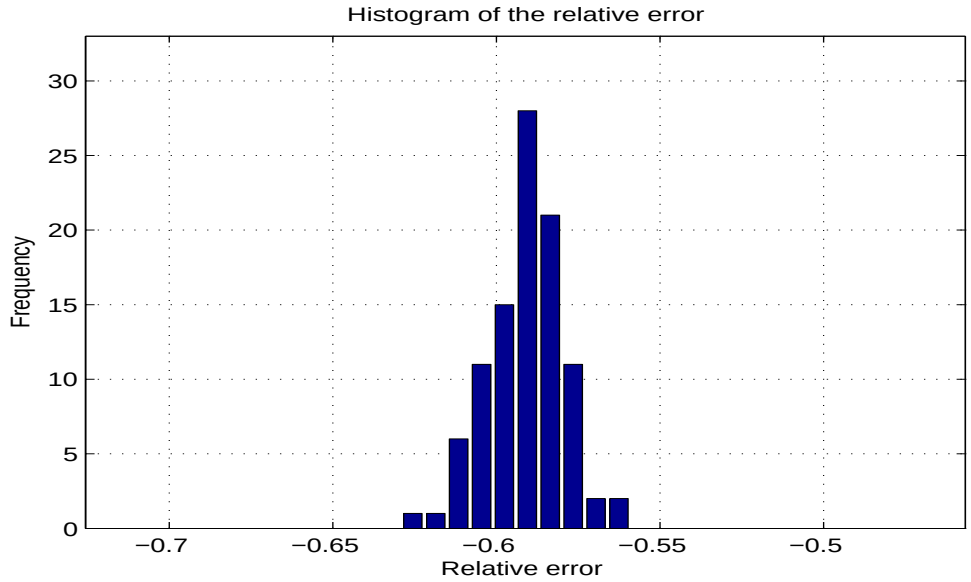

Figure 5.9: *Normalized histogram of the relative error obtained during the experiments performed with the Configuration 1.*

algorithm if the cable is not so long (see (4.12)).

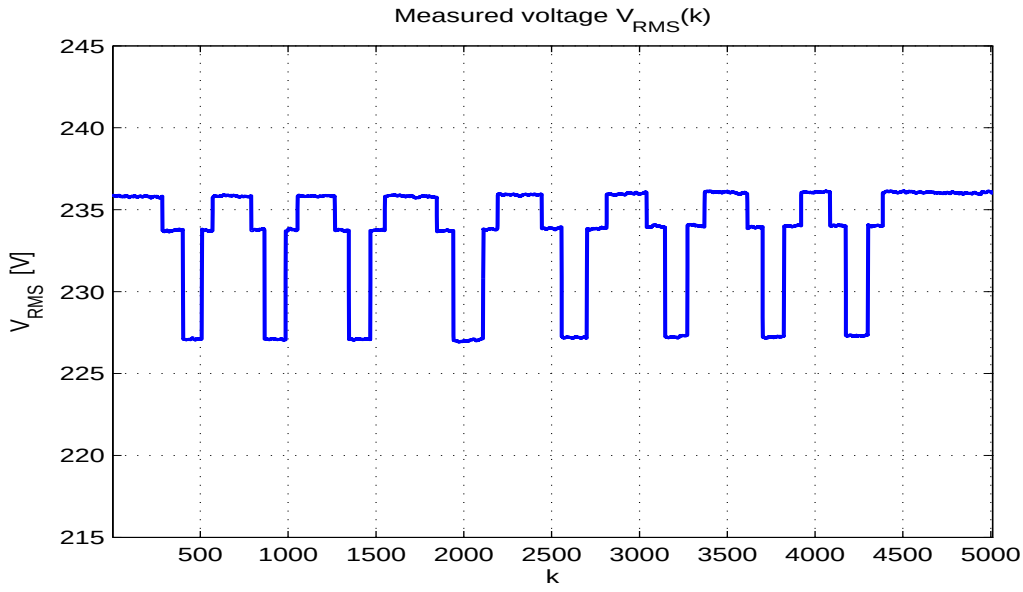

Figure 5.10: *Measured $V_{RMS}(k)$ in Configuration 2.*

The graph of Fig. 5.12 shows that the performance in the presence of the cable does not change so much compared with the results of Basic Configuration (Fig. 5.6).
Data on the normalized histogram of Fig. 5.12:

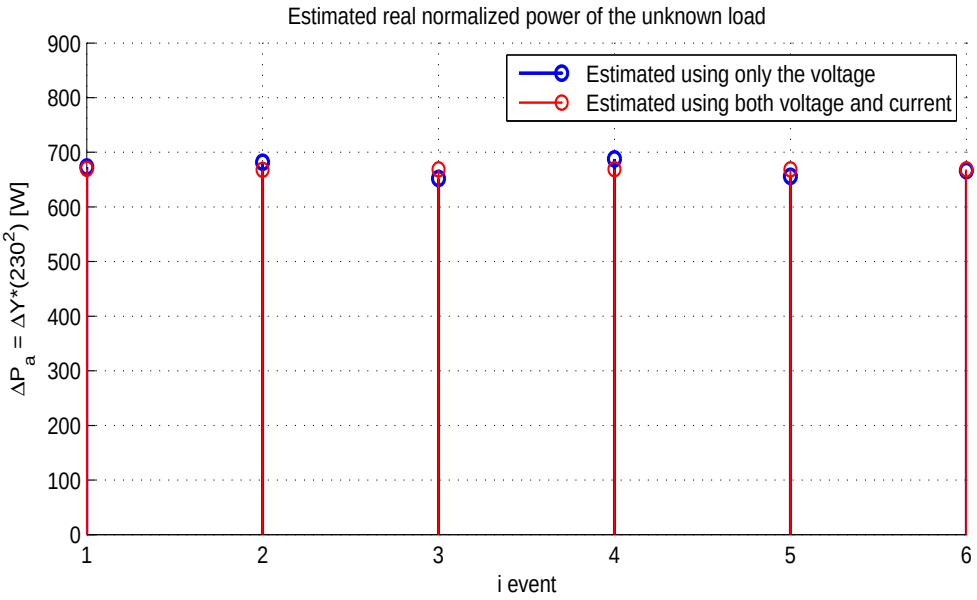

Figure 5.11: *Estimated power of the real power of the unknown load in Configuration 2.*

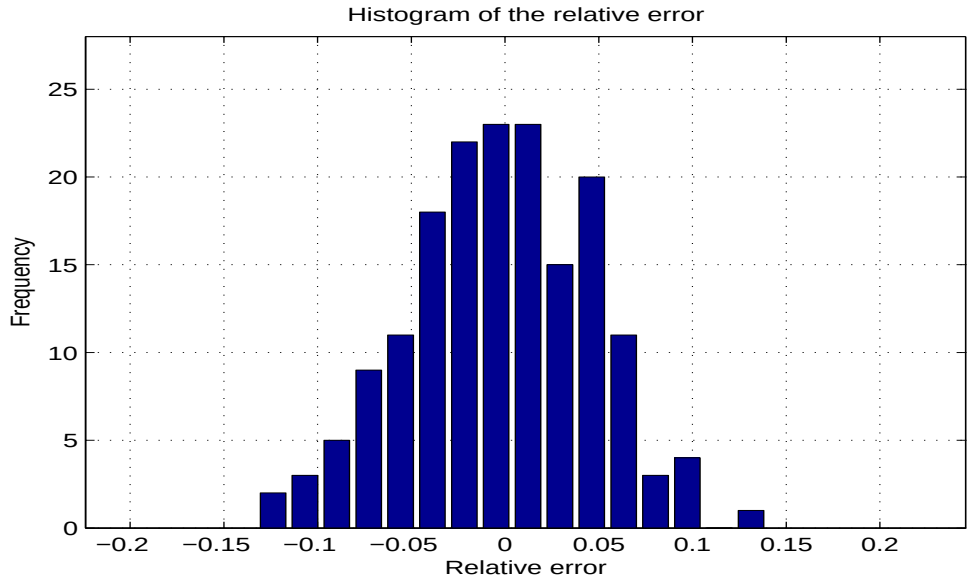

Figure 5.12: *Normalized histogram of the relative error obtained during the experiments performed with the Configuration 2.*

- Width of the interval: 0.017;
- Number of events: 170;
- Mean Error: -0.0019;

Device number	Device name	Nominal power
Device 1	Water Kettle	2200 W
Device 2	Hair dryer (stage 1)	720 W
Device 3	Vacuum cleaner (stage minimum)	320 W
Device 4	Microwave	1100 W
Device 5	Halogen Lamp	400 W
Device 6	Hair dryer (stage 2)	1300 W
Device 7	Vacuum cleaner (stage maximum)	1310 W

Table 5.1: *Devices considered for the experiments.*

- Variance Error: 0.0023 ;

The relevant parameters are the mean and the variance of the relative error, indeed in Basic Configuration and in Configuration 2 we obtain a variance of the relative error of the same order and also the mean. As we expected, Configuration 1 is characterized by a bias in the estimation that we do not find in Configuration 2.

5.4 DEMO

The performances of the algorithm are investigated by using a set of devices with a quite high real power that we could find easily in an environment. With reference to Table 5.1, we have tested the algorithm by estimating Device 1,2,3,4,6,7 and we have built a DEMO to show the results of the algorithm in the case of Device 1,2,3,4.
Device 5 is the Halogen Lamp that we have chosen as reference load, it has a real power of 400 W and no reactive power.
The Matlab algorithms give as results the status of each appliance (appliance ON or OFF) and the energy consumed by each appliance during the execution of the DEMO.
The detection of the appliance, in this simple case, is done by comparing the estimated power with the database of the available devices.
The Graphical output of the DEMO, as shown in Fig. 5.13, is composed of four parts:

- On the upper side the estimated real power is represented with a blue line. This graph depicts only the estimated power of the last 20 s of execution of the DEMO;
- On the middle there is a bar plot that visualizes a blue block, with amplitude equal to 1, when a device is ON;
- On the left of the lower side the total energy consumption for each device is represented (total consumption from the starting point of usage of the DEMO);
- On the right of the lower side there is a pie chart representing how the overall energy consumption is divided between the different devices.

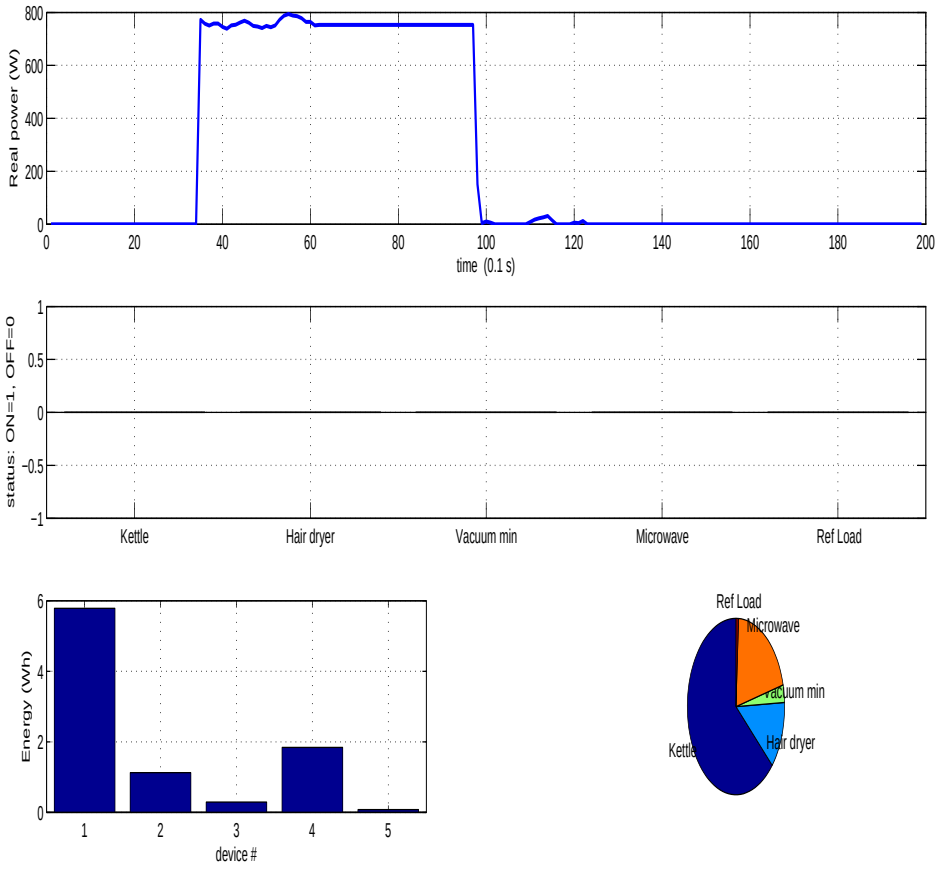

Figure 5.13: *Graphical User Interface used in the demonstrator.*

In Fig. 5.13 we can observe between 30 and 100 s of the upper graph the estimation of the real power of the hair dryer. The estimation takes place until when the long term transient is considered exhausted (as explained in Section 4.9), in the case of the hair dryer we could set immediately the real power because there are no relevant changes after the switching on but in other cases this is not verified as we have already explained.
To support this last consideration Fig. 5.14 shows the trend of the real power in the case in which first the Device 3 is turned on/off (between 0-10 s) and, after that, also the Device 7 is turned on/off (15-20 s). As it can be inferred from Fig. 5.14 in these two cases of interest the voltage does not assume immediately the final value but it is characterized from a strange trend associated to the long term transient. Another important characteristic of our DEMO is that it does not recognize simultaneous events but it can detect when more than one device are working. For instance, if the water kettle is turned on, after the recognition and estimation of this device, if another device is switched on the DEMO shows the total power consumption in the electrical branch circuit that is equal to the sum of the two estimated power.

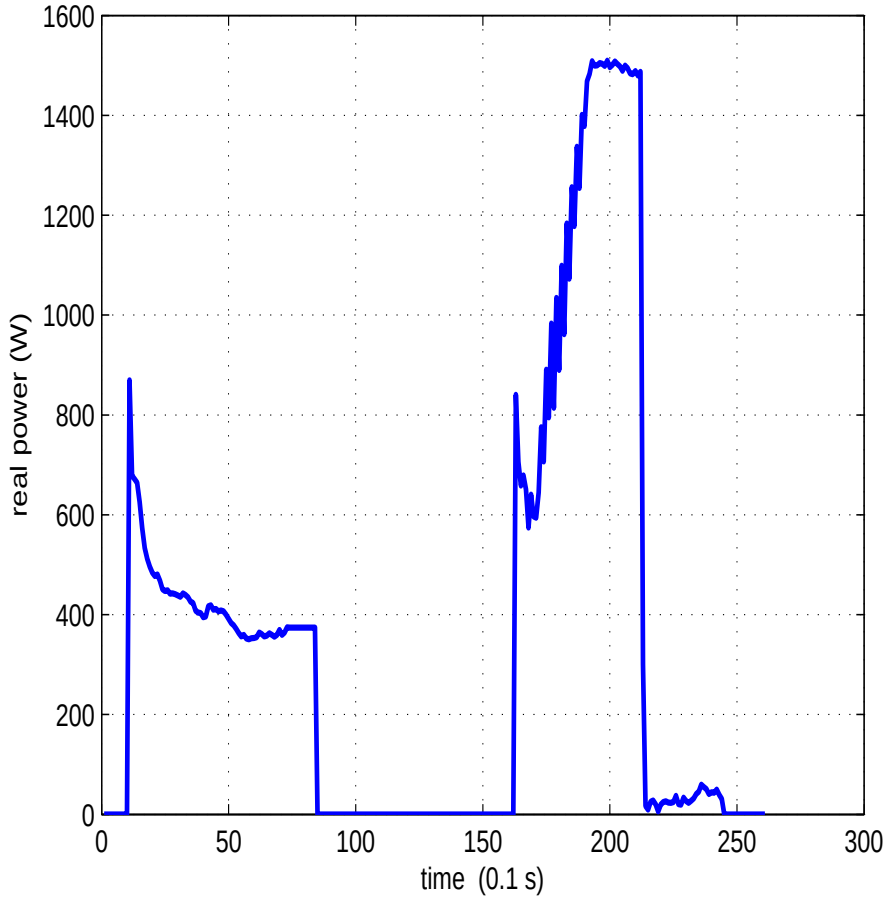

Figure 5.14: *Estimated change in term of Real Power with Device 3 and Device 7.*

5.5 Validation of the Analysis of the existing Crosstalk between different electrical branch circuits

In the present Section some performed experiments are reported with the aim of validating the theoretical analysis of the crosstalk (Section 2.3.1).
The performed experiments consist in the execution of the following steps:

- The reference load of our DEMO (Halogen lamp with a real nominal power of 400W) is turned on/off one time to estimate the equivalent electrical network.
- A water kettle (Device 1 with a real nominal power of 2200 W) is turned on/off for three times in our electrical branch circuit (where the measuring instruments are placed);
- The same water kettle is turned on/off for three times in another electrical branch circuit (different electrical branch circuit from that one in which the voltage probe is placed).

The experiments have been carried out to demonstrate that effectively the presence of the crosstalk between different branch circuits has to be considered in the execution of the algorithm. Fig. 5.15 reports the trend of the voltage in one experiment: after 6/7 s there is the first drop that corresponds to the switching on of the Halogen Lamp, at 10 s it is switched off, between 10/40 s the six large jumps correspond to the three times in which the reference load is switched on/off. Finally between 50/80 s the water kettle is switched on/off three times in another electrical branch circuit. We can clearly see the jumps due to the presence of the appliance in both the branch circuits but with different amplitude.
The event detector recognizes the jumps that are due to the switching on of the unknown device in another electrical branch circuit and the algorithm proceed to estimate the real power of the appliance. In Fig. 5.16 the real power estimated with our method is depicted with a blue line and with a red line the real power, calculated by using voltage and current, is reported.
The estimations of the water kettle when it is placed in the same branch circuit of the voltage sensor give approximately the same results with both methods. The part of the experiments in which the water kettle is placed in a different branch circuit leads to important results:

- Only the voltage method recognizes the existing device because of the presence of the crosstalk.
- The estimation of the real power with the voltage method is completely wrong as we have predicted in Chapter 4, the real power is attenuated by a factor near to the predicted value. Indeed the detected real power is about equal to 200 W.

The introduced experiment shows how the crosstalk really represents an interference for the correct execution of the algorithm. The implementation of a MIMO System, for the explained reason, is suggested.

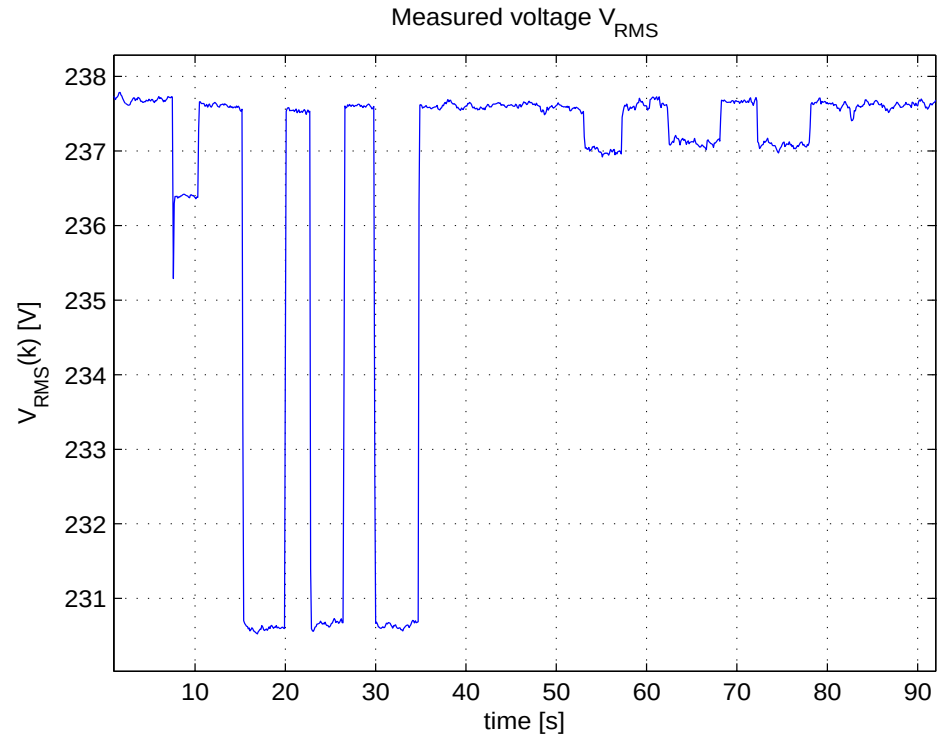

Figure 5.15: *Measured voltage V_{RMS}.*

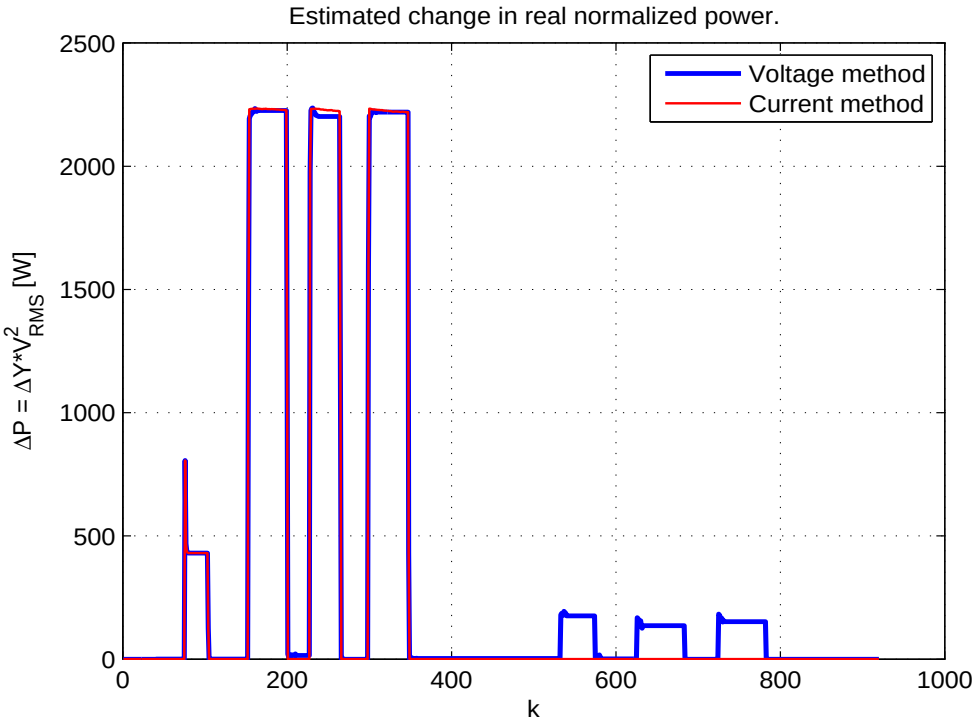

Figure 5.16: *Estimation of the real power.*

		P_{ref} [W]				
		120	160	240	400	2200
P_{x} [W]	120	0.031	0.025	0.023	0.024	0.03
	160	0.025	0.017	0.014	0.013	0.016
	240	0.023	0.014	0.008	0.006	0.007
	400	0.024	0.013	0.006	0.003	0.0024
	720	0.026	0.014	0.006	0.0021	0.0008
	2200	0.03	0.016	0.007	0.002	0.0001

Table 5.2: *Variance of the relative error with* $\sigma_V / V_0 \approx 1.4e-4$.

5.6 Validation of the estimation of the relative load estimation variance

Another relevant examination has been performed in Section 4.5 and it regards the variance of the relative error. Different reference loads and also different unknown loads have been used, in the following Section, to validate the model of the variance of the relative error (see (4.46)). In Table 5.2 a range of possible nominal values of P_{x} (y-axis),P_{ref} (x-axis) are presented and the theoretical value of the variance of the relative error in term of $\left(\frac{\sigma_Y}{Y_L}\right)^2$ is reported as calculated with (4.46).
The value of Table 5.2 are obtained by using the following parameters:

- $\sigma_v = 0.033$ V;
- $V_0 = 238$ V;
- $Z_0 = 0.5\ \Omega$;

A series of experiments has been carried out to validate the theoretical model. Y_{x}, a water kettle (Device 1) was used and, as Y_{ref}, an Halogen Lamp with a nominal power in the first case of 120 W and in the second of 400 W.
One example of execution of the experiments is reported in Fig. 5.17. In this example the reference load is an Halogen lamp with a real power of 400 W.
One experiment consists in a series of rounds. Every round is executed in the following way: first the reference load is turned on/off and the execution of the network takes place, after that the unknown device is turned on/off and the algorithm estimates the real power by taking into account the estimation of the network of the current round.
In Fig. 5.17 in the upper sub-plot the trend of the measured RMS voltage ($N_s = 1000$) is reported. For instance, the first round takes place between $k = 0$ and $k = 180$. At around $k = 100$ there is the first voltage drop that corresponds to the switching on of the reference load, the second drop is larger because it corresponds at the switching on of the water kettle (larger power). In the lower side of Fig. 5.17 the estimated power (with the two different technology) is represented. The first time in which the reference load is turned on its power is estimated only by the method

that uses both current and voltage signals because for the voltage method no estimation of the network is available. The other times in which the reference load is switched on the algorithm estimates its power by using the voltage drop and the previous estimation of the network, when the algorithm recognizes that the device is the reference load it estimates the network again and it sets the power to zero to underlines that the estimation is performed.
During the execution of the algorithm the values of the voltage $V^{(i)}, i = 0, 1, 2$ have been calculated by averaging over $10V_{\text{RMS}}$ values. $V^{(0)}$ is calculated by averaging over 10 values before the switching on of the reference load, instead $V^{(i)}$, $i = 1, 2$ are evaluated by averaging over 10 values after the switching on (and after a transient period) of the reference/unknown load.
Fig. 5.18, 5.19 report the histograms of the relative error in both cases (keeping into account also the sign of the relative error). The number of experiments is limited and this explains the inaccuracy between forecast variance and obtained variance.
It is also necessary to remember that we have carried out an analysis with a lot of simplified hypothesis and so the real variance of the error is obviously higher.
In both of the cases the standard deviation of the voltage and the average value of V_0 are almost the same of the Table 5.2.
Anyway the relevant result is, as it has shown in Table 5.2, the variance of the relative error increases a lot if it is used, as reference load, a load of limited real power. This confirms the theoretical model extracted in Section 4.5. The difference between Fig. 5.18 and Fig. 5.19 is

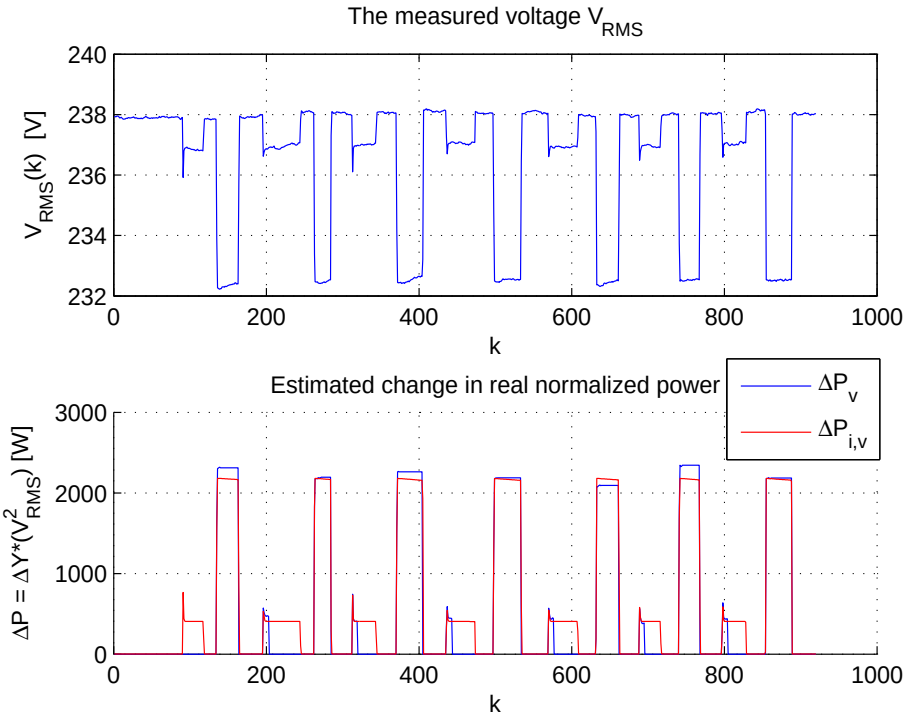

Figure 5.17: *Example:* $P_{ref} = 400$ *W,* $P_x = 2200$ *W.*

immediately evident, we have reported also the parameters that characterize the two different histograms:

- Case 1: $P_{\text{ref}} = 120$ W, the histogram is represented in Fig. 5.18:
  - Width of the interval of the histogram: 0.1;
  - Number of events: 107;
  - Variance of the Relative Error: 0.0843.
- Case 2 $P_{\text{ref}} = 400$ W, the histogram is represented in Fig. 5.19:
  - Width of the interval of the histogram: 0.01;
  - Number of events: 133;
  - Variance of the Relative Error: 0.0019.

The difference between forecast and obtained value of the variance is also explained with the inaccurate estimation of the Z_0 in the forecast. Indeed with the same ratio σ_V / V_0 but with a smaller impedance of the network the variance of the error increases a lot but this is referred to both the cases of interest.

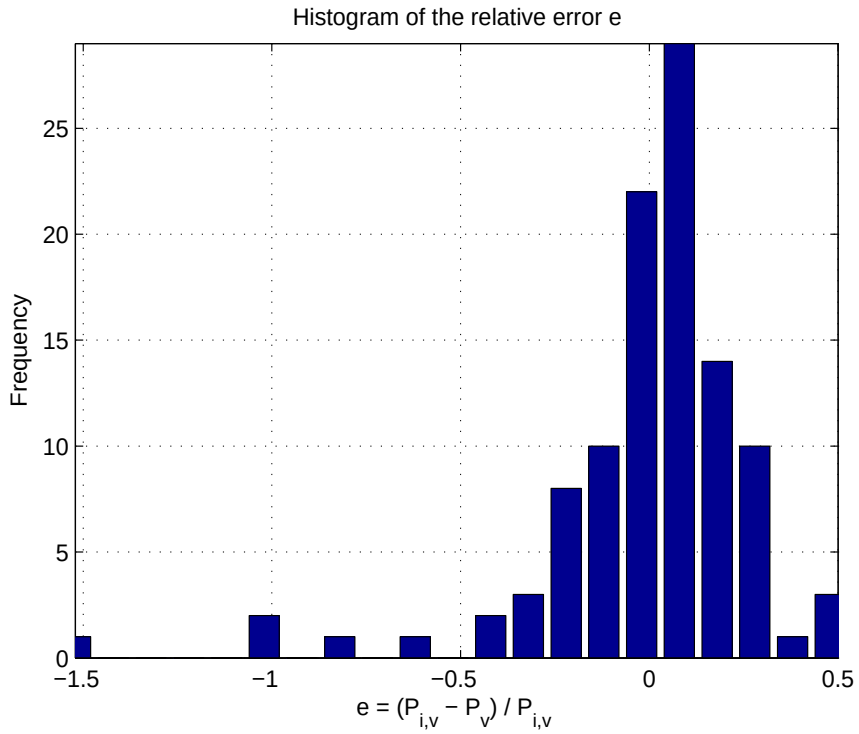

Figure 5.18: *Histogram of the relative error.* $P_{ref} = 120$ *W,* $P_x = 2200$ *W.*

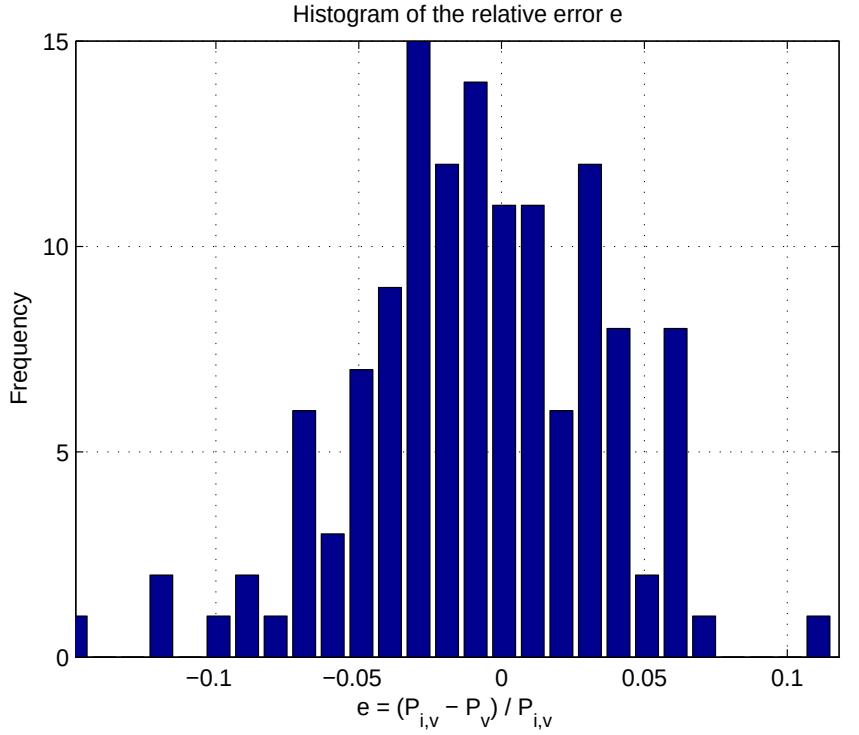

Figure 5.19: *Histogram of the relative error.*$P_{ref} = 400$ *W,* $P_x = 2200$ *W.*

Chapter 6

High Frequency Characterization

6.1 General

In [21], as already introduced in Chapter 1, the authors explain a new approach to identify devices in a home environment based on the device's switching frequency characteristics.
The goal of this Chapter is to verify the reliability of this type of approach to understand if it could be a complementary solution to our method in the detection of devices with a small real power.
The Chapter is divided into the following Sections: Section 6.2 explains the general theory behind this approach, Section 6.3 explains the two tested Configurations and the steps that we execute during the experiments, Section 6.4 focuses on the experiments that we have carried out with laptops, Section 6.5 reports the performed analysis on two devices with a small power consumption, finally Section 6.6 concludes the Chapter with the analysis of other devices with a real power higher than 20 W.

6.2 EMI

The method of [21] focuses on the electrical noise present on a power line when a device is operational that is called electro-magnetic interference (EMI). This last one can be classified into two types: transient and continuous.

Definition 5 *EMI: Electromagnetic interference (or EMI, also called radio frequency interference or RFI when in high frequency or radio frequency) is a disturbance that affects an electrical circuit due to either electromagnetic induction or electromagnetic radiation emitted from an external source.*

Radiated EMI may be broadly categorized into two types; narrowband and broadband. Both transient and continuous noise can either be concentrated within a narrow frequency band or spread over a wider bandwidth. As seen in Chapter 2, an electrical distribution system is interconnected in parallel at the circuit breaker panel and this permits a widely EMI propagation from a given device throughout the electrical infrastructure.

The novel approach of [21] focuses on devices that contain modern SMPS. Indeed, as explained in [21], they generate noise that is synchronous to their power supply's internal oscillator.
This type of appliances has a switching frequency that is much higher than 60 Hz, typical SMPS operate at tens to hundreds of kHz.
For example a compact fluorescent light bulb (CFL) is a device that generates continuous noise, indeed a CFL's power supply employs the same fundamental switching mechanism to generate high voltages necessary to power the lamp. The switching action generates a large amount of EMI centred in frequency around the switching frequency. [21] reports the experiments that they performed in the US where the Federal Communications Commission (FCC) sets rules (47CFR part 15/18 Consumer Emission Limits) for any device that connects to the power line. This limit is 66 dB μ V for frequency range between 150 kHz to 500 kHz, which is nearly -40 dBm across a 50 Ohm load. The ElectricSense, that they have implemented, has a data acquisition system sensitive enough to capture noise from -100 dBm to -10 dBm across a frequency range of 36kHz - 500 kHz.
Our experiments are conducted in EU where the fundamental frequency is 50 Hz (in the US is 60 Hz).
In the mid 1980s, the European Union member states also adopted a number of "new approach" directives with the intention of standardizing technical requirements for products so that they do not become a barrier to trade within the EC. One of these was the EMC Directive (89/336/EC)[23] and it applies to all equipment placed on the market or taken into service. Its scope covers all apparatus "liable to cause electromagnetic disturbance or the performance of which is liable to be affected by such disturbance".
In [21] the authors have shown that when a device is turned on they see a narrowband continuous noise signature that lasts for the duration of the device's operation. The noise centre is strongest in intensity and then extends to lower and higher frequencies with decaying intensity, which can loosely be modelled with a Gaussian function having its mean at the switching frequency.
To perform the following analysis we evaluate the Power Spectral Density associated to voltage signal with the aim of evaluate the components in all the range of frequencies.

6.3 Experimental set-up

We have tried different devices (reported in Table 6.1) in two different situations:

- Configuration 1: the same of Section 2 with a baseline noise given from the existing network;
- Configuration 2: an Ideal Generator of the voltage (ELGAR POWER CW2501) is used to clean the voltage from high frequency components;

The second Configuration is applied to our experiments because one of the unclear point of the approach of [21] was the dependence on the electrical network. We wanted to test the system in an ideal context to prove if the devices really introduce new high frequency components or if they act on the existing components.

Device number	Device name
Device 1	Laptop1
Device 2	Laptop2
Device 3	Laptop3
Device 4	CFL 5 W
Device 5	LED 4 W
Device 6	Water Kettle
Device 7	Radio
Device 8	TV
Device 9	Coffee Machine

Table 6.1: *Devices considered for the experiments.*

Since the variability of the baseline noise, in Configuration 1, it is suggested to average the PSD over time to obtain a stable baseline as we have also done to analyse our experiments. Indeed the PSD is averaged with a window size of 25 (in both Configuration 1 and Configuration 2).
At the beginning the algorithm, implemented in Matlab, computes an average of 10 averaged PSD and stores this as baseline noise. When the amplitude of one frequency of the estimated PSD differs from the baseline noise more than 6 dB it means that a new device is turned on. Every time two different metrics are also analysed:

- $\mathcal{P}_{diff}(f) = 10\log\mathcal{P}_{aft} - 10\log\mathcal{P}_{bef} = 10\log\mathcal{P}_{aft}/\mathcal{P}_{bef}$;
- $\mathcal{P}_{diff2}(f) = 10\,(\mathcal{P}_{aft} - \mathcal{P}_{bef})$.

6.4 Laptop

In this Section I focus on the charger of the laptop that is plugged in/out. In Configuration 1 the first case that we analyse in this Section is: Laptop 1 (in the experiment the Laptop is plugged in and out).
In Fig. 6.1 the frequency spectrogram is reported (it describes how the power of the voltage is distributed within the frequency range and its evolution over time).
From Fig. 6.1 it can be noticed that when the device is plugged in the amplitude of the PSD increases for all the frequencies, in this way the algorithm can easily detect the presence of a new device.
The algorithm stores the new averaged PSD with the device plugged in (averaged over 10 PSD also in this case).
The Gaussian component is estimated by using the PDF of a Gaussian distribution is:

$$Ae^{-\frac{(f-\mu)^2}{2\sigma^2}}; \tag{6.1}$$

where:

- A: maximum amplitude of the component;

- μ: centre frequency f_0 of the component;
- σ^2: variance of the component that is calculated in the following way:

$$\sigma^2 = \frac{1}{2h} \sum_{-h/2}^{h/2} ((\mathcal{P}(f_0 + h)) - A)^2 \tag{6.2}$$

  In the extraction of laptop's features a value of h equal to 50 seems to give a good approximation.

By evaluating the difference as in (6.3) it is possible to extract the features of the new signal (characterization of the device). The feature extraction can be carry out by the individuation of the peak of the amplitude of (6.3) and with the estimation of the Gaussian fit of the component of the device. In Fig. 6.2 PSD, both without any device and with the charger plugged in, are reported and the following conclusions can be inferred:

- The charger amplifies the Gaussian component at 60 kHz. It seems to amplify both the amplitude and the variance of this component. In Fig. 6.3 the difference between the two PSD ,estimated as in 6.3, is reported and we can distinguish a Gaussian slope as it is rounded in the figure (red line) by following the procedure of extraction of the Gaussian fit explained previously.
- The charger clears the track from 80 kHz to 160 kHz by decreasing the amplitude of the PSD.

The same trial has been performed with two different laptops with different charger to evaluate if the laptops share the same behaviour for the frequency components. The same kind of the figures already explained for the Laptop 1 are reported in Fig. 6.5,6.6,6.7,6.9,6.10.
It is interesting to underline how the most relevant component is detected around the same centre frequency. The data about the two wider component of (6.3) for the three laptops are reported in Table 6.4.

	Laptop1	Laptop2	Laptop3
Amplitude fist component [dB]	12.3	7.3	10
Frequency first component [kHz]	60.8	59.3	60
Amplitude second component [dB]	6	- 5.5	-7.1
Frequency second component [kHz]	68.8	99.8	99.8

The higher component of difference (6.3) remains quite constant in spite of the changing of the laptop and of the charger. The second component, in case of Laptop 2 and 3, remarks how the laptop seems to clear the component at higher frequency. The same component is found in the analysis of Laptop 1 as third components in term of absolute amplitude. In Fig. 6.11 the Frequency Spectrogram is reported in the case in which the following procedure is applied:

1. Nothing is on, the baseline noise of Configuration 1 is recorded;

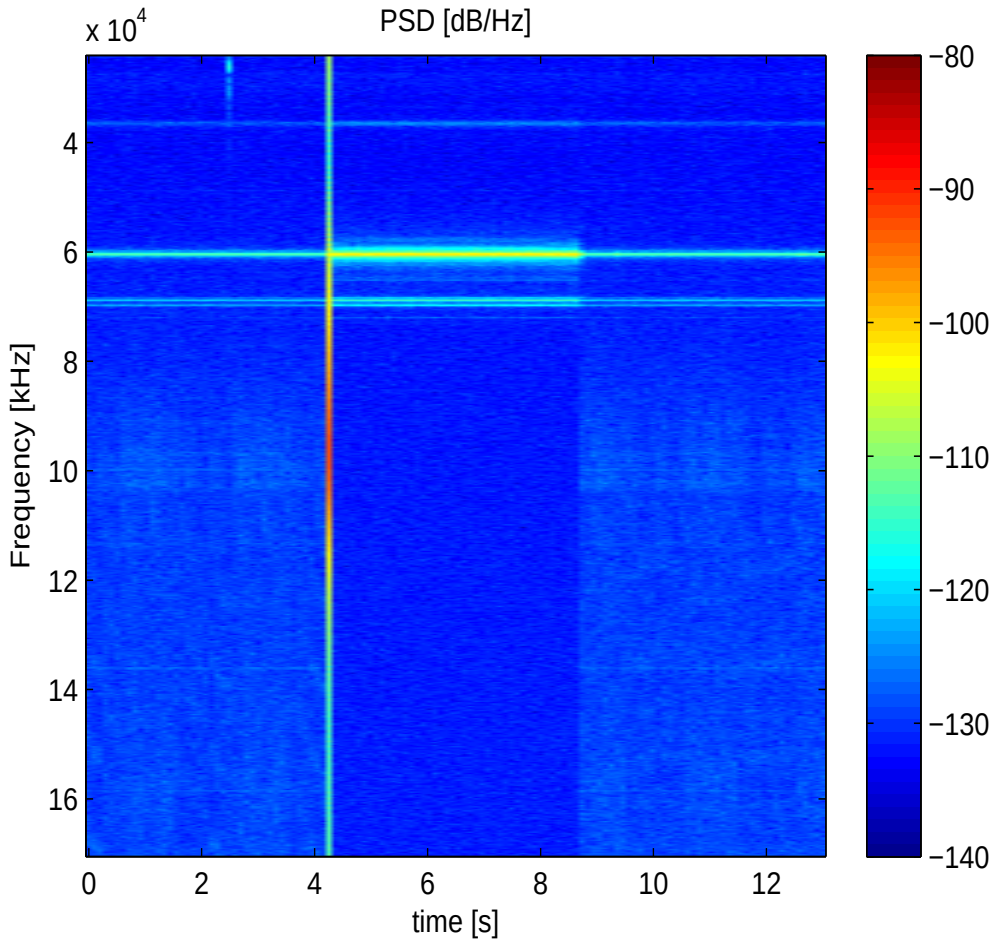

Figure 6.1: *Frequency spectrogram of an experiment with Laptop 1 in Configuration 1.*

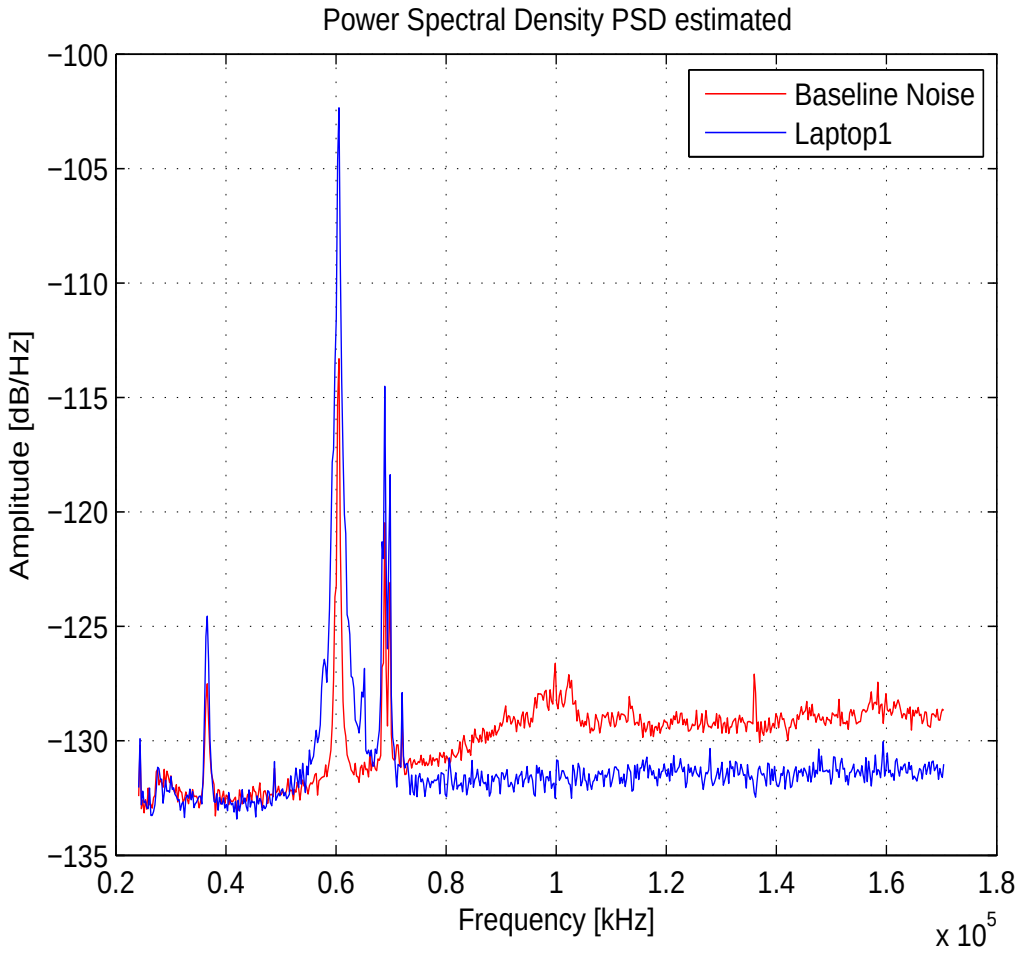

Figure 6.2: *Comparison between the background noise observed on a particular power line (Configuration 1) and the noise observed when the Laptop 1 is turned on.*

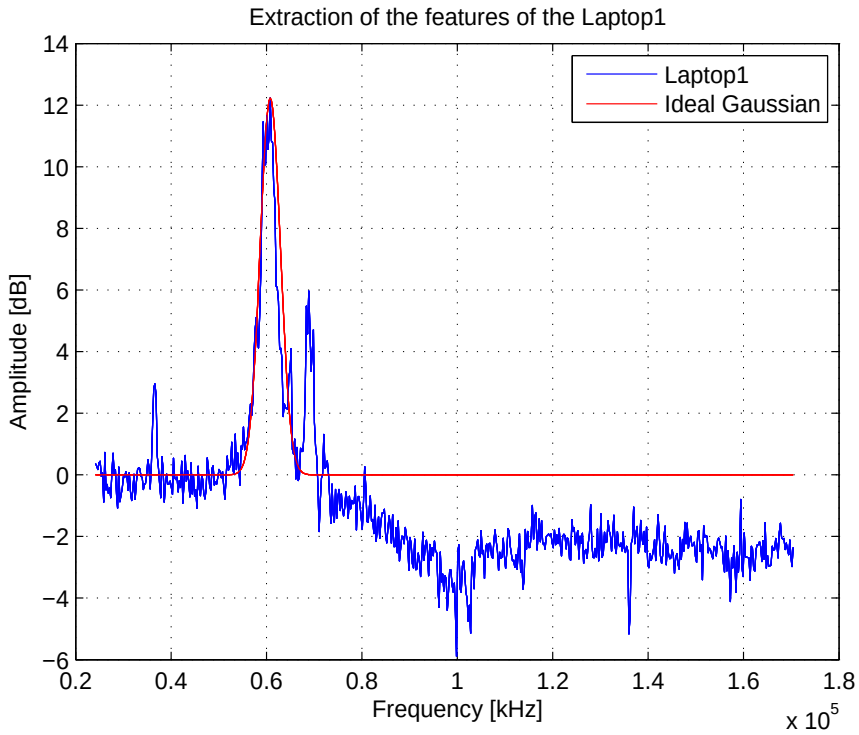

Figure 6.3: *Feature extraction. Extraction of the first relevant component of difference (6.3) in the case of Laptop 1 (Configuration 1).*

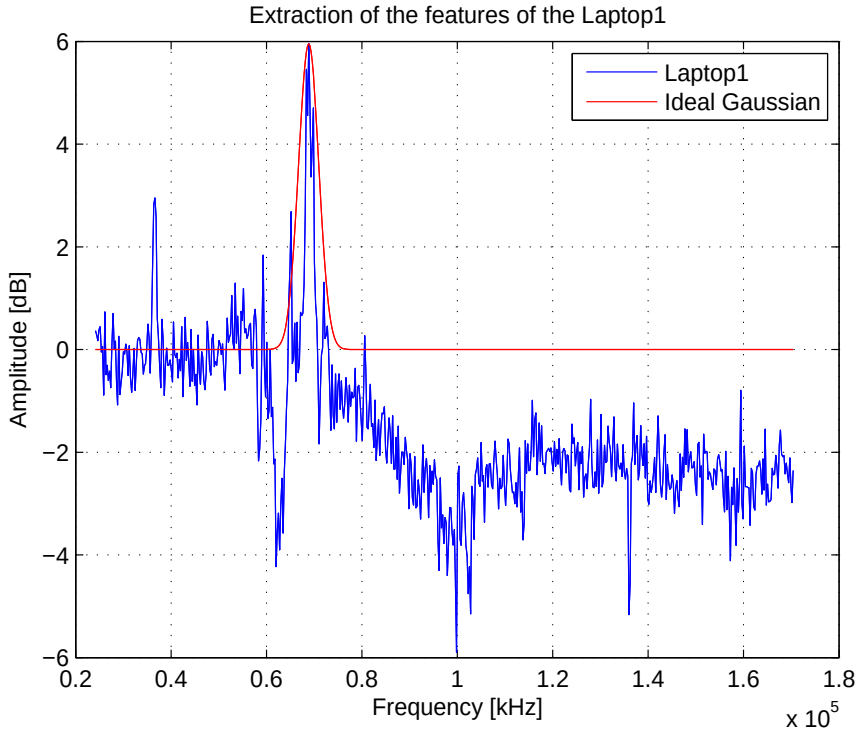

Figure 6.4: *Feature extraction. Extraction of the second relevant component of difference (6.3) in the case of Laptop 1 (Configuration 1).*

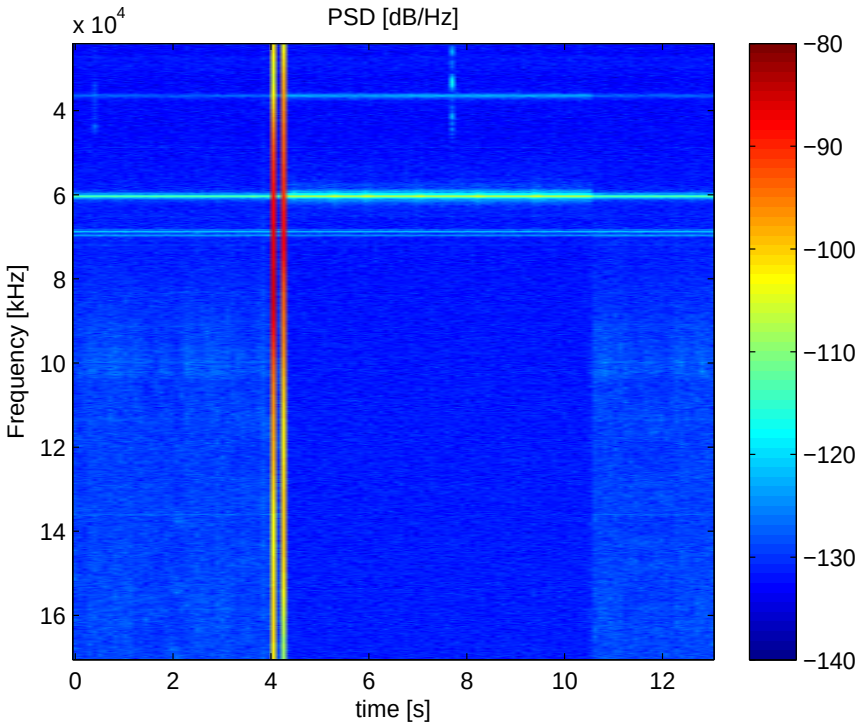

Figure 6.5: *Frequency spectrogram of an experiment with Laptop 2 in Configuration 1.*

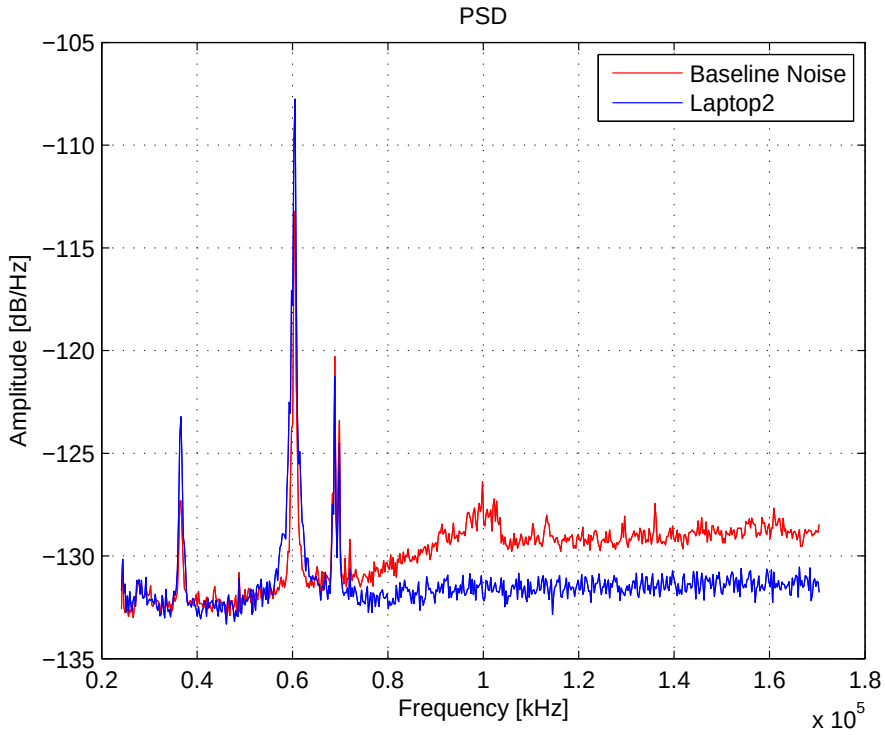

Figure 6.6: *Comparison between the background noise observed on a particular power line (Configuration 1) and the noise observed when the Laptop 2 is turned on.*

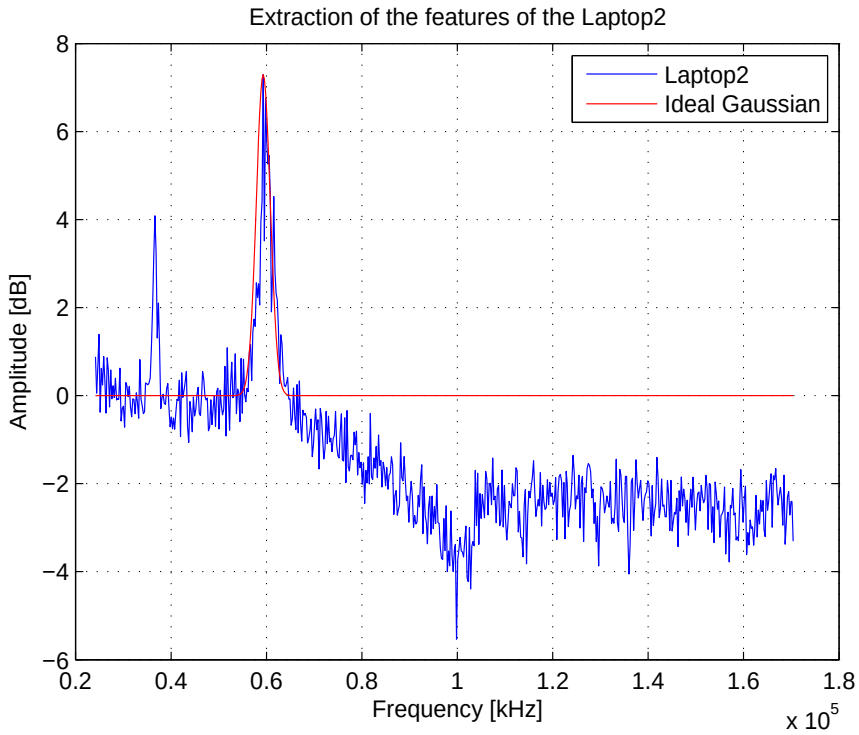

Figure 6.7: *Feature extraction. Extraction of the first relevant component of difference (6.3) in the case of Laptop 2 (Configuration 1).*

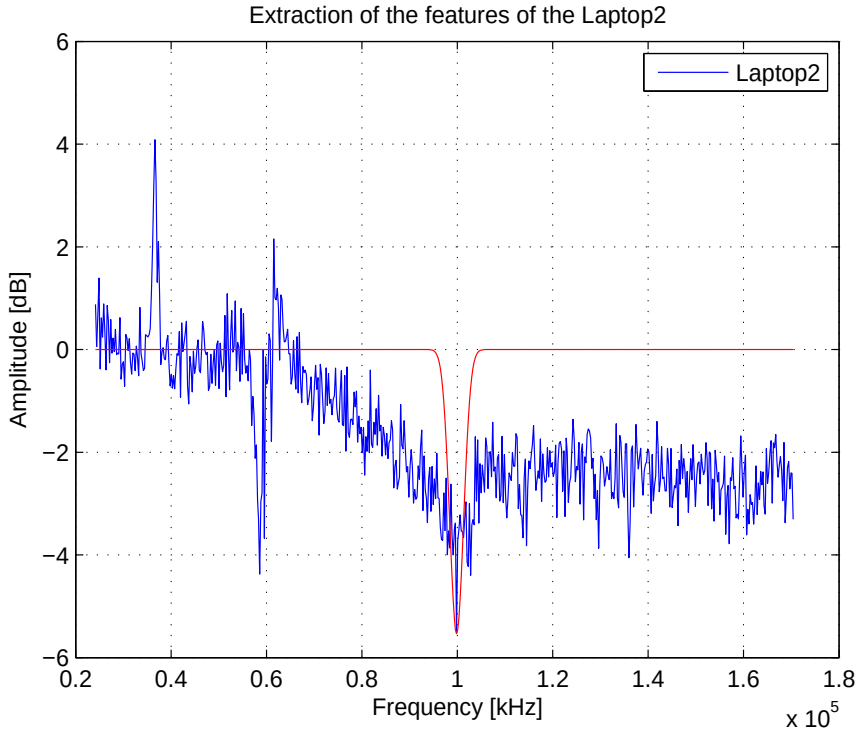

Figure 6.8: *Feature extraction. Extraction of the second relevant component of difference (6.3) in the case of Laptop 2 (Configuration 1).*

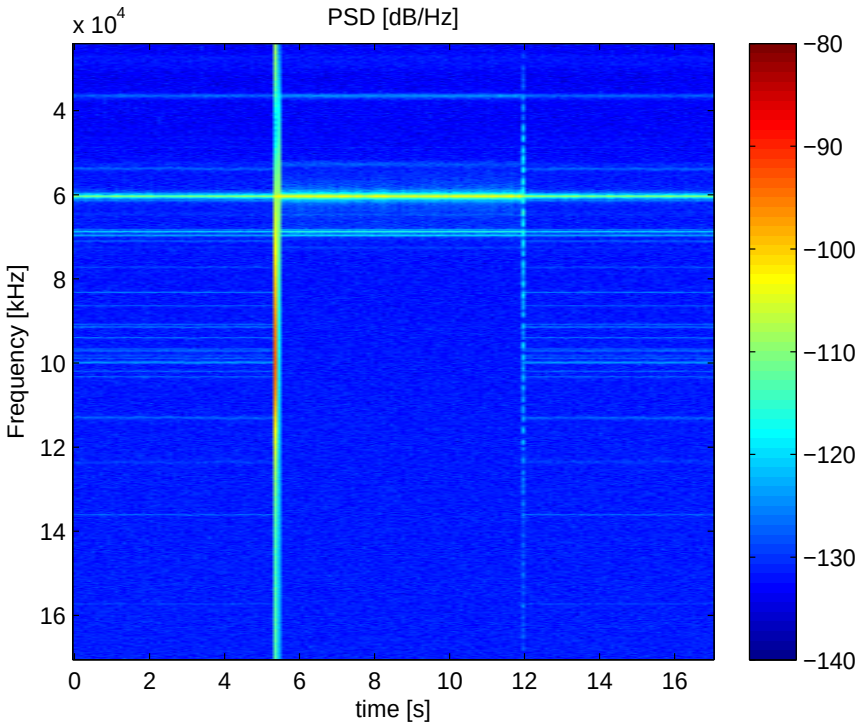

Figure 6.9: *Frequency spectrogram of an experiment with Laptop 3 in Configuration 1.*

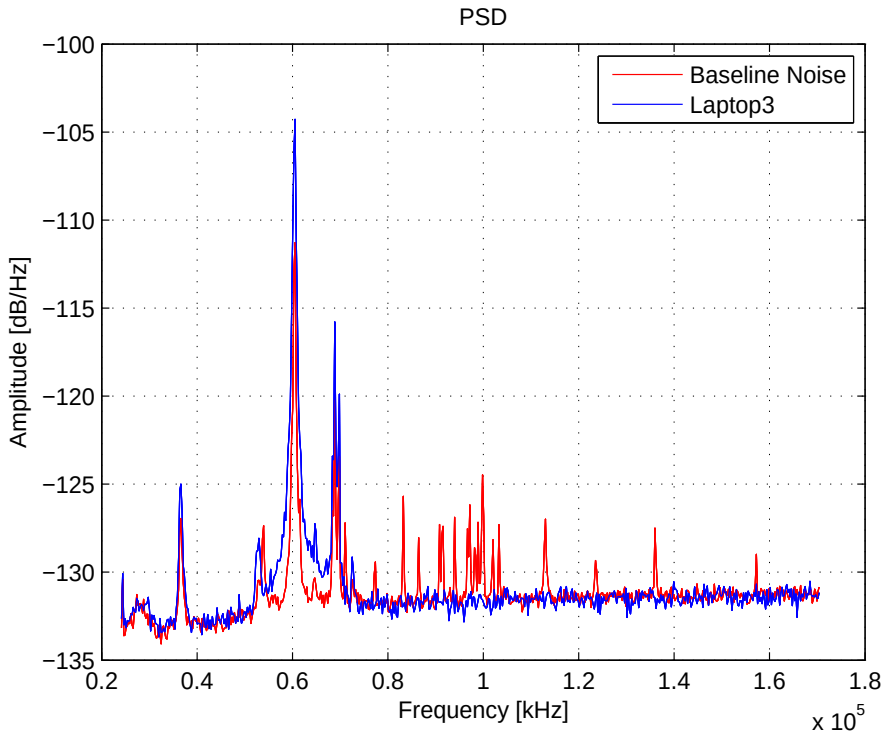

Figure 6.10: *Comparison between the background noise observed on a particular power line (Configuration 1) and the noise observed when the Laptop 3 is turned on.*

2. The Laptop 1 is turned on (at around 6s in the considered experiment);
3. The Laptop 2 is turned on (at around 8s in the considered experiment);
4. The Laptop 3 is turned on (at around 11s in the considered experiment);
5. The Laptop 3 is turned off (at around 16s in the considered experiment);
6. The Laptop 2 is turned off (at around 18s in the considered experiment);
7. The Laptop 1 is turned off (at around 21s in the considered experiment);

With this experiment we want to see in which way the frequency components sum up. The

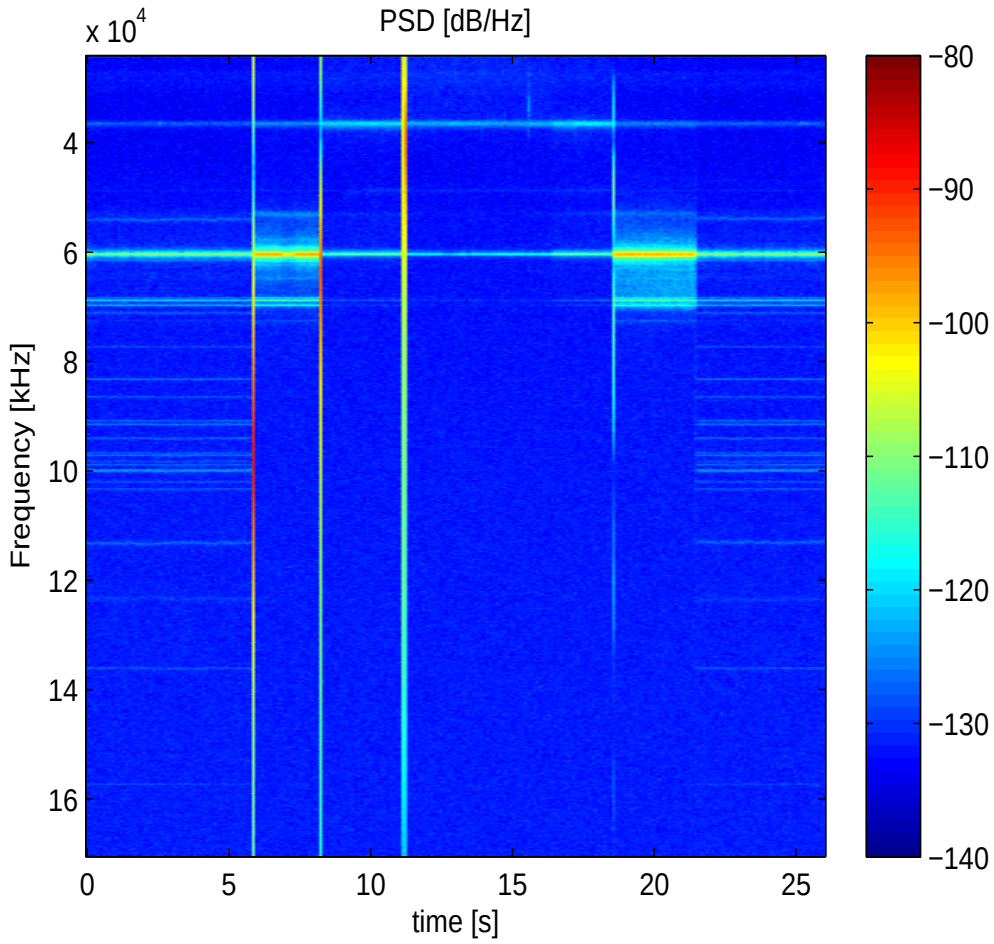

Figure 6.11: *Frequency spectrogram (Configuration 1).*

same experiment has been performed also by changing the order of the plugging of the different laptops, the relevant aspect is that the effects of the switching do not sum in a linear way. Indeed in Fig. 6.12 if, for instance, we consider the main component, the first Laptop add this component

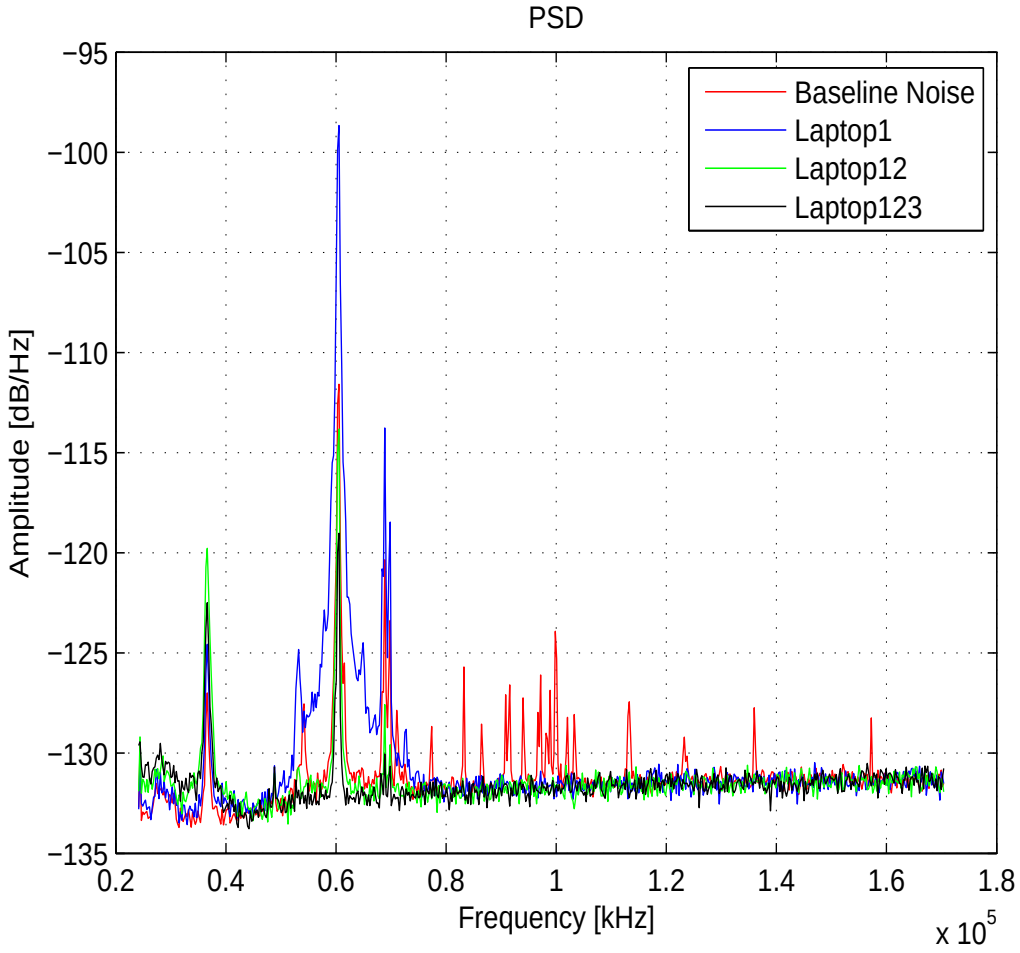

Figure 6.12: *Background noise observed on a particular power line (Configuration 1) without laptops, with Laptop 1 on, both Laptop 1 and Laptop 2 on, Laptop 1 Laptop 2 and Laptop 3 on.*

to the background but then, by switching on other laptops, the component is absorbed and reduce in term of band (as if the laptop acts as narrow band filter). The same experiments (only one laptop for each experiment) have been executed with the ideal background to show the own high frequency components of the devices. With the ideal voltage source we expected to find no high frequency components, instead of this the background (no loads on) shows a component at about 110kHz. The effect of the turning on of a generic laptop (Fig. 6.13,Fig. 6.14) is to absorb this component. The laptops have not any more effect at around 60kHz as it happens in Configuration 1. These last considerations lead us to suppose that the laptops have not own frequency components but they act on the existing components. In Fig. 6.15 the case in which, first is switched on Laptop 1, then Lapton 2 is switched on/off and finally Laptop 1 is switched off, is reported to test again, but in an ideal context, how the components sum up. In Fig. 6.15 the non linearity is clear but, at least, the effect of the laptops seem to be always absorption of the existing main component of the background.

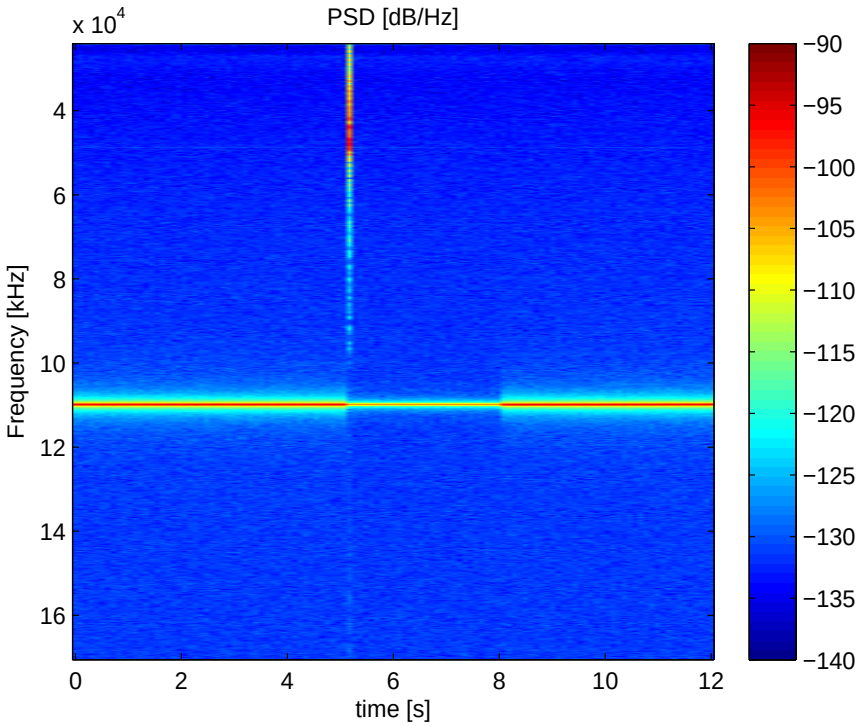

Figure 6.13: *Frequency spectrogram. Laptop 1 Configuration 2.*

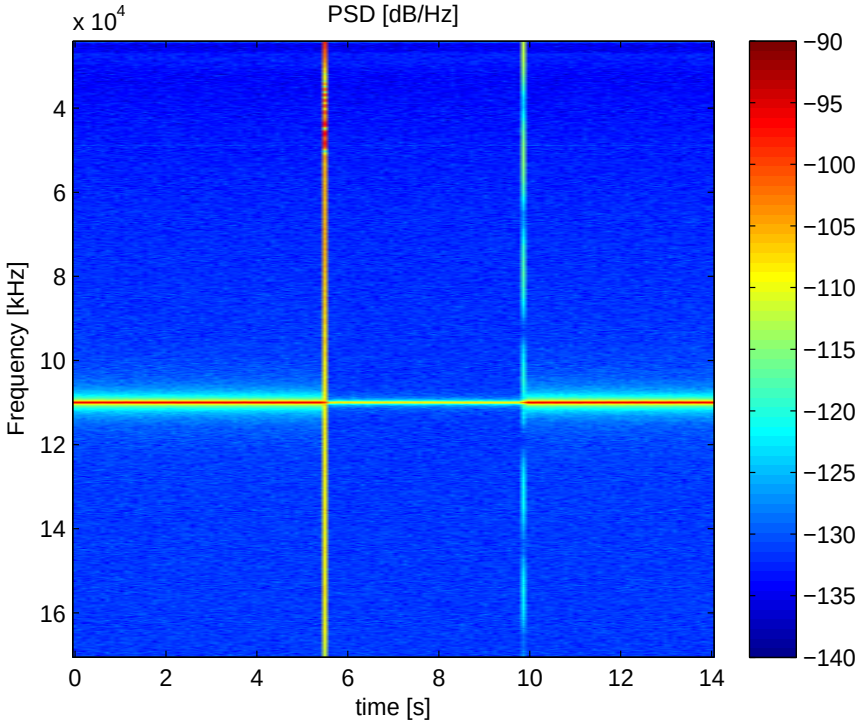

Figure 6.14: *Frequency spectrogram. Laptop 2 Configuration 2.*

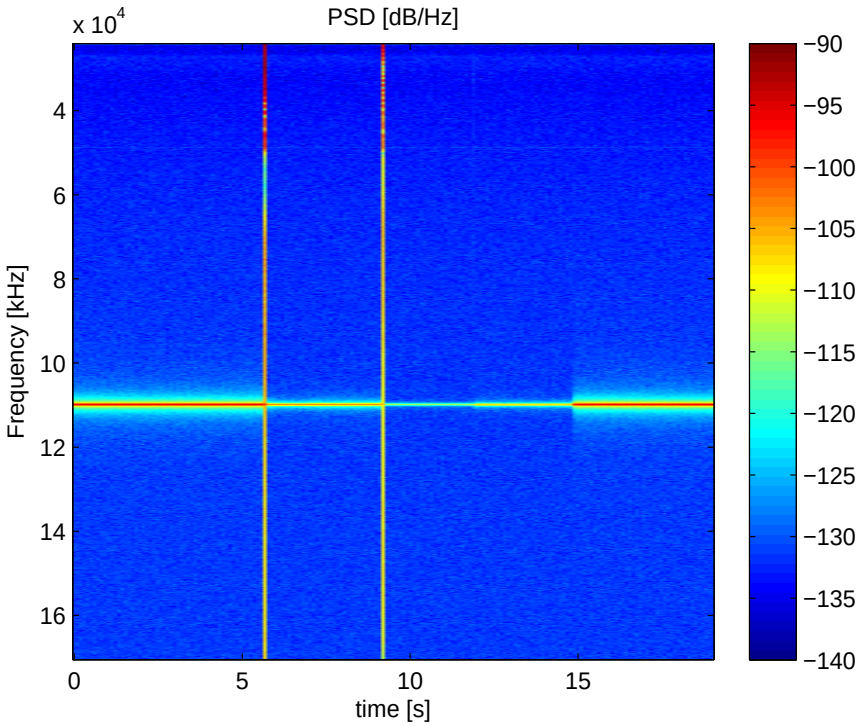

Figure 6.15: *Frequency spectrogram (Configuration 2).*

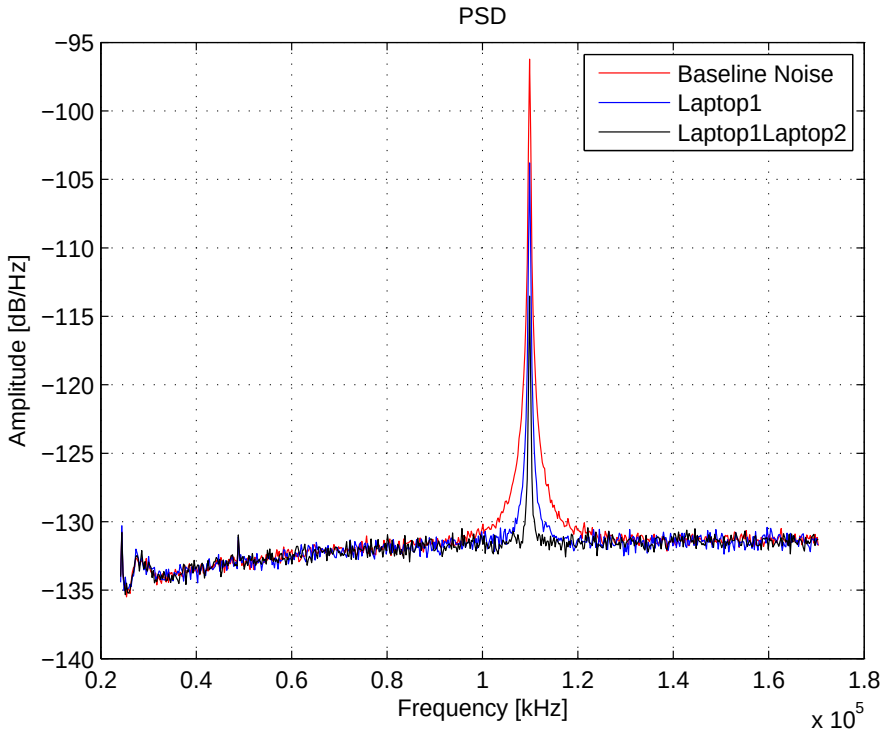

Figure 6.16: *Background noise observed on a particular power line (Configuration 2) without laptops, with Laptop 1 on, both Laptop 1 and Laptop 2 on.*

6.5 Small Power Devices

We have tried different devices, the only ones with which clear features have been extracted are small power devices.
In particular, for instance, we have tried to switch on/off a LED Lamp with a real power of 4 W. Fig. 6.17 shows the frequency spectrograph in Configuration 1, Fig. 6.18 reports the same experiment performed in Configuration 2. Fig. 6.19 and 6.20 shows the same types of experiments executed to find the high frequency components of a CFL Lamp of 5 W. Also Fig. 6.19 and Fig. 6.20 show that CFL 5W introduces new high frequency components, in this case a distinct trend can be recognize, indeed after the switching on a component at around 50 kHz arises and then this component gradually moves toward 40 kHz. A different case is represented by the CFL Lamp of 14 W, indeed, as shown in Fig. 6.21, after the switching on of the lamp we do not clearly recognize new high frequency components. The lamp seems to introduces new components at around 50 kHz but with a small amplitude.

6.6 Other devices

The small devices (Section 6.5) seem to introduce high frequency components instead of only absorbing the existing ones as the laptops. After these trials we have executed the same type of experiments with other devices to prove if device, with a power higher than 20 W, have own high frequency characteristics.
In this Section I report only the spectrogram related to Configuration 2 because with the Ideal Background it is possible to underline the presence of novel components.
Fig. 6.22,6.23 and 6.24 depict the spectrogram associated to the switching on/off of a Coffee Machine, a TV, a Radio.
In all these cases it is possible to recognize the switching on and off (more difficult) but the devices do not introduce new components. These results show that devices absorbing high power could not introduce new components but only act on the existing components that depends on the electrical network (not reliable approach).

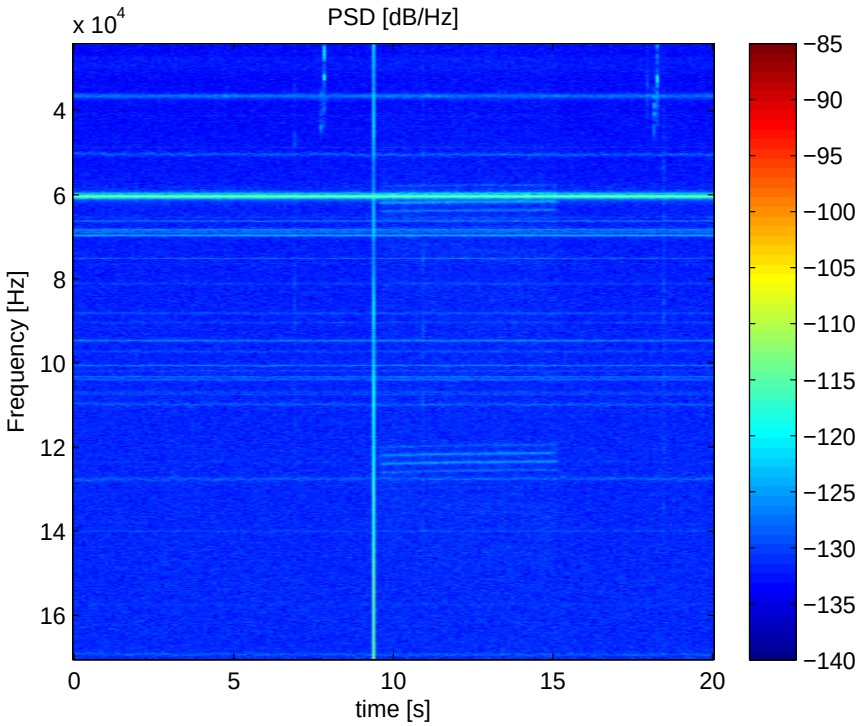

Figure 6.17: *Frequency spectrogram of an experiment with LED 4 W in Configuration 1.*

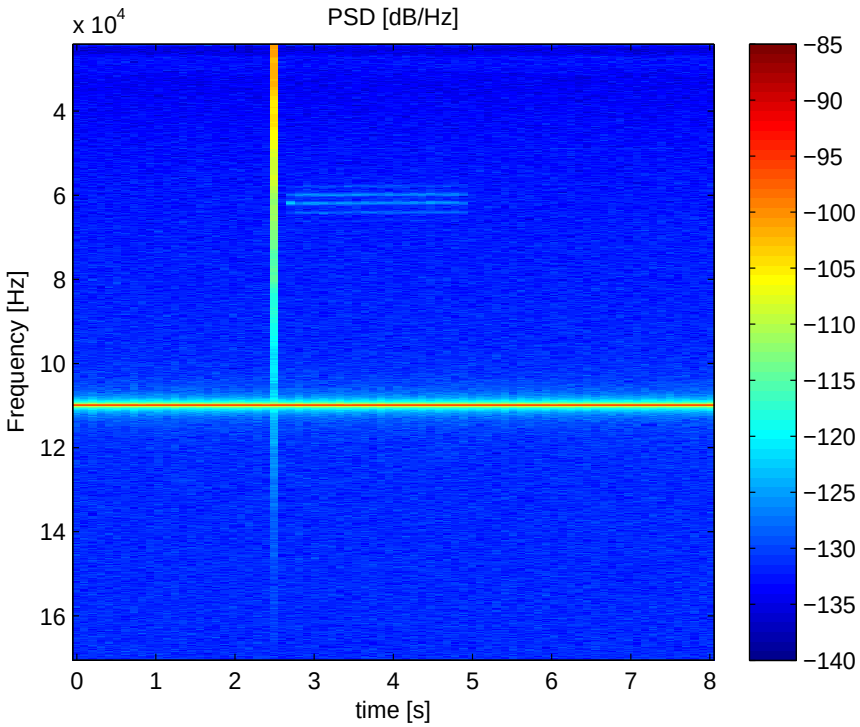

Figure 6.18: *Frequency spectrogram of an experiment with LED 4 W in Configuration 2.*

Fig. 6.17 and Fig. 6.18 show as the LED Lamp really introduces new high frequency components. This is testified from the presence in both Configurations of new components between 60 and 70 kHz. In Configuration 1 the lamp is switched on at around 9s and is switched off at around 15s, in Configuration 2 the same round is executed between 2.5 and 4.5 s. In these time intervals we can clearly see the new high frequency components.

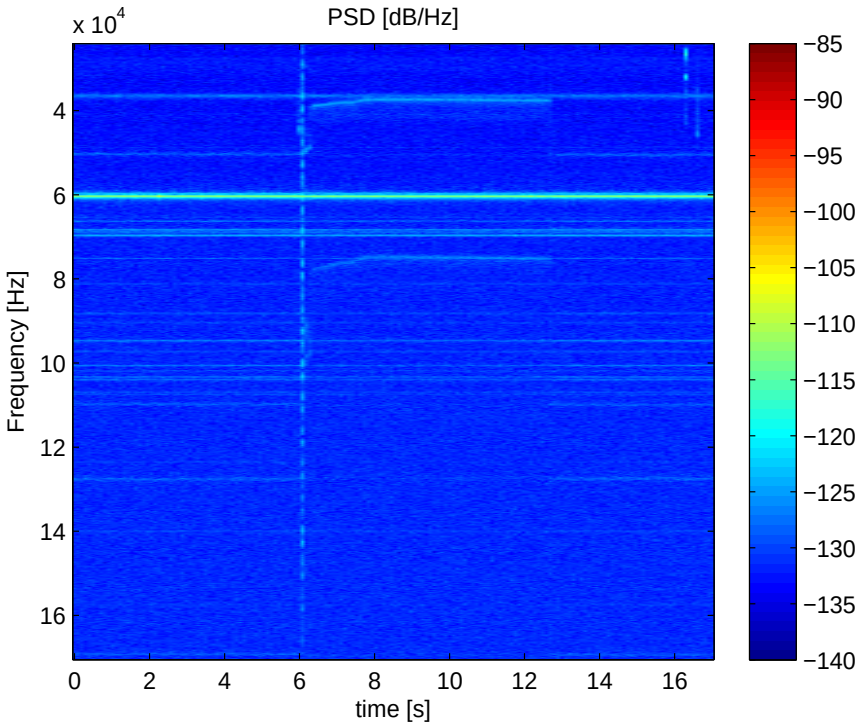

Figure 6.19: *Frequency spectrogram of an experiment with CFL 5 W in Configuration 1.*

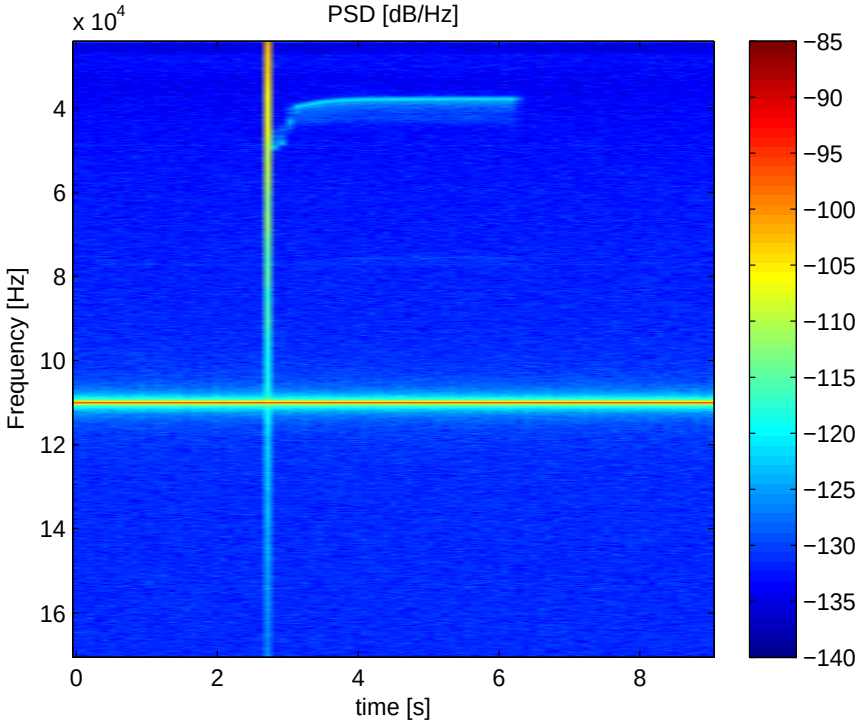

Figure 6.20: *Frequency spectrogram of an experiment with CFL 5 W in Configuration 2.*

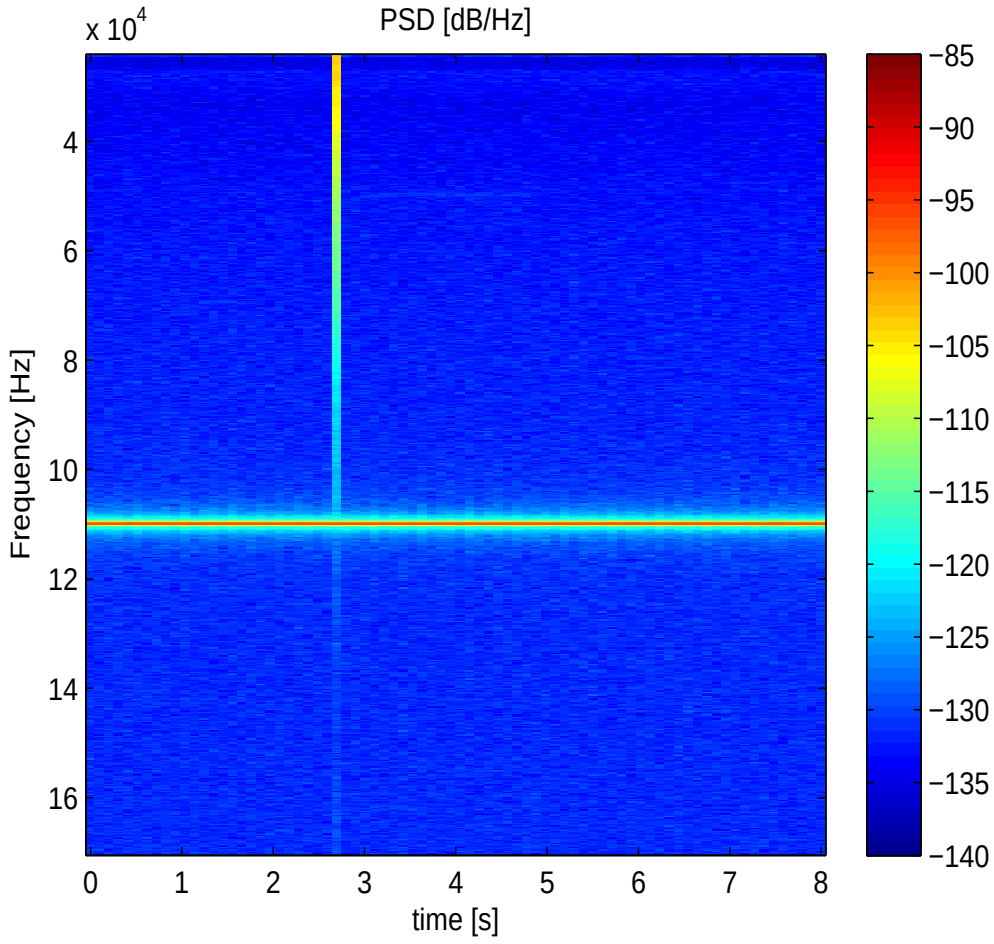

Figure 6.21: *Frequency spectrogram of an experiment with CFL Lamp of 14 W in Configuration 2.*

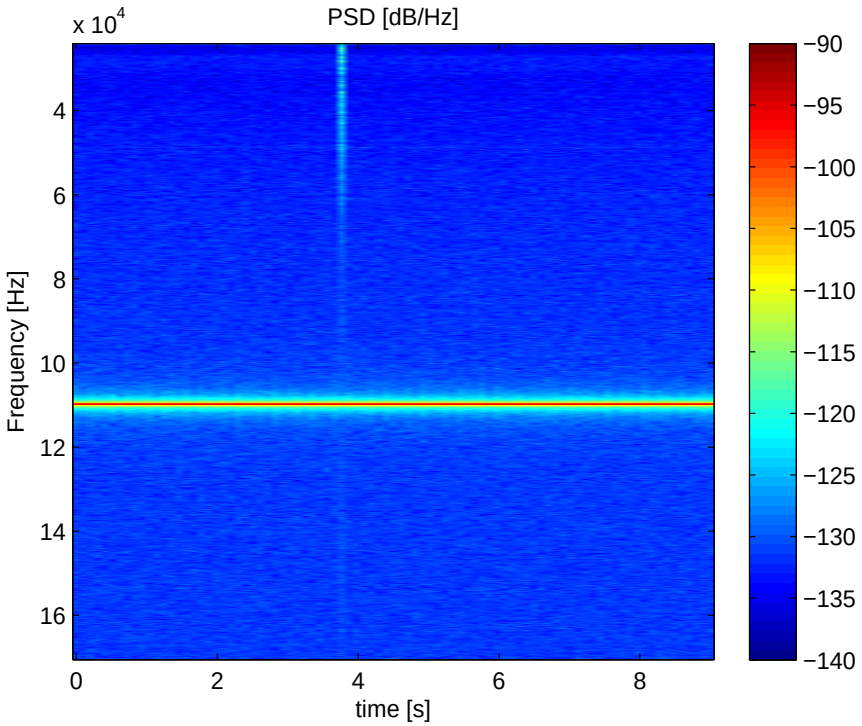

Figure 6.22: *Frequency spectrogram of an experiment with a Coffee Machine in Configuration 2.*

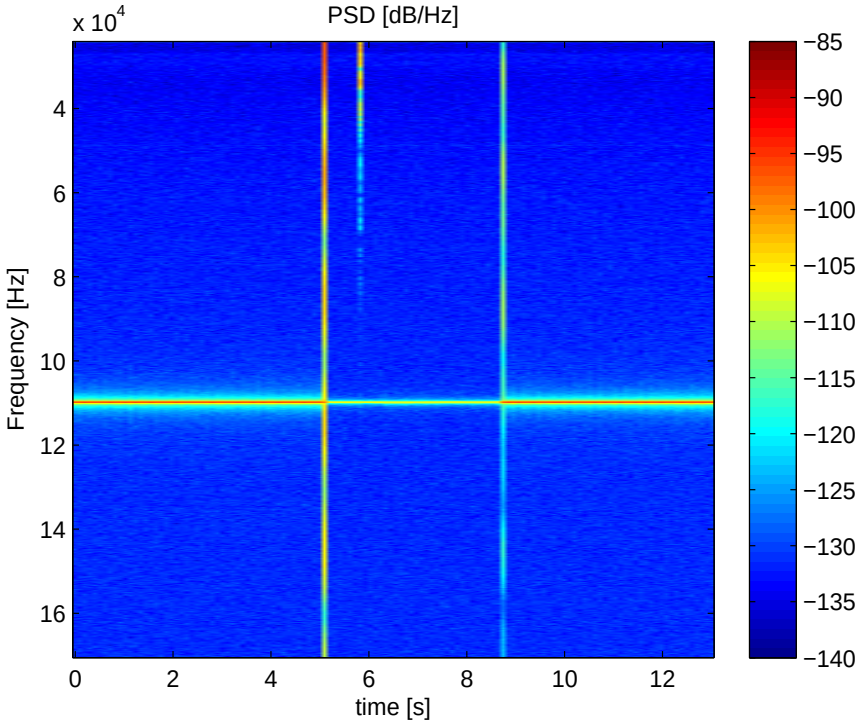

Figure 6.23: *Frequency spectrogram of an experiment with a Philips TV in Configuration 2.*

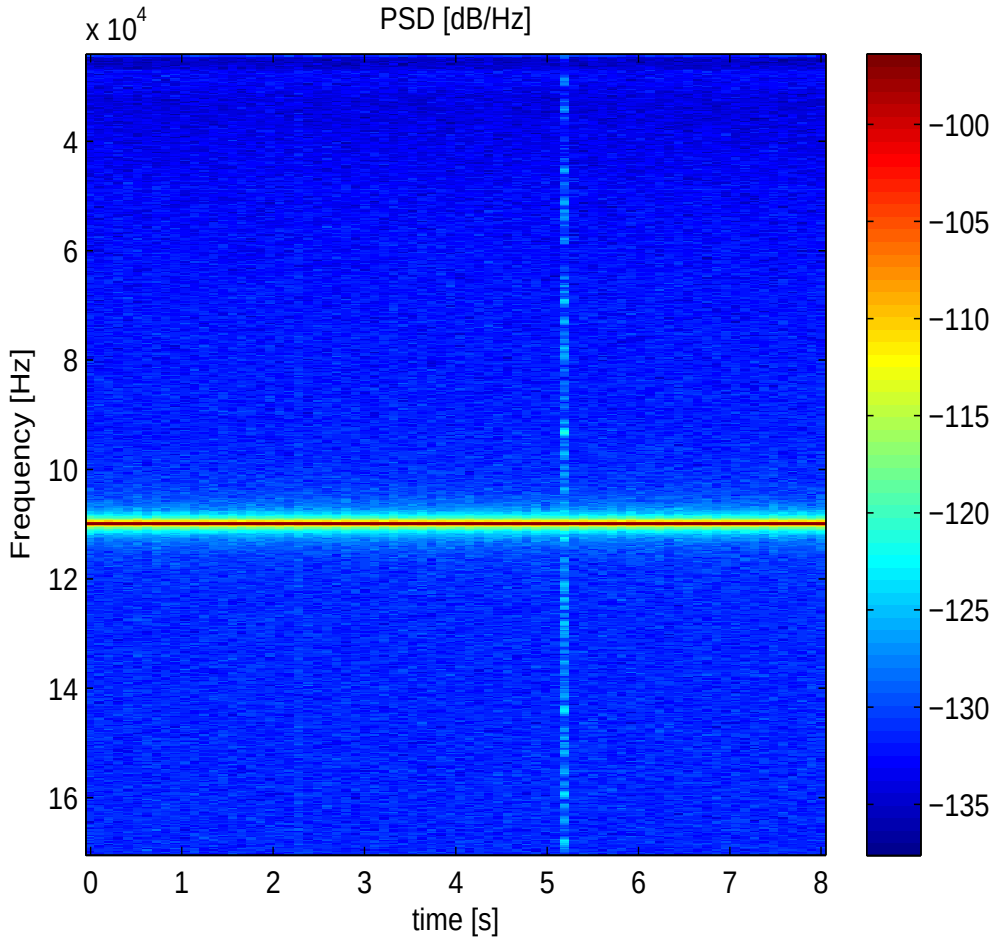

Figure 6.24: *Frequency spectrogram of an experiment with a Radio in Configuration 2.*

Chapter 7

Conclusions and Future works

7.1 Conclusions

The proposed method describes a very simple technology to provide energy disaggregation.
Initial results show that this novel approach for energy management provides good performance for loads characterized by large power and a simple transition from off to on state (the event detector depends on the long-term electric transient).
A definitive positive aspect is that, with this technology, loads with also reactive components could be monitored by using only a single voltage sensor and a mainly resistive load.
In the positive aspects we need to cite again the lower cost (only the voltage probes) for implementation of the novel technology.
The conclusion of our investigation about high frequency components of the voltage signal (Chapter 6) are:

- from our analysis it seems that only devices with really small power (4/5 W) (Section 6.5) introduce high frequency components. The other devices, that [21] analyses, seem only to absorb the high frequency components of the house wiring. The appliance signature could depend, in this way, on the socket of application of the algorithm, if the signature consists on the absorption of components dependent from the house wiring;
- the appliance signature are different if more that one device (of the same type) are switched on and this testifies the non linearity of this type of signature;
- modern appliances are not always equipped with SMPS;
- this type of approach anyway allows only the detection of the appliances not the estimation ot their power.

7.2 Future Works

Our method has as limitation the range of possible appliances, indeed , as it is indicated in the Chapter 3, the method can not estimate loads with a real power lower than about 80/100 W.

The final goal of a energy management should provide energy monitoring of all the devices that are present in households, the final solution should include also devices with small power. A future development could be the analysis of devices with small power to understand if really the approach [21] has no sense (Chapter 6). If additional studies will give the same results of Chapter 6 it will be necessary to find another way to detect power consumption of small devices. Otherwise the final technology could include both the voltage method and the high frequency method for "small" devices. The second one will need to build a database of the appliances for every new environment of application to associate the power nominal consumption when a device is detected (this approach can not estimate the power consumption).
Another problem that we have indicated in Chapter 3 and 4 is the instability that characterizes the phase of the voltage signal. The implementation of a PLL system is suggested to solve that problem and test the system about the estimation of the complex power (not only real power).
For a practical implementation, in a domestic environment, further studies about the stability of the voltage and the stability of the ratio V_0/Z_0 are suggested.
As future development of the voltage technology it is also suggested to implement a MIMO system with a sensor for each electrical branch circuit. The system should include more than one electrical branch circuit and the algorithm should provide the disaggregation of the energy so the analysis of the attenuation between different electrical branch circuits, in a generic environment, is necessary.

Bibliography

[1] M. Bertocco, A. Sona,“Manuale di compatibilit elettromagnetica”, 2010.

[2] K. Ehrhardt-Martinez, K. A. Donnelly, J. A. Laitner,“Advanced Metering Initiatives and Residential Feedback Programs: a Meta-Review for Household Electricity-Saving Opportunities”,*ACEEE*, 2010.

[3] S. Park, H. Kim, H. Moon, J. Heo, S. Yoon, “Concurrent Simulation Platform for Energy-Aware Smart Metering Systems”, *IEEE Trans. Consumer Electron*, vol. 56, num. 3, pp. 1918-1926, Aug. 2010.

[4] K. Balasubramanian and A. Cellatoglu, “Improvements in Home Automation Strategies for Designing Apparatus for Efficient Smart Home”, *IEEE Trans. Consumer Electron*, vol. 54, num. 4, pp. 1681-1687, Nov. 2008.

[5] G. W. Hart, “Nonintrusive Appliance Load Monitoring,” *Proceedings of the IEEE*, pp. 1870-1891, Dec 1992.

[6] Cox R.; Leeb S. B.; Shaw S. R.; Kirtley J. L., “Transient event detection for Nonintrusive Load Monitoring and Demand Side Management Using Voltage Distortion”, *IEEE Applied Power Electronics Conference and Exposition (APEC)*, pp. 1751-1757, March 2006.

[7] Leeb S. L., Shaw S. R., Kirtley J. L.,“Transient event detection in Spectral envelope estimates for nonintrusive load monitoring.”,*IEEE transaction on power delivery*, vol. 10, num. 3, July 1995.

[8] Norford, L. K. Leeb, S. B.,“Non-Intrusive electrical load monitoring in commercial buildings based on steday-state and transient load-detection alogorithms”, *Energy and Buildings*, num. 24, 1996.

[9] Shaw S. R., Leeb S. B., Norford L. K., Cox R. W.,“Nonintrusive load monitoring and diagnostics in power systems”, *IEEE Transactions on Instrumentation ans measurement*, vol. 57, num. 7, July 2008.

[10] Chang H. H., Lin C. L., Yang H. T., “Load recognition for different loads with the same real power and reactive power in non-intrusive load monitoring systems”, *12th International Conference on Computer Supported Cooperative Work in Design*, 2008.

[11] Laughman C., Lee K., Cox R., Shaw S., Leeb S., Nordford L., Armstrong P., "Power signature analysis", *IEEE power and energy magazine*, March/April 2003.

[12] Phhala H., "Non-Intrusive appliance load monitoring system based on a modern kWh-meter", *VTT publications*, 1998.

[13] A. Cole, A. Albicki,"Data extraction for effective non-intrusive identification of residential power loads", *Instrumentation and Measurement Technology Conference*, vol. 2, pp. 812-815, 1998.

[14] H. Najmeddine, et al.,"State of the art on load monitoring methods", *IEEE international conference on power and energy*, Dec. 2008.

[15] L. Farinaccio, R. Zmeureanu,"Using a pattern recognition approach to disaggregate the total electricity consumption in a house into the major end-uses", *Energy and buildings*, vol. 30(3), pp. 245-259.

[16] D. Benyoucef, P. Klein, T. Bier,"Smart meter with Non-Intrusive Load Monitoring for Use in Smart House", *IEEE International Energy Conference*, 2010.

[17] M. Zeifman, K. Roth, "Nonintrusive Appliance Load Monitoring: Review and Outloook", *IEEE Transactions on Consumer Electronics*, vol. 57, num. 1, 2011.

[18] Patel et al., "At the Flick of a Switch: Detecting and Classifying Unique Electrical Events on the Residential Power Line", *UbiComp 2007: Ubiquitous Computing*,

[19] S. Gupta, M. S. Reynolds, S. N. Patel, "ElectricSense: Single Point Sensing Using EMI for Electrical Event Detection and Classification in the Home ", *UbiComp 2010*, pp. 26-29, 2010.

[20] M. H. J. Bollen,"Understanding Power Quality Problems. Voltage sags and interruptions.", *IEEE Press Series on Power Engineering*, 2000.

[21] B. Franken, V. Ajodhia, K. Petrov, K. Keller, C. Muller, "Regulation of Voltage Quality", *9th International Conference. Electrical Power Quality and Utilisation*, October 2007.

[22] $http://www.swissgrid.ch/content/swissgrid/it/home/experts/topics.htm.$

[23] $http://ec.europa.eu/enterprise/electr_equipment/emc/directiv/text.htm.$

[24] "Tecnhical data: Miniature Circuit Breaker", *http://www05.abb.com/global/scot/scot209.nsf/veritydisplay/e5a4baa7eed9b492c1256a49004a812e$file/gsk0400701s0201.pdf*.

[25] C. Narduzzi, "Dispense di misure elettroniche", 2010.